FUNCTIONAL AND STRUCTURAL CHARACTERIZATION OF TET/JANUS SIGNALING COMPLEXES IN *A. THALIANA* SPERM CELLS

by

Ryan Hockemeyer

A Thesis

Submitted to the Faculty of Purdue University

In Partial Fulfillment of the Requirements for the degree of

Master of Science

Department of Botany and Plant Pathology

West Lafayette, Indiana

August 2020

THE PURDUE UNIVERSITY GRADUATE SCHOOL
STATEMENT OF COMMITTEE APPROVAL

Dr. Leonor Boavida, Chair
Department of Botany and Plant Pathology

Dr. Sharon A. Kessler
Department of Botany and Plant Pathology

Dr. Joseph P. Ogas
Department of Biochemistry

Dr. Daniel B. Szymanski
Department of Botany and Plant Pathology

Approved by:
Dr. Christopher Staiger

This thesis is dedicated to my fiancée Mercedes for supporting and encouraging me throughout my time at Purdue University.

ACKNOWLEDGMENTS

I would like to thank my advisor Dr. Leonor Boavida for providing guidance and assistance throughout my graduate work. I would also like to thank my committee members, Dr. Sharon Kessler, Dr. Joe Ogas, and Dr. Dan Szymanski for advice during this master's project.

Thank you to the current and past members of the Boavida lab: Dr. Nikita Bhatnagar, Mike Alley. I especially thank Dr. Kwok Ki Ho and Dr. Ding-Hua Lee for providing advice and training in the lab. The training and assistance provided by Dr. Leonor Boavida, Dr. Ding-Hua Lee, and Dr. Kwok Ki Ho were essential to complete this thesis and have provided me with skills that will help in my future career.

TABLE OF CONTENTS

LIST OF FIGURES

ABSTRACT

Plants are used as a primary food source by humans. Some plants produce edible roots or leaves, but most crops used today are grown to harvest their nutrient-rich seeds which are a product of double fertilization in flowering plants.

Cell-cell recognition, adhesion, and fusion are widespread phenomena in many biological processes, where fertilization is an exemplary process. Many players have been identified to mediate sperm-egg fusion in both animals and plants. Interestingly several of these components were shown to be structurally and functionally conserved across kingdoms. In animals Tetraspanins act as facilitators of sperm-egg fusion. Tetraspanins are known to associate in clusters in the plasma membrane of cells, where they recruit diverse signaling proteins, forming the so called Tetraspanin-enriched microdomains (TEMs). TEMs are therefore recognized as major signaling platforms mediating specific cellular processes in the plasma membrane of cells. Two *Arabidopsis*-expressed tetraspanins, *TET11* and *TET12*, are highly expressed in the sperm cells (SCs), however their function in fertilization are unknown. Using fluorescence microscopy, we quantified the expression of TETs in SCs and found evidence for the existence of a Tetraspanin-enriched microdomain (TEM) at the SC-SC adhesion interface. Sperm cell factors which are necessary for fertilization were found to accumulate at the TEM, suggesting that plant SC TEMs may function as protective platforms for fertilization factors. Sperm-expressed TETs directly interact with members of a novel, plant-specific family of unknown proteins, *DMP8/9*. DMP8/9 function as negative regulators of SC-SC adhesion and are required for double fertilization. Structural and functional analysis suggest that these two proteins may perform unique functions

as membrane remodelers in SCs. In addition, we provide evidence of a new GEX2 function as a SC-SC adhesion factor and potential partner of TET-DMP complexes at the SC-SC interface.

CHAPTER 1. INTRODUCTION

Flowering plants, also known as angiosperms, are the primary source of nutrients and energy for humans. They are the basis for many industries in modern society including lumber, agriculture, and pharmaceuticals. Dead land plants are the primary source of coal and other organic molecules in the soil (Delwiche and Cooper, 2015). Of all the plants used by humans, angiosperms are the most important for humans as they evolved to produce nutrient-rich seeds.

There are almost 300,000 species of angiosperms (Thorne, 2002). Today's major crops (rice, maize, wheat, etc.) have been selectively bred over 10,000 years to increase production and nutrition of the seeds. Many modern crop plants have impaired seed dispersal strategies and depend on humans for their propagation. This domestication of wild ancestors was necessary for human survival as ancient civilizations transitioned from hunters and gatherers to agriculturally dependent societies during the agriculture revolution (Doebley et al., 2006).

Many resources used in the plant sciences are allocated to understating and improving crops. This research is applied to produce crops that are less susceptible to disease and pests or use water in a more efficient manner. Detailed research into the mechanisms underlying plant fertilization has only been made possible by recent advances in our understanding of the male and female gamete transcriptomes and early stages of zygotic activation (Becker et al., 2003; Borges et al., 2008; Wuest et al., 2010; Anderson et al., 2017; Zhao et al., 2019). Understanding fertilization can lead to advances in both applied and basic plant sciences. For example, in applied plant sciences like crop breeding, haploid-inducer genes are highly sought after because of the economic savings and increased speed with which new inbred and hybrid lines are developed (Rajcan et al., 2011). Research into sexual reproduction in angiosperms can reveal factors necessary for fertilization and provide methods to improve haploid induction. Fertilization

involves the precise signaling between male and female sex cells, the gametes, unique in their functions and features. When gametes meet a process of cell-cell recognition and adhesion allow these cells to fuse and create a diploid cell which develops into a new brand organism that carries new characteristics resulting from the combination of genetic material from both parents. Understanding fundamental principles of fertilization in plants can shed light on many aspects of genetic and cellular signaling which are relevant not only for plant biology but also to understand basic cell-to-cell signaling mechanisms that are conserved as fundamental processes for the development and reproduction of all multicellular organisms.

1.1 Sexual Reproduction in Flowering Plants

Angiosperms alternate between a diploid dominant sporophytic and a reduced haploid gametophytic generation (Niklas and Kutschera, 2010). In modern flowering plants, the dominant generation is the sporophyte while the gametophytic generation is reduced in the flowers. Gametophytes are multicellular structures that hold the gametes. The gametophyte of the plant is dependent on the sporophyte for nutrition and protection within the flower (Sprunck, 2020).

Angiosperms enclose their haploid gametes within gametophytes which result from meiotic divisions of predetermined cells (Bleckmann et al., 2014). The female gametophyte, or embryo sac, develops in an ovule enclosed in the protective carpel (Irish, 2017). The male gametophytes are the pollen grains which develop in the anther. Both male and female gametophytes are multicellular structures and the development and function of gametes that they enclose depend on gametophytic accessory cells (Gross-Hardt et al., 2007). The embryo sac develops within a highly specialized sporophytic reproductive structure, the ovule. In the sporophytic tissues of the ovule a megasporocyte, or Megaspore Mother Cell (MMC) undergoes two rounds of meiosis and three mitotic divisions to produce the typical 8 cell *Polygonum* structure

of the *Arabidopsis* embryo sac (Yadegari and Drews, 2004). These cellular divisions lead to the formation of a mature embryo sac containing two synergids, the egg cell, a diploid central cell, and three antipodals. The haploid egg cell and a diploid central cell are the true female gametes, while synergids are accessory cells that are responsible for pollen tube attraction and reception (Johnson et al., 2019).

Mature haploid pollen grains have a unique "cell within a cell" structure. The two non-motile male gametes, the sperm cells, float within the cytoplasm of the large vegetative cell. The pollen grain is protected by a highly resistant cell wall which facilitates dispersion, protects the male gametes after dehiscence, and is the site of the first contact and signaling events during pollination (Dresselhaus and Franklin-Tong, 2013).

Upon dehiscence from the anther the pollen grain starts a long journey which eventually culminates in double fertilization, a hallmark of angiosperm sexual reproduction (Johnson et al., 2019). Pollen grains are released from the anthers in a quiescent and dehydrated state. The pollen disperses through wind and insects until it eventually lands on the stigma of a compatible flower (Pacini, 2015). Stigmas are the receptive structures of the flower and can be of two types, dry stigmas and wet stigmas. Wet stigmas secrete a sticky matrix that supports pollen germination and growth (Lennon et al., 1998). Upon capture by the stigmatic surface, the first contact surface between pollen and the female reproductive tissues a number of cell-cell interactions are initiated that will determine the success of sexual reproduction.

Sexual reproduction in angiosperms is complex and regulated by numerous pollen-pistil checkpoints (Dresselhaus and Franklin-Tong, 2013). After a compatible interaction between the pollen and the receptive stigma, the pollen hydrates by uptaking water from the stigma (Hiscock and Allen, 2008). The pollen grain germinates to produce a polarized structure, the pollen tube

which functions as a vehicle for the transport of sperm cells (Zhang et al., 2017). The pollen tube is in a constant exchange of signals with the female tissues and is precisely guided through signaling cues towards an ovule (Kim et al., 2003). Pollen tube competition and several signal check points imposed by the transmitting tract ensure that only one pollen tube reaches an ovule. After arrival, the pollen tube enters through the ovule funiculus and penetrates the embryo sac through the micropyle opening before growing on the surface of the synergids and eventually bursting to release the sperm cells within the interface of the two female gametes, the egg and the central cell. Double fertilization is tightly controlled and allows each sperm cell to fuse with a single female gamete. The two fusion events result in two distinct fertilization products, the zygote and the endosperm. The zygote develops into the future plant while the triploid endosperm supports embryo development (Johnson et al., 2019). Seeds are thus the result of a process that increases genetic diversity and assures the species propagation.

1.1.1 Male Gametophyte Development

Modern angiosperms use small male microspores and larger female megaspores, known as heterospory (Petersen and Burd, 2017). Male gametophyte development occurs in two phases, microsporogenesis and microgametogenesis (Ma, 2005). Diploid Pollen Mother Cells (PMC) develop within the sporogenous tissue of the anthe locules. During microsporogenesis, the PMCs undergo meiosis to produce tetrads of haploid microspores. At tthis stage the haploid microspores are connected to one another within the tetrad by the callosic cell wallsand through cytoplasmic bridges (McCormick, 2004). Thiscytoplasmic continuum within the tetrad assures synchronization of microspore development. After meiosis, the microspores enlarge in volume and size and are dependent on the surrounding anther sporogenous tissue, the tapetum, for their development (microsporogenesis). After microspore development, the callose wall that connects microspores

within the tetrads is digested by enzymes secreted by the nutrient-rich tissue in the anther, the tapetum (Scott et al., 2004). The microspores are released from the tetrad into the anther locule where they begin microgametogenesis (Scott et al., 2004). At this stage, the transcriptome of microspores undergoes drastic changes which prepare individual microspores for the following stages of pollen development and maturation (Honys and Twell, 2004). The first step during microgametogenesis is an asymmetric cell division named Pollen Mitosis I (PMI) which will form two cells with very distinct cell fates, a small generative cell (GC) and a large vegetative cell. The asymmetry of this first cell division is necessary for generative cell differentiation. Disruption of microtubules during pollen development leads to a symmetric cellular division where both daughter cells adopt a vegetative cell fate (Park et al., 1998). The *gemini pollen1* (*gem1*) is defective in nuclear migration and cytokinesis at PMI. Microspores divide symmetrically and fail to differentiate sperm cells (Park et al., 1998). After PMI, the polarized generative cell is engulfed by the vegetative cell, migrating into a central position in the pollen vegetative cell's cytoplasm (Berger and Twell, 2011). Following PMI, the vegetative cell exits the cell cycle and supports the development of the male gametes. In species with tricellular pollen, the generative cell then undergoes a second, symmetric mitotic event or Pollen Mitosis II (PMII) to produce the two sperm cells (SCs). Finally, after completion of PMII, a physical connection between the two male gametes and the vegetative pollen nucleus formed, producing the male germ unit (MGU) assemblage (Borg et al., 2009). In angiosperms pollen development is a widely conserved process, with the greatest differences being at the timing of PMII. In some species, like tomato, pollen development is paused after the first mitotic division, producing bicellular pollen. In species with bicellular type pollen, PMII occurs during pollen tube growth in the transmitting tract (Gomez et al., 2015).

DUO POLLEN 1 (DUO1) is a transcription factor which is expressed in the generative cell and is required for male gamete differentiation and progression through the cell cycle (Brownfield et al., 2009). The *duo1* mutants successfully complete microspore development and the asymmetric division at PMI, however, male gametophyte development is arrested at PMII and the generative cell fails to accomplish PMII (Durbarry et al., 2005), leading to the formation of a bicellular pollen grain containing a non-functional sperm cell-like cell (Brownfield et al., 2009).

After generative cell division and sperm cell differentiation the pollen grain is released from the anthers into the environment in a quiescent and dehydrated state. Pollen grains are then prepared to travel long distances and resist environmental stress before they land on the receptive stigma of a flower and complete double fertilization.

1.1.2 Pollination

Pollination begins when a pollen grain lands on the stigma of a compatible flower. The evolution of the pollen tube and the requirement of stigmatic germination is associated with mechanisms that prevent self-pollination, thus promoting outcrossing and genetic diversity within a population (Qiu et al., 2012). Although extensive work has been performed in pollen-stigma interactions, little is known about self-incompatibility in economically important crop species. Most crop species like maize, soybeans, and wheat are self-compatible while many fruit and vegetable species are self-incompatible. Self-incompatibility is best understood and mostly studied in the Brassicaceae family although *Arabidopsis thaliana*, a preferred model plant system for genetic studies, is self-compatible.

The first step of pollen contact with the stigma is mediated by the components existent on the pollen and papilla cell walls. The pollen coat is primarily composed of proteins and lipids. Following pollen capture by a receptive stigmatic papilla cell, the pollen coat migrates to the

interface with the stigma developing a 'foot' promotes pollen adhesion to the stigma (Bosch and Wang, 2020). Pollen-papilla interaction is necessary for pollen recognition and hydration. Incompatible pollen grains will fail to hydrate (Rozier et al., 2020), indicating that the incompatibility response occurs within the first few minutes of pollen-papilla interactions. The protein-rich pollen coat secretes the S-locus protein 11 (SP11), a cysteine-rich peptide involved in cell-cell communication and recognition (Marshall et al., 2011). SP11 binds to the papilla-expressed S-locus receptor kinase which induces a signaling cascade, that prevents hydration and germination of an incompatible pollen grain (Takayama et al., 2000). Another example of pollen-stigma incompatibility signaling is the ligand-receptor interaction of the stigmatic S-Receptor Kinase (SRK) and the pollen-expressed S-Locus Cysteine-Rich Protein (SCR) (Ivanov et al., 2010). Pollen landing on the stigma induces translocation of SCR from the pollen coat into the papilla cells (Iwano et al., 2003). Interaction between SRK and SCR is necessary for the self-incompatibility (SI) response and leads to rejection of the pollen grain (Ivanov et al., 2010). These mechanisms are examples of self-recognition where pollen grains produced in a plant are prohibited from fertilizing ovules of the same plant.

After a pollen compatible recognition step by the stigma, the pollen grain uptakes water from the stigma, hydrates and germinates, producing a pollen tube. This process is accompanied by reconstitution of the pollen membranes and remodeling of the actin cytoskeleton, leading to accumulation of actin cytoskeleton at the pollen-papilla contact site (Iwano et al., 2007). While actin is accumulating at the contact site in pollen grains, the papilla cell enriches the area just below the contact site with Ca^{2+}, with the highest concentration occurring while the pollen grain penetrates the papilla cell wall (Iwano et al., 2004). The pollen tube grows toward the base of the

papilla cell along the surface of the plasma membrane and into the style of the pistil (Bosch and Wang, 2020).

1.1.3 Pollen Tube Growth

Pollen tubes are rapidly elongating, polarized cells that undergo tip growth to perform their ultimate function, the delivery of male gametes to a single ovule. They are one of the fastest growing cells, reaching speeds of 2.7 µm/s in maize (Shamsudhin et al., 2016). To maintain this speed in the female tissue, the cytoplasm of the pollen tube is highly organized and withstands a tremendous amount of turgor pressure. Pollen tubes never divide, so to maintain the high turgor pressure, the old parts of the tube are isolated by the deposition of callose plugs (Qin et al., 2012). Pollen tubes are organized into three primary zones: the apical region, subapical region, and the basal region (Lee and Yang, 2008). The basal region contains a large vacuole that helps maintain the turgor pressure. All major organelles are carried into the apical and subapical regions via cytoplasmic streaming (de Graaf et al., 2005; Lee and Yang, 2008). Pollen tubes use a reverse fountain cytoplasmic streaming to maintain a constant supply of cell wall materials at the apical region and maintain turgor pressure within the tube (Chebli et al., 2013). The vesicle cargo is transported to the apical region of the growing pollen tube (Grebnev et al., 2017). Actin is primarily responsible for the quick transport of vesicles containing cell wall components while the largest and most important feature, the male germ unit (MGU), is transported using microtubules (Åström et al., 1995). As mentioned previously, the MGU organization is essential for double fertilization. In mutants where this connection is broken, like *GERM UNIT MALFORMED (GUM),* the vegetative nucleus migrates through the pollen tube alone. *gum* mutants had severe fertilization impacts and the mutant allele was rarely observed in the next generation (Lalanne and Twell, 2002).

Pollen tube growth is a highly dynamic process that puts immense strain on the walls of the tube. The pollen tube wall must be flexible to allow the rapid elongation of the tube but also rigid to withstand turgor pressure. The composition of the pollen tube wall is variable in the basal and subapical/apical regions. Pectin and callose compose a majority of the cell wall with little cellulose (Guan et al., 2013). The pollen tube regulates the plasticity of the cell wall by esterification of pectin. The apical region contains a high amount of methyl-esterified pectins which are subsequently de-esterified as it transitions into the basal region (Guan et al., 2013). The de-esterification of pectin allows the molecules to form calcium bridges. The de-esterified pectin produces a gel-like substance which promotes wall rigidity (Hepler et al., 2013). Calcium also plays a role as an important messenger in pollen tubes. Cytosolic Ca^{2+} is important in regulating pollen tube elongation and directional growth (Zheng et al., 2019). A gradient maintained at the tip of the pollen tube is necessary for elongation (Steinhorst and Kudla, 2013) and asymmetric enrichment of calcium at the tip promotes reorientation of the tube (Malho and Trewavas, 1996). Pollen tube growth is a complex and dynamic process. It requires both nutrients and guidance from the female tissue to complete the journey to the ovule.

1.1.4 Pollen-Pistil Interactions and Guidance

Pollen interactions within the female reproductive tract (transmitting tissue) are necessary for efficient pollen tube growth. The transmitting tract cells are surrounded by an extracellular matrix (ECM) that provides support and nutrients for pollen tube growth (Palanivelu and Preuss, 2006). The formation of water, γ-amino butyric acid (GABA), and calcium gradients direct the pollen tube through the transmitting tract (Bleckmann et al., 2014). After reaching the ovary the pollen tubes are guided towards the female gametophyte (ovule) by small range and long range signals (Palanivelu and Preuss, 2006). Guidance to the ovule is highly regulated permitting a single

pollen tube to target a single ovule, thus is considered a limiting factor for polyspermic fertilization events.

Several factors have been identified that could function as micropylar guidance factors, including GABA and D-serine (Palanivelu et al., 2003; Michard et al., 2011). Oscillations of Ca^{2+} in the pollen tube cytoplasm have been observed to be dependent on the distance between the female gametophyte and growing pollen tube, demonstrating that ovules secrete long-distance signals to communicate with pollen tubes (Iwano et al., 2012). Small peptides in the LURE protein family are secreted by synergid cells to attract a single pollen tube to the ovule (Okuda and Higashiyama, 2010). The mechanisms controlling pollen tube exit from the transmitting tract and into the funiculus are not well understood. This process is believed to be tightly regulated based on the observation that only one pollen tube is permitted to enter the funiculus of an unfertilized ovule (Bleckmann et al., 2014). The pollen tube exits the funiculus and is guided through the micropyle of the ovule during micropylar guidance (Shimizu and Okada, 2000). After entering through the micropyle the tube contacts the filiform apparatus of the synergid cells. The filiform apparatus is an invaginated, thick cell wall at the micropylar pole of the synergid cells (Bleckmann et al., 2014). The pollen tube grows along the synergid cell until its growth is arrested and the pollen tube bursts (Leydon et al., 2013).

The female gametophyte controls pollen tube bursting and reception via interactions mediated by the synergid-expressed NORTIA and FERONIA proteins (Kessler and Grossniklaus, 2011). After reception of the tube, competition between male- and female-expressed Rapid Alkalinization Factors (RALF) proteins mediate bursting. BUPS1/2 and ANX1/2 are pollen-expressed receptors localized to the tip of the pollen grain. Two RALFs (RALF4/19) are specifically expressed in the pollen tube. RALF34 is expressed in mature ovules with expression

concentrating around the micropylar pole of the synergid cell. Interactions between ANX/BUPS with male-expressed RALF4/19 inhibit bursting, but interacting with the female-expressed RALF34 promotes bursting (Ge et al., 2017).

1.1.5 Regulation of Double Fertilization

Angiosperms have evolved a unique type of fertilization called double fertilization (Berger et al., 2008). After pollen tube burst and due to the internal cytoplasmic pressure, the sperm cells are propelled to the interface between both female gametes, the egg and central cell. In contrast to animals, where microtubules seem to be required for sperm nuclei targeting (Fatema et al., 2019), plants use F-actin to assist male nucleus migration to the female nucleus (Kawashima et al., 2014). Actin coronas surround the sperm cells at pollen tube burst, before fusion of the gametes (Ye et al., 2002).

Interactions between the male and female gametes lead to recognition and eventual fusion of their plasma membranes (plasmogamy). The sperm cells remain at the interface of the female gametes for approximately 7 minutes before plasmogamy (Hamamura et al., 2011). During this time, the gametes adhere, interact, and exchange signals that activate the fusion machinery in both gametes and allow the precise targeting of the sperm cells to each of the female gametes. The molecular mechanisms and interactions controlling this process are still poorly understood. Activation of both gametes is necessary for successful fertilization. In the unicellular green algal *Chlamydomonas*, activation of the gametes is induced by the adhesion between two cells of the opposite sex (Pan and Snell, 2000). Upon activation of *Chlamydomonas* gametes, a serine protease is secreted that activates metalloproteases required to degrade the extracellular matrix surrounding each cell (Buchanan et al., 1989).

In Arabidopsis, after sperm cell arrival, the egg cell secretes a small, cysteine-rich peptide called EGG CELL 1 (EC1). EC1 binds to an unknown sperm cell receptor resulting in SC activation and re-localization of HAP2 to the SC membrane (Sprunck et al., 2012). GEX2 is a SC-specific, single-pass transmembrane protein that contains an immunoglobulin-like domain and promotes SC-female gamete adhesion (Mori et al., 2014). Fertilization in animals is also dependent on adhesion proteins containing immunoglobulin-like domains (Nishimura and L'Hernault, 2016). HAP2 mediates the plasma membrane fusion of the male and female gametes (von Besser et al., 2006). HAP2 is a widely conserved fusion protein, and the protein is hypothesized to be an ancient gamete fusion factor (Feng et al., 2018) with homologs identified in all major eukaryotic taxa except fungi (Wong and Johnson, 2010). *DMP8* and *DMP9* belong to a small gene family of unknown transmembrane proteins (Kasaras and Kunze, 2010) and were recently found to be involved in sperm cell-egg cell fusion (Cyprys et al., 2019).

One sperm cell fuse with the egg cell to form the embryo while the second fuses with the central cell to create the nourishing endosperm that supports embryo and seed development. Failure in double fertilization results in the recruitment of an additional pollen tube (polytubey) which releases an additional pair of sperm cells into the ovule (Kasahara et al., 2012). Polyspermic fusions of the egg cell are viable in plants, while excess of paternal copies in endosperm usually leads to seed abortion as a result of unbalanced parental genome dosage (Zhang et al., 2016).

In both animal and plant gametes, calcium is used as a secondary messenger during fertilization. In mice, calcium oscillations are observed in the zygote following sperm fusion with the egg. The calcium oscillations stimulate mitochondrial energy production and seem to contribute to the egg polyspermy block (Miao and Williams, 2012). In plants, the contact of sperm and egg also induce calcium oscillations. In maize, an *in vitro* fertilization system revealed that

cytoplasmic calcium oscillations are induced upon fusion of sperm and egg cell, but not by adhesion of the male and female gametes (Digonnet et al., 1997). Following sperm-egg fusion and the propagation of a calcium wave, a cell wall rapidly forms, which is thought to block additional sperm cell fusions (polyspermy block) (Antoine et al., 2001). In *Arabidopsis* cytosolic calcium changes seemed to be coordinated with pollen tube discharge in the synergids and male-female gamete fusion (Hamamura et al., 2011; Denninger et al., 2014). The functional role of these calcium spikes are unknown, but they could play a role in egg cell polyspermy block.

In *Arabidopsis*, fusion of both SCs with both female gametes are interdependent but appear to be random, in that neither SC has a preference for either the central cell or egg cell (Berger et al., 2008). The two fusion events are not equal though, the fusion of the sperm and egg cell results in the diploid embryo while the fusion with the central cell produces the triploid endosperm. Balance between the maternal and paternal gene doses in the endosperm (2:1 maternal : paternal) is critical for proper endosperm development (Lin, 1984). Disturbing this 2:1 ratio results in defects of the endosperm and can lead to seed abortion (Povilus et al., 2018).

Early zygotic development was thought for long to be strictly under maternal control and the sperm cells contributing merely with genetic information. Transcriptomic profiling of the developing zygote has shown that most of the initial transcripts required for zygotic development originate from both maternal and paternal copies. In addition to its genome, the sperm also contributes mRNAs, epigenetic factors (micro RNAs and small RNAs), and maybe proteins to the egg cell. In the endosperm, the paternal-derived *miR159* induces nuclear division in the endosperm. *miR159* targets *MYB33* and *MYB65* whose expression levels are high before fertilization but drastically decrease following sperm fusion. Interfering with the delivery of this microRNA results in severe seed abortion (Zhao et al., 2018).

In animals, it is believed that the delivery of a phospholipase, PLC ζ-1 functions as a sperm oocyte activation factor (Nozawa et al., 2018). Mice sperm lacking PLC ζ-1 can fuse with the egg cell but fail to induce the calcium oscillations and abort at one or two cell stage. *MATRILINEAL (MTL)* is a sperm cell specific phospholipase which has been shown to play a role in double fertilization in maize (Kelliher et al., 2017). It has been shown that *mtl* mutant sperm cells induce zygotic activation independent of paternal contribution (haploid induction). It is interesting that both mice and maize require male-specific phospholipase activity in order to complete successful fertilization. In *Arabidopsis* the *SHORT SUSPENSOR* (*SSP*) transcripts are expressed in sperm cells, but do not appear to be translated (Bayer et al., 2009). SSP is a membrane-associated receptor-like kinase in which the transcripts are delivered from the sperm cells into the egg cell. SSP is then translated in the zygote where it activates a YODA (YDA)/Map kinase (MPK) signaling pathway that is required to set up the apical–basal axis of the embryo. The *ssp* mutants show shorter suspensors as a result of fewer cells (Babu et al., 2013).

Although extensive research has led to the identification of gamete factors, the signaling pathways connecting these factors are unknown and proteins necessary for male-male interactions during pollen tube growth and male gamete activation remain elusive.

1.2 Function of Tetraspanins as Regulators of Intercellular Signaling

Tetraspanins (TETs) are evolutionarily conserved membrane proteins present in all multicellular organisms and seem to function as common denominators of processes involving cell-cell interactions. They function as organizers of signaling clusters at the plasma membrane (Yunta and Lazo, 2003). TETs are characterized by containing 4 transmembrane domains, intracellular N- and C-termini, one small extracellular loop (EC1), and one large extracellular loop (EC2). Animal TETs also contain a conserved CCG amino acid motif in EC2 along with other

cysteine residues that form disulfide bonds and contribute to the final structure of the protein (Termini and Gillette, 2017).

Tetraspanins are known to regulate important functions, like adhesion, through a series of complicated direct and indirect interactions. TETs regularly interact with other TETs to form homo- and hetero- dimers (Boavida et al., 2013). The dimers are formed before transport to the plasma membrane and have been detected in the Golgi (Kovalenko et al., 2004). In animals, Tetraspanins form both direct and indirect interactions with integrins (Berditchevski, 2001). Integrins are well known for their function as adhesion receptors (Horstkorte and Fuss, 2012). Integrins propagate signals through a variety of molecules, including focal adhesion kinases (FAKs) (Cary and Guan, 1999). These FAKs are also regulated by tetraspanins, and knockdown of TETs leads to a reduction in FAK phosphorylation (Yamada et al., 2008). This pathway demonstrates the complexity of tetraspanin-mediated signaling. Tetraspanins are implicated in almost every aspect of the signal propagation and removal of one tetraspanin gene can have detrimental effects on the cell. TETs are also known to directly interact with ADAM matrix metalloprotease (MMP) proteins. ADAM10, a well-studied member of the ADAM protease family, interacts with many TETs in animals like CD9, CD81, and CD82 (Arduise et al., 2008). These interactions are important in the regulation of secretion of hormones and peptides in mice

Although not direct interactors, TETs are linked to the cytoskeleton through indirect interactions. Both CD9 and CD81 function in regulating the actin cytoskeleton through their direct interaction with EWI-2 and EWI-F. The EWIs bind to exrin-radixin-moesin (ERM) which directly interact with the cytoskeleton (Berditchevski, 2001).

1.2.1 Tetraspanin-Enriched Microdomains

Tetraspanins in animals are known to be important for several biological processes like cell-cell adhesion and fusion (Hemler, 2005). They form signaling platforms that represent scaffolds of signaling proteins and are associated with microdomains. The Tetraspanin-enriched microdomain (TEM) is a functional unit located in the plasma membrane. Within the TEMs, tetraspanins mediate many different interactions, including; formation of both homo- and heterodimers (Boavida et al., 2013), interactions with other membrane proteins (Charrin et al., 2014), and interactions with lipids (Reimann et al., 2017). The size of any given TEM can range dramatically between cell types, in animals TEMs have been observed to range from 16 nm particles to areas of 400 nm^2 (Yáñez-Mó et al., 2009). Functionally related receptors are recruited to the microdomain which acts as an organized, physical unit in the bilayer (M et al., 2009). Proteomic analysis of animal TEMs shows that there are numerous categories of proteins represented in these domains including adhesion molecules, receptors/signaling molecules, membrane proteases, and proteins involved in fusion (Le Naour et al., 2006).

The plasma membrane is a heterogeneous structure composed of proteins, phospholipids, and cholesterol to name a few. The size of TEMs allows them to incorporate many different molecules which provides a mechanism to regulate signaling events and recruit functionally related receptors (Yáñez-Mó et al., 2009). Tetraspanins interact with different membrane-associated receptors at different levels of interaction which can be identified using different extraction methods (Charrin et al., 2003). The first level of interaction, which can withstand harsh detergent treatments such as Triton X-100, are direct protein-protein interactions. The direct protein interactions include those between tetraspanins as well as between TETs and another membrane protein such as metalloproteases (Hemler, 2005). The second level of interactions within TEMs are indirect interactions. Secondary interactions are stabilized by palmitoylation of

both tetraspanins and their indirect-interacting partners. These secondary partners include proteins belonging to the immunoglobulin family, adhesion molecules, and signaling enzymes (Boucheix and Rubinstein, 2001). TETs maintain their direct, first-level interactions in the absence of palmitoylation sites, but many of the secondary interactions are prevented (Berditchevski et al., 2002).

TEMs are not the only organized unit within the plasma membrane. Lipid rafts are another organized domain. Lipid rafts, similar to TEMs, are enriched in both cholesterol and sphingolipids. Although lipid rafts and TEMs show some similarities, TEMs show many critical differences which distinguish the two domains. Lipid raft interactions are disrupted when treated with Triton X-100, whereas TEMs maintain their direct protein-protein interactions. Palmitoylation of proteins in lipid rafts decreases their solubility, in comparison, TEMs rely on palmitoylation to facilitate second-level interactions. Both TEMs and lipid rafts are enriched with cholesterol and divide into low-density fractions in sucrose gradients. Finally, they are differentiated by their tolerance to cholesterol depletion. Lipid rafts are sensitive to cholesterol depletion while TEMs are resistant to depletion (Le Naour et al., 2006).

Recent publications of tetraspanins in plants have demonstrated their involvement in development and cell communication. Lipid rafts and detergent-resistant membranes have been identified in plants (Grennan, 2007), but despite established methods to identify TEMs, their presence in plants is currently unknown.

1.2.2 Tetraspanin Functions in Plants

Research of *Arabidopsis*-expressed TETs has shown their involvement in a variety of different processes including leaf development, plant immunity, and root growth. In the *A. thaliana*

genome, 17 members of this protein family were identified. Plant tetraspanins are expressed in many different cell types and show diverse expression patterns (Boavida et al., 2013).

The first TET described in detail was TET1 by Cnops et al. 2006 who identified its role in leaf development and venation. In this study, the researchers used six mutated *tet1* alleles, all of which contained mutations in the large extracellular loop of the tetraspanin. Mutation of TET1 resulted in significant decrease in mean lamina area of the first leaves and large intercellular gaps, lacking palisade and spongy cells (Cnops et al., 2006).

TET13 was identified to promote primary root growth and mutants showed reduced amounts of cells within the root meristem (Wang et al., 2015). TET13 is also involved in lateral root initiation (Wang et al., 2015). In roots and leaves, *TET5* and *TET6* function redundantly. Double *tet5/tet6* mutants showed larger leaves, increased fresh weight, and longer primary roots. The increased leaf size phenotype resulted from an increased in cell number rather than increase in cell size, suggesting that the tetraspanins could be involved in regulating the cell cycle in vegetative tissues (Wang et al., 2015).

Recently, TETs have been demonstrated to function in *A. thaliana* immunity (Cai et al., 2018). During *B. cinerea* infection *TET8* and *TET9* are induced and actively accumulate at the infection site of the cell. *TET8/9* plant-derived coated-exosomes carry small RNAs that target virulent genes in fungi (Cai et al., 2018). These findings suggest that *TET8* and *TET9* have a function in membrane fusion and cell-cell communication.

Although tetraspanins have been studied in animals for decades they have only recently begun to gain attention in the plant field. The goal of this thesis is to characterize SC-expressed tetraspanins as well as their interactors. The chapters of this thesis contribute to our understanding of cell signaling during double fertilization and to mechanisms that contribute to successful

fertilization in angiosperms. This thesis provides evidence of an essential tetraspanin-enriched microdomain which could protect fertilization factors in the SCs. Understanding how these factors interact with one another and contribute to double fertilization will provide new insights into fertilization mechanisms and contribute to advance, develop, or improve breeding strategies and seed production in economically important crops.

1.3 References

Anderson, SN, CS Johnson, J Chesnut, DS Jones, I Khanday, M Woodhouse, C Li, LJ Conrad, SD Russell, and V Sundaresan. 2017. "The Zygotic Transition Is Initiated in Unicellular Plant Zygotes With Asymmetric Activation of Parental Genomes." *Developmental cell* 43 (3). doi: 10.1016/j.devcel.2017.10.005.

Antoine, AF, JE Faure, C Dumas, and JA Feijó. 2001. "Differential Contribution of Cytoplasmic Ca2+ and Ca2+ Influx to Gamete Fusion and Egg Activation in Maize." *Nature cell biology* 3 (12). doi: 10.1038/ncb1201-1120.

Arduise, C, T Abache, L Li, M Billard, A Chabanon, A Ludwig, P Mauduit, C Boucheix, E Rubinstein, and F Le Naour. 2008. "Tetraspanins Regulate ADAM10-mediated Cleavage of TNF-alpha and Epidermal Growth Factor." *Journal of immunology (Baltimore, Md. : 1950)* 181 (10). doi: 10.4049/jimmunol.181.10.7002.

Babu, Y., T. Musielak, A. Henschen, and M. Bayer. 2013. "Suspensor Length Determines Developmental Progression of the Embryo in Arabidopsis1[W][OA]." In *Plant Physiol*, 1448-58.

Bayer, M, T Nawy, C Giglione, M Galli, T Meinnel, and W Lukowitz. 2009. "Paternal Control of Embryonic Patterning in Arabidopsis Thaliana." *Science (New York, N.Y.)* 323 (5920). doi: 10.1126/science.1167784.

Becker, J. D., L. C. Boavida, J. Carneiro, M. Haury, and J. A. Feijó. 2003. "Transcriptional Profiling of Arabidopsis Tissues Reveals the Unique Characteristics of the Pollen Transcriptome1[w]." In *Plant Physiol*, 713-25.

Berditchevski, F. 2001. "Complexes of Tetraspanins With Integrins: More Than Meets the Eye." *Journal of cell science* 114 (Pt 23).

Berditchevski, F, E Odintsova, S Sawada, and E Gilbert. 2002. "Expression of the Palmitoylation-Deficient CD151 Weakens the Association of Alpha 3 Beta 1 Integrin With the Tetraspanin-Enriched Microdomains and Affects Integrin-Dependent Signaling." *The Journal of biological chemistry* 277 (40). doi: 10.1074/jbc.M205265200.

Berger, F, and D Twell. 2011. "Germline Specification and Function in Plants." *Annual review of plant biology* 62. doi: 10.1146/annurev-arplant-042110-103824.

Berger, F., Y. Hamamura, M. Ingouff, and T. Higashiyama. 2008. "Double fertilization - caught in the act." *Trends Plant Sci* 13 (8):437-43. doi: 10.1016/j.tplants.2008.05.011.

Bleckmann, A., S. Alter, and T. Dresselhaus. 2014a. "The beginning of a seed: regulatory mechanisms of double fertilization." *Front Plant Sci* 5. doi: 10.3389/fpls.2014.00452.

Boavida, L. C., P. Qin, M. Broz, J. D. Becker, and S. McCormick. 2013. "Arabidopsis tetraspanins are confined to discrete expression domains and cell types in reproductive tissues and form homo- and heterodimers when expressed in yeast." *Plant Physiol* 163 (2):696-712. doi: 10.1104/pp.113.216598.

Borg, M, L Brownfield, and D Twell. 2009. "Male Gametophyte Development: A Molecular Perspective." *Journal of experimental botany* 60 (5). doi: 10.1093/jxb/ern355.

Borges, F, G Gomes, R Gardner, N Moreno, S McCormick, JA Feijó, and JD Becker. 2008. "Comparative Transcriptomics of Arabidopsis Sperm Cells." *Plant physiology* 148 (2). doi: 10.1104/pp.108.125229.

Bosch, M., and L. Wang. 2020. "Pollen–stigma interactions in Brassicaceae: complex communication events regulating pollen hydration." *J Exp Bot* 71 (9):2465-8. doi: 10.1093/jxb/eraa117.

Boucheix, C, and E Rubinstein. 2001. "Tetraspanins." *Cellular and molecular life sciences : CMLS* 58 (9). doi: 10.1007/PL00000933.

Brownfield, L, S Hafidh, M Borg, A Sidorova, T Mori, and D Twell. 2009. "A Plant Germline-Specific Integrator of Sperm Specification and Cell Cycle Progression." *PLoS genetics* 5 (3). doi: 10.1371/journal.pgen.1000430.

Buchanan, MJ, SH Imam, WA Eskue, and WJ Snell. 1989. "Activation of the Cell Wall Degrading Protease, Lysin, During Sexual Signalling in Chlamydomonas: The Enzyme Is Stored as an Inactive, Higher Relative Molecular Mass Precursor in the Periplasm." *The Journal of cell biology* 108 (1). doi: 10.1083/jcb.108.1.199.

Cai, Q, L Qiao, M Wang, B He, FM Lin, J Palmquist, SD Huang, and H Jin. 2018. "Plants Send Small RNAs in Extracellular Vesicles to Fungal Pathogen to Silence Virulence Genes." *Science (New York, N.Y.)* 360 (6393). doi: 10.1126/science.aar4142.

Cary, LA, and JL Guan. 1999. "Focal Adhesion Kinase in Integrin-Mediated Signaling." *Frontiers in bioscience : a journal and virtual library* 4. doi: 10.2741/cary.

Charrin, S, S Jouannet, C Boucheix, and E Rubinstein. 2014. "Tetraspanins at a Glance." *Journal of cell science* 127 (Pt 17). doi: 10.1242/jcs.154906.

Charrin, S, S Manié, M Billard, L Ashman, D Gerlier, C Boucheix, and E Rubinstein. 2003. "Multiple Levels of Interactions Within the Tetraspanin Web." *Biochemical and biophysical research communications* 304 (1). doi: 10.1016/s0006-291x(03)00545-x.

Chebli, Y., J. Kroeger, and A. Geitmann. 2013. "Transport logistics in pollen tubes." *Mol Plant* 6 (4):1037-52. doi: 10.1093/mp/sst073.

Cnops, G., P. Neyt, J. Raes, M. Petrarulo, H. Nelissen, N. Malenica, C. Luschnig, O. Tietz, F. Ditengou, K. Palme, A. Azmi, E. Prinsen, and M. Van Lijsebettens. 2006. "The TORNADO1 and TORNADO2 genes function in several patterning processes during early leaf development in Arabidopsis thaliana." *Plant Cell* 18 (4):852-66. doi: 10.1105/tpc.105.040568.

Cyprys, P., M. Lindemeier, and S. Sprunck. 2019. "Gamete fusion is facilitated by two sperm cell-expressed DUF679 membrane proteins." *Nat Plants* 5 (3):253-257. doi: 10.1038/s41477-019-0382-3.

de Graaf, B. H., A. Y. Cheung, T. Andreyeva, K. Levasseur, M. Kieliszewski, and Hm Wu. 2005. "Rab11 GTPase-Regulated Membrane Trafficking Is Crucial for Tip-Focused Pollen Tube Growth in TobaccoW." In *Plant Cell*, 2564-79.

Delwiche, C. F., and E. D. Cooper. 2015. "The Evolutionary Origin of a Terrestrial Flora." *Curr Biol* 25 (19):R899-910. doi: 10.1016/j.cub.2015.08.029.

Denninger, P, A Bleckmann, A Lausser, F Vogler, T Ott, DW Ehrhardt, WB Frommer, S Sprunck, T Dresselhaus, and G Grossmann. 2014. "Male-female Communication Triggers Calcium Signatures During Fertilization in Arabidopsis." *Nature communications* 5. doi: 10.1038/ncomms5645.

Digonnet, C, D Aldon, N Leduc, C Dumas, and M Rougier. 1997. "First Evidence of a Calcium Transient in Flowering Plants at Fertilization." *Development (Cambridge, England)* 124 (15).

Doebley, J. F., B. S. Gaut, and B. D. Smith. 2006. "The molecular genetics of crop domestication." *Cell* 127 (7):1309-21. doi: 10.1016/j.cell.2006.12.006.

Dresselhaus, T, and N Franklin-Tong. 2013. "Male-female Crosstalk During Pollen Germination, Tube Growth and Guidance, and Double Fertilization." *Molecular plant* 6 (4). doi: 10.1093/mp/sst061.

Durbarry, A., I. Vizir, and D. Twell. 2005. "Male Germ Line Development in Arabidopsis. duo pollen Mutants Reveal Gametophytic Regulators of Generative Cell Cycle Progression1[w]." In *Plant Physiol*, 297-307.

Fatema, U., M. F. Ali, Z. Hu, A. J. Clark, and T. Kawashima. 2019. "Gamete Nuclear Migration in Animals and Plants." *Front Plant Sci* 10. doi: 10.3389/fpls.2019.00517.

Feng, J., X. Dong, J. Pinello, J. Zhang, C. Lu, R. E. Iacob, J. R. Engen, W. J. Snell, and T. A. Springer. 2018. "Fusion surface structure, function, and dynamics of gamete fusogen HAP2." *Elife* 7. doi: 10.7554/eLife.39772.

Ge, Z., T. Bergonci, Y. Zhao, Y. Zou, S. Du, M. C. Liu, X. Luo, H. Ruan, L. E. Garcia-Valencia, S. Zhong, S. Hou, Q. Huang, L. Lai, D. S. Moura, H. Gu, J. Dong, H. M. Wu, T. Dresselhaus, J. Xiao, A. Y. Cheung, and L. J. Qu. 2017. "Arabidopsis pollen tube integrity and sperm release are regulated by RALF-mediated signaling." *Science* 358 (6370):1596-1600. doi: 10.1126/science.aao3642.

Gomez, J. F., B. Talle, and Z. A. Wilson. 2015. "Anther and pollen development: A conserved developmental pathway." *J Integr Plant Biol* 57 (11):876-91. doi: 10.1111/jipb.12425.

Grebnev, G., M. Ntefidou, and B. Kost. 2017. "Secretion and Endocytosis in Pollen Tubes: Models of Tip Growth in the Spot Light." *Front Plant Sci* 8. doi: 10.3389/fpls.2017.00154.

Grennan, A. K. 2007. "Lipid Rafts in Plants." In *Plant Physiol*, 1083-5.

Gross-Hardt, R, C Kägi, N Baumann, JM Moore, R Baskar, WB Gagliano, G Jürgens, and U Grossniklaus. 2007. "LACHESIS Restricts Gametic Cell Fate in the Female Gametophyte of Arabidopsis." *PLoS biology* 5 (3). doi: 10.1371/journal.pbio.0050047.

Guan, Y., J. Guo, H. Li, and Z. Yang. 2013. "Signaling in pollen tube growth: crosstalk, feedback, and missing links." *Mol Plant* 6 (4):1053-64. doi: 10.1093/mp/sst070.

Hamamura, Y, C Saito, C Awai, D Kurihara, A Miyawaki, T Nakagawa, MM Kanaoka, N Sasaki, A Nakano, F Berger, and T Higashiyama. 2011. "Live-cell Imaging Reveals the Dynamics of Two Sperm Cells During Double Fertilization in Arabidopsis Thaliana." *Current biology : CB* 21 (6). doi: 10.1016/j.cub.2011.02.013.

Hemler, M. E. 2005. "Tetraspanin functions and associated microdomains." *Nat Rev Mol Cell Biol* 6 (10):801-11. doi: 10.1038/nrm1736.

Hepler, PK, CM Rounds, and LJ Winship. 2013. "Control of Cell Wall Extensibility During Pollen Tube Growth." *Molecular plant* 6 (4). doi: 10.1093/mp/sst103.

Hiscock, SJ, and AM Allen. 2008. "Diverse Cell Signalling Pathways Regulate Pollen-Stigma Interactions: The Search for Consensus." *The New phytologist* 179 (2). doi: 10.1111/j.1469-8137.2008.02457.x.

Honys, D., and D. Twell. 2004. "Transcriptome analysis of haploid male gametophyte development in Arabidopsis." In *Genome Biol*, R85.

Horstkorte, Rüdiger, and Babette Fuss. 2012. "Chapter 9 - Cell Adhesion Molecules." In *Basic Neurochemistry (Eighth Edition)*, edited by Scott T. Brady, George J. Siegel, R. Wayne Albers and Donald L. Price, 165-179. New York: Academic Press.

Irish, V. 2017. "The ABC model of floral development." *Curr Biol* 27 (17):R887-r890. doi: 10.1016/j.cub.2017.03.045.

Ivanov, R., I. Fobis-Loisy, and T. Gaude. 2010. "When no means no: guide to Brassicaceae self-incompatibility." *Trends Plant Sci* 15 (7):387-94. doi: 10.1016/j.tplants.2010.04.010.

Iwano, M, H Shiba, K Matoba, T Miwa, M Funato, T Entani, P Nakayama, H Shimosato, A Takaoka, A Isogai, and S Takayama. 2007. "Actin Dynamics in Papilla Cells of Brassica Rapa During Self- And Cross-Pollination." *Plant physiology* 144 (1). doi: 10.1104/pp.106.095273.

Iwano, M, H Shiba, T Miwa, FS Che, S Takayama, T Nagai, A Miyawaki, and A Isogai. 2004. "Ca2+ Dynamics in a Pollen Grain and Papilla Cell During Pollination of Arabidopsis." *Plant physiology* 136 (3). doi: 10.1104/pp.104.046961.

Iwano, M., Q. A. Ngo, T. Entani, H. Shiba, T. Nagai, A. Miyawaki, A. Isogai, U. Grossniklaus, and S. Takayama. 2012. "Cytoplasmic Ca2+ changes dynamically during the interaction of the pollen tube with synergid cells." *Development* 139 (22):4202-9. doi: 10.1242/dev.081208.

Iwano, M., H. Shiba, M. Funato, H. Shimosato, S. Takayama, and A. Isogai. 2003. "Immunohistochemical studies on translocation of pollen S-haplotype determinant in self-incompatibility of Brassica rapa." *Plant Cell Physiol* 44 (4):428-36. doi: 10.1093/pcp/pcg056.

Johnson, M. A., J. F. Harper, and R. Palanivelu. 2019. "A Fruitful Journey: Pollen Tube Navigation from Germination to Fertilization." *Annu Rev Plant Biol* 70:809-837. doi: 10.1146/annurev-arplant-050718-100133.

Kasahara, R., Maruyama D., Hamamura Y., Sakakibara T., Twell D., Higashiyama T. 2012. "Fertilization recovery after defective sperm cell release in Arabidopsis." *Curr Biol* 22 (12):1084-9. doi: 10.1016/j.cub.2012.03.069.

Kasaras, A, and R Kunze. 2010. "Expression, Localisation and Phylogeny of a Novel Family of Plant-Specific Membrane Proteins." *Plant biology* 12 Suppl 1. doi: 10.1111/j.1438-8677.2010.00381.x.

Kawashima, T., D. Maruyama, M. Shagirov, J. Li, Y. Hamamura, R. Yelagandula, Y. Toyama, and F. Berger. 2014. "Dynamic F-actin movement is essential for fertilization in Arabidopsis thaliana." *Elife* 3. doi: 10.7554/eLife.04501.

Kelliher, T, D Starr, L Richbourg, S Chintamanani, B Delzer, ML Nuccio, J Green, Z Chen, J McCuiston, W Wang, T Liebler, P Bullock, and B Martin. 2017. "MATRILINEAL, a Sperm-Specific Phospholipase, Triggers Maize Haploid Induction." *Nature* 542 (7639). doi: 10.1038/nature20827.

Kessler, S. A., and U. Grossniklaus. 2011. "She's the boss: signaling in pollen tube reception." *Curr Opin Plant Biol* 14 (5):622-7. doi: 10.1016/j.pbi.2011.07.012.

Kim, S, JC Mollet, J Dong, K Zhang, SY Park, and EM Lord. 2003. "Chemocyanin, a Small Basic Protein From the Lily Stigma, Induces Pollen Tube Chemotropism." *Proceedings of the National Academy of Sciences of the United States of America* 100 (26). doi: 10.1073/pnas.2533800100.

Kovalenko, O. V., X. Yang, T. V. Kolesnikova, and M. E. Hemler. 2004. "Evidence for specific tetraspanin homodimers: inhibition of palmitoylation makes cysteine residues available for cross-linking." In *Biochem J*, 407-17.

Lalanne, E, and D Twell. 2002. "Genetic Control of Male Germ Unit Organization in Arabidopsis." *Plant physiology* 129 (2). doi: 10.1104/pp.003301.

Le Naour, F, M André, C Boucheix, and E Rubinstein. 2006. "Membrane Microdomains and Proteomics: Lessons From Tetraspanin Microdomains and Comparison With Lipid Rafts." *Proteomics* 6 (24). doi: 10.1002/pmic.200600282.

Lee, Y. J., and Z. Yang. 2008. "Tip growth: Signaling in the apical dome." *Curr Opin Plant Biol* 11 (6):662-71. doi: 10.1016/j.pbi.2008.10.002.

Lennon, Kristen A., Stéphane Roy, Peter K. Hepler, and E. M. Lord. 1998. "The structure of the transmitting tissue of Arabidopsis thaliana (L.) and the path of pollen tube growth." *Sexual Plant Reproduction* 11 (1):49-59. doi: 10.1007/s004970050120.

Leydon, AR, KM Beale, K Woroniecka, E Castner, J Chen, C Horgan, R Palanivelu, and MA Johnson. 2013. "Three MYB Transcription Factors Control Pollen Tube Differentiation Required for Sperm Release." *Current biology : CB* 23 (13). doi: 10.1016/j.cub.2013.05.021.

Lin, BY. 1984. "Ploidy Barrier to Endosperm Development in Maize." *Genetics* 107 (1).

Ma, H. 2005. "Molecular Genetic Analyses of Microsporogenesis and Microgametogenesis in Flowering Plants." *Annual review of plant biology* 56. doi: 10.1146/annurev.arplant.55.031903.141717.

Malho, R., and A. J. Trewavas. 1996. "Localized Apical Increases of Cytosolic Free Calcium Control Pollen Tube Orientation." In *Plant Cell*, 1935-49.

Marshall, E, LM Costa, and J Gutierrez-Marcos. 2011. "Cysteine-rich Peptides (CRPs) Mediate Diverse Aspects of Cell-Cell Communication in Plant Reproduction and Development." *Journal of experimental botany* 62 (5). doi: 10.1093/jxb/err002.

McCormick, S. 2004. "Control of male gametophyte development." *Plant Cell* 16 Suppl:S142-53. doi: 10.1105/tpc.016659.

Miao, Y. L., and C. J. Williams. 2012. "Calcium signaling in mammalian egg activation and embryo development: Influence of subcellular localization." *Mol Reprod Dev* 79 (11):742-56. doi: 10.1002/mrd.22078.

Michard, E, PT Lima, F Borges, AC Silva, MT Portes, JE Carvalho, M Gilliham, LH Liu, G Obermeyer, and JA Feijó. 2011. "Glutamate Receptor-Like Genes Form Ca2+ Channels in Pollen Tubes and Are Regulated by Pistil D-serine." *Science (New York, N.Y.)* 332 (6028). doi: 10.1126/science.1201101.

Mori, T., T. Igawa, G. Tamiya, S. Y. Miyagishima, and F. Berger. 2014. "Gamete attachment requires GEX2 for successful fertilization in Arabidopsis." *Curr Biol* 24 (2):170-5. doi: 10.1016/j.cub.2013.11.030.

Niklas, K. J., and U. Kutschera. 2010. "The evolution of the land plant life cycle." *New Phytol* 185 (1):27-41. doi: 10.1111/j.1469-8137.2009.03054.x.

Nishimura, H, and SW L'Hernault. 2016. "Gamete Interactions Require Transmembranous Immunoglobulin-Like Proteins With Conserved Roles During Evolution." *Worm* 5 (3). doi: 10.1080/21624054.2016.1197485.

Nozawa, K, Y Satouh, T Fujimoto, A Oji, and M Ikawa. 2018. "Sperm-borne Phospholipase C zeta-1 Ensures Monospermic Fertilization in Mice." *Scientific reports* 8 (1). doi: 10.1038/s41598-018-19497-6.

Okuda, S., and T. Higashiyama. 2010. "Pollen tube guidance by attractant molecules: LUREs." *Cell Struct Funct* 35 (1):45-52. doi: 10.1247/csf.10003.

Pacini, E. 2015. "Pollination☆." In *Reference Module in Earth Systems and Environmental Sciences*. Elsevier.

Palanivelu, R, L Brass, AF Edlund, and D Preuss. 2003. "Pollen Tube Growth and Guidance Is Regulated by POP2, an Arabidopsis Gene That Controls GABA Levels." *Cell* 114 (1). doi: 10.1016/s0092-8674(03)00479-3.

Palanivelu, Ravishankar, and Daphne Preuss. 2006. "Distinct short-range ovule signals attract or repel Arabidopsis thaliana pollen tubes in vitro." *BMC Plant Biology* 6 (1):1-9. doi: doi:10.1186/1471-2229-6-7.

Pan, J, and WJ Snell. 2000. "Signal Transduction During Fertilization in the Unicellular Green Alga, Chlamydomonas." *Current opinion in microbiology* 3 (6). doi: 10.1016/s1369-5274(00)00146-6.

Park, SK, R Howden, and D Twell. 1998. "The Arabidopsis Thaliana Gametophytic Mutation Gemini pollen1 Disrupts Microspore Polarity, Division Asymmetry and Pollen Cell Fate." *Development (Cambridge, England)* 125 (19).

Petersen, Kurt B., and Martin Burd. 2017. "Why did heterospory evolve?" *Biological Reviews* 92 (3):1739-1754. doi: 10.1111/brv.12304.

Povilus, RA, PK Diggle, and WE Friedman. 2018. "Evidence for Parent-Of-Origin Effects and Interparental Conflict in Seeds of an Ancient Flowering Plant Lineage." *Proceedings. Biological sciences* 285 (1872). doi: 10.1098/rspb.2017.2491.

Qin, P, D Ting, A Shieh, and S McCormick. 2012. "Callose Plug Deposition Patterns Vary in Pollen Tubes of Arabidopsis Thaliana Ecotypes and Tomato Species." *BMC plant biology* 12. doi: 10.1186/1471-2229-12-178.

Qiu, Yin-Long, Alexander B. Taylor, and Hilary A. McManus. 2012. "Evolution of the life cycle in land plants." *Journal of Systematics and Evolution* 50 (3):171-194. doi: 10.1111/j.1759-6831.2012.00188.x.

Rajcan, I., J. G. Boersma, and E. J. Shaw. 2011. "4.11 - Plant Genetic Techniques: Plant Breeder's Toolbox." In *Comprehensive Biotechnology (Second Edition)*, edited by Murray Moo-Young, 133-147. Burlington: Academic Press.

Reimann, R., B. Kost, and J. Dettmer. 2017. "TETRASPANINs in Plants." *Front Plant Sci* 8. doi: 10.3389/fpls.2017.00545.

Rozier, F, L Riglet, C Kodera, V Bayle, E Durand, J Schnabel, T Gaude, and I Fobis-Loisy. 2020. "Live-cell Imaging of Early Events Following Pollen Perception in Self-Incompatible Arabidopsis Thaliana." *Journal of experimental botany* 71 (9). doi: 10.1093/jxb/eraa008.

Scott, RJ, M Spielman, and HG Dickinson. 2004. "Stamen Structure and Function." *The Plant cell* 16 Suppl (Suppl). doi: 10.1105/tpc.017012.

Shamsudhin, N., N. Laeubli, H. B. Atakan, H. Vogler, C. Hu, W. Haeberle, A. Sebastian, U. Grossniklaus, and B. J. Nelson. 2016. "Massively Parallelized Pollen Tube Guidance and Mechanical Measurements on a Lab-on-a-Chip Platform." In *PLoS One*.

Shimizu, KK, and K Okada. 2000. "Attractive and Repulsive Interactions Between Female and Male Gametophytes in Arabidopsis Pollen Tube Guidance." *Development (Cambridge, England)* 127 (20).

Sprunck, S. 2020. "Twice the Fun, Double the Trouble: Gamete Interactions in Flowering Plants." *Current opinion in plant biology* 53. doi: 10.1016/j.pbi.2019.11.003.

Sprunck, S., S. Rademacher, F. Vogler, J. Gheyselinck, U. Grossniklaus, and T. Dresselhaus. 2012. "Egg cell-secreted EC1 triggers sperm cell activation during double fertilization." *Science* 338 (6110):1093-7. doi: 10.1126/science.1223944.

Steinhorst, L., and J. Kudla. 2013. "Calcium - a central regulator of pollen germination and tube growth." *Biochim Biophys Acta* 1833 (7):1573-81. doi: 10.1016/j.bbamcr.2012.10.009.

Takayama, S, H Shiba, M Iwano, H Shimosato, FS Che, N Kai, M Watanabe, G Suzuki, K Hinata, and A Isogai. 2000. "The Pollen Determinant of Self-Incompatibility in Brassica Campestris." *Proceedings of the National Academy of Sciences of the United States of America* 97 (4). doi: 10.1073/pnas.040556397.

Termini, C. M., and J. M. Gillette. 2017. "Tetraspanins Function as Regulators of Cellular Signaling." *Front Cell Dev Biol* 5:34. doi: 10.3389/fcell.2017.00034.

Thorne, Robert F. 2002. "How many species of seed plants are there?" *TAXON* 51 (3):511-512. doi: 10.2307/1554864.

von Besser, K., A. C. Frank, M. A. Johnson, and D. Preuss. 2006. "Arabidopsis HAP2 (GCS1) is a sperm-specific gene required for pollen tube guidance and fertilization." *Development* 133 (23):4761-9. doi: 10.1242/dev.02683.

Wang, F., A. Muto, J. Van de Velde, P. Neyt, K. Himanen, K. Vandepoele, and M. Van Lijsebettens. 2015. "Functional Analysis of the Arabidopsis TETRASPANIN Gene Family in Plant Growth and Development1[OPEN]." In *Plant Physiol*, 2200-14.

Wong, JL, and MA Johnson. 2010. "Is HAP2-GCS1 an Ancestral Gamete Fusogen?" *Trends in cell biology* 20 (3). doi: 10.1016/j.tcb.2009.12.007.

Wuest, SE, K Vijverberg, A Schmidt, M Weiss, J Gheyselinck, M Lohr, F Wellmer, J Rahnenführer, C von Mering, and U Grossniklaus. 2010. "Arabidopsis Female Gametophyte Gene Expression Map Reveals Similarities Between Plant and Animal Gametes." *Current biology : CB* 20 (6). doi: 10.1016/j.cub.2010.01.051.

Yadegari, R, and GN Drews. 2004. "Female Gametophyte Development." *The Plant cell* 16 Suppl (Suppl). doi: 10.1105/tpc.018192.

Yamada, M, Y Sumida, A Fujibayashi, K Fukaguchi, N Sanzen, R Nishiuchi, and K Sekiguchi. 2008. "The Tetraspanin CD151 Regulates Cell Morphology and Intracellular Signaling on laminin-511." *The FEBS journal* 275 (13). doi: 10.1111/j.1742-4658.2008.06481.x.

Ye, XL, EC Yeung, and SY Zee. 2002. "Sperm Movement During Double Fertilization of a Flowering Plant, Phaius Tankervilliae." *Planta* 215 (1). doi: 10.1007/s00425-002-0736-2.

Yunta, M, and PA Lazo. 2003. "Tetraspanin Proteins as Organisers of Membrane Microdomains and Signalling Complexes." *Cellular signalling* 15 (6). doi: 10.1016/s0898-6568(02)00147-x.

Yáñez-Mó, M, O Barreiro, M Gordon-Alonso, M Sala-Valdés, and F Sánchez-Madrid. 2009. "Tetraspanin-enriched Microdomains: A Functional Unit in Cell Plasma Membranes." *Trends in cell biology* 19 (9). doi: 10.1016/j.tcb.2009.06.004.

Zhang, Hy, M. Luo, S. D. Johnson, Xw Zhu, L. Liu, F. Huang, Yt Liu, Pz Xu, and Xj Wu. 2016. "Parental Genome Imbalance Causes Post-Zygotic Seed Lethality and Deregulates Imprinting in Rice." In *Rice (N Y)*.

Zhang, J, Q Huang, S Zhong, A Bleckmann, J Huang, X Guo, Q Lin, H Gu, J Dong, T Dresselhaus, and LJ Qu. 2017. "Sperm Cells Are Passive Cargo of the Pollen Tube in Plant Fertilization." *Nature plants* 3. doi: 10.1038/nplants.2017.79.

Zhao, P, X Zhou, K Shen, Z Liu, T Cheng, D Liu, Y Cheng, X Peng, and MX Sun. 2019. "Two-Step Maternal-to-Zygotic Transition With Two-Phase Parental Genome Contributions." *Developmental cell* 49 (6). doi: 10.1016/j.devcel.2019.04.016.

Zhao, Youshang, Songyun Wang, Wenye Wu, Lei Li, Ting Jiang, and Binglian Zheng. 2018. "Clearance of maternal barriers by paternal miR159 to initiate endosperm nuclear division in Arabidopsis." *Nature Communications* 9 (1):5011. doi: 10.1038/s41467-018-07429-x.

Zheng, R. H., S. D. Su, H. Xiao, and H. Q. Tian. 2019. "Calcium: A Critical Factor in Pollen Germination and Tube Elongation." In *Int J Mol Sci*.

Åström, Helena, Outi Sorri, and Marjatta Raudaskoski. 1995. "Role of microtubules in the movement of the vegetative nucleus and generative cell in tobacco pollen tubes." *Sexual Plant Reproduction* 8 (2):61-69. doi: 10.1007/BF00230890.

CHAPTER 2. FUNCTION OF TETRASPANIN-ENRICHED DOMAINS IN SPERM CELLS

2.1 Abstract

In animal cells, Tetraspanins (TETs) function as membrane scaffold molecules forming the so-called Tetraspanin-Enriched Microdomains (TEMs) at the cell surface. These microdomains are unique in their composition and functions, representing clusters of signaling proteins, lipids and other associated subcellular components which are anchored by TETs to the cell surface. In Arabidopsis, *TET11* and *TET12* are expressed specifically in the plasma membrane of sperm cells (SCs) localizing in a polarized manner to the sperm cell-sperm cell (SC-SC) adhesion interface. However, the biological meaning and function of this specific cellular localization is currently unknown. In this chapter, we examined the spatial organization and quantified the distribution of TETs and other known factors at the sperm cell surface using spinning disk microscopy. To determine the function of *TET12* and address a possible genetic redundancy with *TET11* in sperm cells and during double fertilization, we used CRISPR/Cas9 gene editing technology to generate *TET12* mutant lines in wild type and in the background of *TET11* knockout T-DNA insertion mutant. Our results provide convincing evidence for the existence of a Tetraspanin-enriched microdomain at the adhesion interface of SCs. We determined that the SC-specific factors *GEX2*, *HAP2, JANUS2(DMP9),* localize at the SC-SC interface with a similar pattern, suggesting that TEMs may function as potential signaling platforms in SCs. In agreement with these results, our preliminary analysis of *TET12* CRISPR lines, indicate that *TET12* perform essential functions in double fertilization.

2.2 Introduction

2.2.1 Plasma Membrane Microdomains

The plasma membrane, also known as the cell membrane, is a physical barrier that encloses the cell and protects the intracellular components from the external environment. The plasma membrane is a thin semi-permeable membrane consisting of a lipid bilayer with associated lipids and proteins (Cacas et al., 2012). The embedded molecules allow cells to sense and respond to the extracellular signals, which is essential to maintain cell homeostasis also contributing to the overall tissue and organism balance (Qiu et al., 2003; Blazek et al., 2015).

Most cells show some form of asymmetry in their shape or organization of components. The organization of the plasma membrane is fundamental for cellular signaling, transport of molecules, and cellular adhesion (Alexandersson et al., 2004). While proteins can randomly distribute across the membrane, a growing body of evidence supports the hypothesis that proteins are organized in complexes, can aggregate into clusters, form membrane gradients, or establish cell polarity (Simons and Toomre, 2000). The spatial organization of proteins and lipids in membranes is thus tightly linked to cell functions and can be affected by external signals or physiological conditions (Marhava et al., 2020).

In both animals and plants, there are plenty of examples of asymmetrically distributed proteins in polarized cells. In animal cells such as neurons, membrane proteins are polarized to the axon and dendrite regions where they facilitate communication with other nearby cells (Bentley and Banker, 2016). In plant cells, the auxin transporters PIN1 and PIN2 are polarly localized to either the basal or apical region of the root cortex and epidermal cells (Wisniewska et al., 2006). In the root cortex tissue, both PIN1 and PIN2 localize to the basal region of the cell while in epidermal cells PIN1 is specifically localized to the basal area and PIN2 is found in the apical

region. This asymmetry is important to regulate auxin efflux throughout the meristematic tissues of the plant (Wisniewska et al., 2006). The mobilization of proteins across subcellular compartments of the cell can be highly dynamic. For instance, the Mildew Resistance Locus-O membrane protein NORTIA (NTA) is redistributed from Golgi-associated compartments to the membrane-rich region of the synergid filiform apparatus upon pollen tube reception (Yuan et al., 2020).

The formation of clusters containing membrane proteins (nano- and micro-domains) depend on many variables, including their affinity to specific lipid compositions (e.g. lipid rafts) (Brown and London, 1998; Hooper, 1999), protein-protein interactions (e.g. tetraspanin domains) (Harder et al., 1998), and constraints imposed by the cytoskeleton (Holowka et al., 2000). Tetraspanin-enriched microdomains (TEM) localized at the cell surface are characterized by unique lipid and protein compositions (Yáñez-Mó et al., 2009). Tetraspanins (TETs) are known to function as 'master organizers' of membranes interacting with each other, other membrane proteins, and signaling molecules in a cell-type specific manner. Thus, specific Tetraspanin signaling platforms can regulate different cellular functions in different cell types (Reimann et al., 2017).

Although evidence of membrane microdomains in plants is not as abundant when compared to animals, there is convincing data to support the presence of protein clusters within the plasma membrane of plant cells. Some examples come from the study of root hairs, pollen tubes, embryogenesis, and leaf primordia initiation (Raggi et al., 2020). For instance, the aquaporin protein PIP2;1, an integral membrane protein that regulates water transport across the plasma membrane of root cells (Li et al., 2011) and SUT1, a potato sucrose transporter (Krügel et al., 2008) localize within clusters on the plasma membrane. SUT1 membrane clusters range from 200-300

nm in size and are associated with detergent-resistant membrane (DRM) fractions (Krügel et al., 2008). The ability to detect heterogeneous distributions of membrane proteins at nano or microscale levels using quantitative approaches is therefore critical to understand the composition of organized membrane signaling platforms, their regulation, and the dependency of particular signaling events.

2.2.2 Expression of Tetraspanins in Plant Gametes

In animal systems, Tetraspanins (TETs) are recognized as a major cell surface scaffold molecule, functioning as a facilitator of numerous biological processes involving cell-cell interactions (Hemler, 2005). In *Arabidopsis thaliana* 17 members were identified and their expression patterns characterized in detail in reproductive (Boavida et al., 2013) and vegetative tissues (Wang et al., 2015). In reproductive tissues, TET members show a cell-type specific expression, with different TET members showing overlapping patterns (Boavida et al., 2013). In addition, their expression patterns are regulated during pollination, pollen tube growth, and

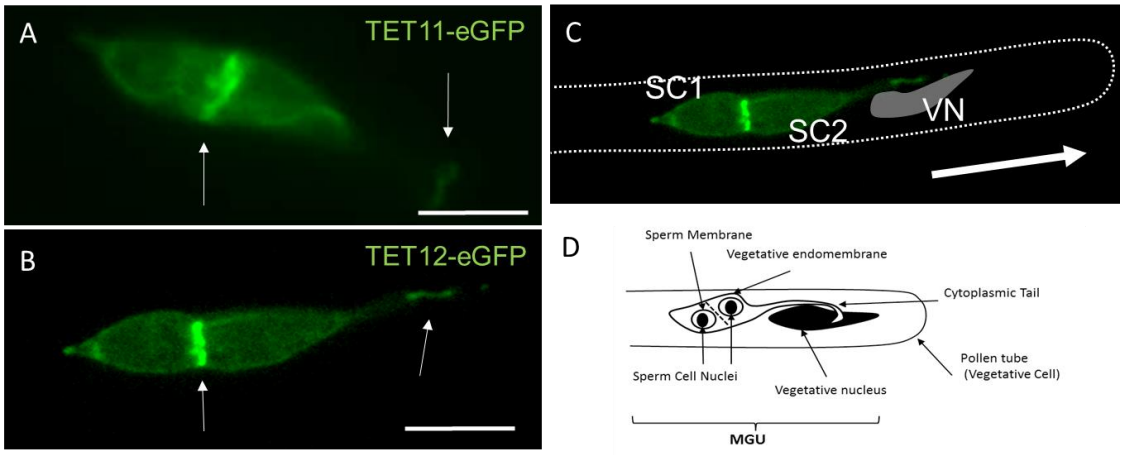

Figure 2.1. Expression of Tetraspanins in sperm cells and Male Germ Unit (MGU) organization within the pollen tube. Representative fluorescence images of (A) translational GFP fusion of *TET11* (*TET11-GFP*); (B) translational GFP fusion of *TET12* (*TET12-GFP*); (C) Representation of positioning of sperm cells (SC) within a pollen tube and association with Vegetative Nucleus (VN); (D) Graphical representation of MGU assembly. Arrows in A and B point to location of adhesion domain between SCs and cytoplasmic tail extending from one of the SCs to the VN. Arrow in C indicates direction of pollen tube growth. Scale bars: 5 µm. *Adapted from Boavida et al. (2013).*

fertilization. For instance, *AtTET8*/*AtTET9* are expressed in egg and central cell while *AtTET11*/*AtTET12* are expressed in sperm cells (SCs). As Arabidopsis tetraspanins are known to form both homo- and hetero-dimers (Boavida et al., 2013) these two pairs of gamete-expressed *TETs* are excellent candidates to investigate possible functions during double fertilization.

TET8 is induced upon fertilization, localizing at the plasma membrane of the zygote, while *TET9* is expressed in all female gametophytic cells (synergids, egg cell, central cell, and antipodals) before fertilization. *TET9* is evenly distributed at the plasma membrane of synergids and at the egg cell surface, while in the central cell *TET9* localizes in unknown, intracellular organelles (Boavida et al., 2013). *TET9* is mobilized to a restricted domain on the membrane surface of the egg cell upon pollination and is internalized after fertilization (Leonor Boavida, *unpublished results*). However, the role and dynamics of the expression patterns and the biological meaning for this regulation in double fertilization is still not understood.

AtTET11 and *AtTET12* are specifically expressed in sperm cells and their localization pattern is unique. Upon pollen germination *TET11*/*TET12* mobilize to a membrane domain that physically connects the plasma membrane of both SCs (Fig 2.1). Plant gametes lack structural support from cell walls found in other plant cells; thus, their cell surfaces are flexible and cell-cell interactions between gametes could occur directly across their plasma membranes. Sperm cells have their individual membranes, which do not directly face the cytoplasm of the pollen vegetative cell (Fig. 2.2) (Leonor Boavida, *unpublished results*). Prior to Pollen Mitosis II (PMII), an outer membrane of vegetative origin engulfs the generative cell. The division of the generative cell leads to the formation of two twin sperm cells which contain their own membranes (Fig. 2.2B-D) and are both enclosed by an outer vegetative membrane. The sperm cells remain connected by an adhesion domain. The localization of *TET11*/*TET12* appears polarized to the adhesion domain

between adjacent SCs (Fig. 2.1A and B). This domain is remarkably stable and is maintained along the entire journey of pollen tube growth across the female tissues towards an ovule (around 8 hours). Transmission electron microscopy reveals that sperm cell plasma membranes do not seem to be in direct contact at this SC-SC interface, but instead are separated by an interstitial space of

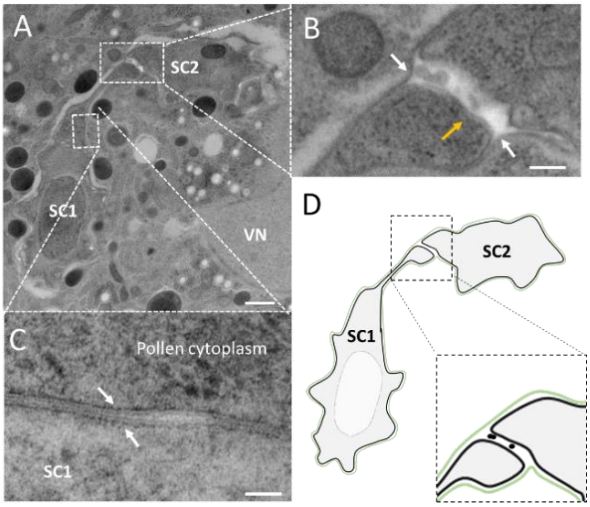

Figure 2.2. Transmission electron microscopy of a pollen grain showing association of Sperm Cells (SC) to the Vegetative Nucleus (VN). (A) Overview of MGU with Sperm cells (SC1 and SC2) and VN. Scale bar 500nm. Dashed boxes are insets of B and C. (B) Inset shown in A of sperm cell-sperm cell adhesion interface. White arrows point to outer vegetative cell membrane, yellow arrow point to inner SC plasma membrane. Scale bar 100nm. (C) Inset of A showing detail of double membrane surrounding the Sperm Cell 1 (SC1), white arrows point to outer vegetative membrane and inner sperm cell membrane. Scale bar 50nm. (D) Graphical representation of A, showing vegetative membrane in green and sperm cell membrane in black. Inset with detail of double membranes at the SC interface and at the sperm cell surface. Image acquired by Leonor Boavida.

50-100 nm (Fig. 2.2B). Although the exact composition of this interface is unknown, it is possible that direct protein-protein interactions across the plasma membrane interface could facilitate adhesion and communication between the twin sperm cells. A cytoplasmic extension connects a single SC to the Vegetative Nucleus (VN) forming the Male Germ Unit (MGU) assembly (Fig. 2.1D).

Upon delivery into the embryo sac, the sperm cells are propelled to the interface between the egg and central cell, remaining attached for a few minutes. Cellular communication and recognition between male and female gametes occur during this period. The SCs then separate and precisely fuse with each of the female gametes (Hamamura et al., 2011). The signaling mechanisms leading to sperm-sperm cell adhesion and their regulated separation are some of the most critical events in double fertilization, yet no molecular components or mechanisms are known.

While the MGU organization was reported in several plant species, the relevance of these cellular associations remains unknown. The most prevalent hypothesis is that the adhesion contacts between SCs and the pollen Vegetative Nucleus (VN) are essential to assure the simultaneous delivery of the sperm cells into the embryo sac, thus facilitating double fertilization (McCue et al., 2011).

The fact that in animal cells, Tetraspanins interact with specific lipids and proteins in the so-called TET-enriched microdomains (TEM), led us to hypothesize that polarized localization of TETs in sperm cells reflect the spatial organization of signaling and adhesion components. A second possible hypothesis is that this membrane domain functions as a "protective" environment for fertilization factors during pollen tube growth. Two recently discovered *TET11/TET12* interactors, *DMP8/9 (JANUS1/2)* seem to support the hypothesis that TET-JANUS complexes are involved in stabilizing adhesion factors at the SC surface. To test these hypotheses, we quantified and analyzed the distribution patterns of TETs and known signaling factors at the sperm cell surface and within the SC-SC adhesion domain.

2.3 Materials and Methods

2.3.1 Plant Material and Growth Conditions

Mutant lines and ecotypes if not otherwise indicated were obtained from ABRC stock center (https://abrc.osu.edu/). Arabidopsis seeds were surface sterilized using the vapor phase methodology with chlorine gas. Briefly, seeds were aliquoted into 1.5mL eppendorf tubes at ~ 30µL volume. The eppendorf tubes containing the seeds were placed open in a desiccator located in a fume hood. Three ml of concentrated HCl was quickly added to a beaker containing 50 mL of bleach (5-10% NaOCl) and the desiccator was immediately sealed. Primary transformants were

sterilized for 4-6 hours and F2 seeds or greater were sterilized for 2 hours. After sterilization, seeds were removed from the desiccator and covered with aluminum foil to avoid contamination. The seeds were transferred to a flow hood and the tubes were left open for 30 minutes to allow diffusion of chlorine gas before plating. Sterilized seeds were plated on 1x basal Murashige and Skoog (MS) (Sigma) medium supplemented with Gamborg vitamins (Sigma), 0.5 g L^{-1} MES (Sigma), 1% (w/v) Sucrose (Fisher Scientific), and 0.8% (w/v) plant agar (Fisher Scientific) and the pH adjusted to 5.7. Seeds were stratified for 48 h at 4ºC in the dark before transfer to a growth chamber with long-day conditions (16 h light/8h dark at 21ºC). Transgenic plants and mutant lines were selected in MS medium containing the appropriate selection agent. After 14 days seedlings were transferred to soil and grown in short-day conditions (8h light/16 h dark at 22ºC) for 2 weeks to promote vegetative growth. Flowering was induced by transferring the plants to long day conditions (16h light/8h with dark day/night temperatures of 22ºC/18ºC).

All transgenic marker lines used in this study were generated previously to this study (Boavida 2013 and unpublished results from Leonor Boavida). The *quartet 1-2* (*qrt1-2*) mutant (Preuss et al., 1994) in the Columbia ecotype was used for stable transformations. Briefly, ten to twenty resistant plants resulting from each transformation were analyzed for expression patterns and presence of single insertions. One or two lines with stable GFP expression were chosen for propagation and used to recover homozygous lines to use in further analysis. Lines with possible phenotypes in plant development and seed set were discarded if the phenotypes were proven not to be related with protein expression levels. All the analysis of this study was performed using homozygous stable lines.

2.3.2 DNA Extractions

DNA extractions were performed according to (Edwards et al., 1991; Cenis, 1992) with small adaptations. DNA extraction buffer was prepared with 1M Tris HCl (pH: 8), 5M NaCl, 0.5M EDTA, and 20% SDS. Young, fresh rosette leaves were collected and grinded in a 1.5 ml eppendorf tube with 300 ul of DNA extraction buffer using a plastic pellet or a grinding machine. 150 ul of 3M sodium acetate (pH = 5.2) was added to the tube. The samples were vortexed and incubated at -20^{o}C for 10 minutes. After incubation, samples were spun at 14,800 rpm for 3 minutes. The supernatant was transferred to a clean 1.5 mL eppendorf tube. Isopropanol was added at a 1:1 ratio (450ul). Samples were incubated at room temperature (RT) for 15 min before centrifugation at 14,800 rpm for 5 min. The supernatant was removed, and the DNA pellet washed by adding 450ul of ice-cold 70% ethanol. The samples were spun for 1 minute at 14,800 rpm. The ethanol was removed, and samples were air-dried for 1 hour before elution with 30 ul of 1x TE buffer. Extracted genomic DNA was stored at -20^{o}C.

2.3.3 Characterization of Insertion and Marker lines

Genotyping of *janus1/2* (SK30238/SK29952 were obtained from the Saskatoon collection http://aafc-aac.usask.ca/FST/) (Robinson et al., 2009) and *TET11* (SAIL_897_B02) homozygous mutant lines was performed by PCR using genomic DNA extracted from individual plants. All PCR amplifications used DreamTaq polymerase (Thermo Fisher) according with manufacturer's instructions. Two primer pairs were used to determine the plant genotype. For *TET11* SAIL line, the primer pairs were L151 and L152 for the genomic region flanking the T-DNA insertion and L151 and L040 were used as a second primer pair to amplify the region between the T-DNA left border and the flanking genomic sequence. For *janus1/2* the primer pairs for the genomic region were L534 and L575 and L537 and L535 respectively. The second primer pair for *janus1/2* was

L535 and L423 and L575 and L038 respectively to amplify the region between the T-DNA left border and flanking genomic sequence. Sequences of the primers used in this study can be found in Appendix A.

2.3.4 Seed Set Analysis

Pistils 7-10 Days After Pollination (DAP) were collected from self-pollinated plants and dissected under a stereoscope to expose ovules. The number of developing seeds, aborted seeds, and undeveloped ovules were counted for each silique. A minimum of 5 siliques were used for quantification of seed set.

2.3.5 Pollen Germination Assays

Arabidopsis pollen was collected from fresh day open flowers and germinated *in vitro* as previously described (Boavida and McCormick, 2007). Briefly, ~ 40 open flowers were incubated in 1 mL of freshly prepared pollen germination medium (5mM $CaCl_2$, 0.01% H_3BO_3, 5mM KCl, 10% sucrose, 1mM $MgSO_4$, pH adjusted to 7.5-7.8) and vortexed for 3 minutes to release the pollen from anthers. After removing flower parts and debris with a tweezer, the solution was centrifuged at 8,000 rpm for 3 min and the supernatant removed. The pollen pellet was then resuspended in 100-200 µL of fresh pollen germination medium, depending on the size of the pellet. The pollen solution was transferred to a 25mm glass-bottom petri dish coated with 0.01% poly-L lysine (Sigma). The dish was placed in a humidity chamber as described in (Johnson-Brousseau and McCormick, 2004) and incubated at 22^{o}C for 4 hours.

2.3.6 Microscopy Imaging and Data Processing

For quantification of protein enrichment in sperm cells**,** germinated pollen tubes were imaged using a spinning disk CSU-10 confocal head (Yokogawa Electric) mounted on a Zeiss Observer.Z1 inverted microscope equipped with a Prime 95B camera (Teledyne Photometrics) controlled by the Slidebook software (Intelligent Imaging Innovations). Optical sections of 0.25 µm collected from sperm cell pairs expressing single or double fluorophores were acquired using a 100x Plan-APO oil-immersion objective (1.46 NA) with the following settings: GFP and mCherry excited by 488 nm and 561 nm laser lines, respectively. Samples were exposed for 500*ms* using 30% laser power using the respective band-pass filters (482/35 and 617/73; Semrock). A minimum of 20 sperm cell pairs were analyzed for quantification of protein abundance.

Image analysis and 2D projections were performed using ImageJ/Fiji (Schindelin et al., 2012). All images were processed using the following functions available in Fiji prior to analysis: smooth, sharpen, de-speckle, and background subtraction with a rolling-ball radius of 30 pixels. No contrast or brightness adjustments were done on the images prior to analysis. To quantify fluorescent intensity, single optical sections corresponding to median planes for each sperm cell pair were selected. A freehand line (width = 5 pixels) was drawn on the SC-SC adhesion domain or in the outer sperm membrane and the mean intensity values recorded. Fold enrichment was determined as the ratio between the mean fluorescence intensity at the adhesion domain and the outer sperm membrane. Co-localization analysis was carried out using the Fiji plugin Coloc2 (Schindelin et al., 2012).

2.3.7 Statistical Analysis

Statistical analysis and graphs were generated using R (R Development Core Team, 2010) and GraphPad (Prism version 8.4.2; GraphPad Software). One-Way or two-way *ANOVA* was used

to analyze significant differences between multiple groups. Two-sided, unpaired *Student's t-test* was used to determine significance between two groups.

2.3.8 Identification of CRISPR/Cas9 Edited Plants

The two CRISPR/Cas9 constructs targeting *TET12* and *JANUS1/2* genomic regions, respectively were generated by Dr. Mily Ron, a lab collaborator from UC Davis. Both plasmid constructs were transformed separately or simultaneously into *Col qrt*, *janus1/2* and *tet11* homozygous lines using the Agrobacterium flower dip method (Bent, 2006). The plasmid constructs are shown in Figure 2.7A and Figure 2.7B. The seeds were selected first based on RFP, mCitrine or double fluorescence to identify positive transformants (T0s). Fluorescent positive seeds were plated under antibiotic selection to assure that only positive transformants were analyzed (see Fig. 2.7C for selection scheme).

Genomic DNA was extracted from rosette leaves of positive plants and PCR was used to amplify the sequence predicted to contain the editing events. The PCR products were first run on an electrophoresis gel to identify possible indel events (shift on band size). The PCR products were purified using the QIAquick PCR Purification Kit (Qiagen) and sent for Sanger sequencing.

Prior to December 2019, sequencing reactions were performed using Purdue's Genomic Core Facility. Reactions that occurred following January 2020 were performed by Genewiz.

Purdue Genomics Core Facility: 10 µl reactions were used for Sanger sequencing. 5 µl of PCR product diluted with water was provided at a concentration dependent on PCR product size (100-200 bp: 3 ng/ µl; 200-500 bp: 10 ng/µl; 500-1000 bp: 20 ng/µl; 1000-2000 bp: 40 ng/µl; plasmid DNA: 10 ng/µl). 10 µM of the respective primer was added with 2 µl of Terminator Ready Reaction mix and Big Dye Sequencing Buffer (Fisher). Sequencing reactions were performed in a thermal cycler with the following conditions: *1)* 96 ^{o}C for 1 min; *2)* 96 ^{o}C for 10 sec; *3)* appropriate

primer annealing temperature for 5 sec; *4)* 60 ºC for 4 min. After the reaction, the sequencing products were precipitated by adding an equivalent volume of water, 2 µl of 3M NaAc (pH: 4.6), 2 µl of 0.125M EDTA, and 50 µl of 100% ethanol. The solution was transferred to a 1.5 mL eppendorf tube, vortexed, and stored at -20 ºC for 10 min upon which the mix was centrifuged at 14,800 rpm for 15 min at RT. The supernatant was carefully removed, and the pellet washed twice with ice-cold 70% ethanol. The pellet was left to dry in the dark for 1 hour, before elution in 15 ul of MiliQ water. The sequencing products were then delivered to Purdue's Genomic Core Facility.

Genewiz: The purified PCR product was mixed with the appropriate primer according to the Genewiz guidelines for Sanger sequencing. All sequences were analyzed with SnapGene software.

Sequencing reads obtained from individual plants were submitted to Synthego ICE software (https://ice.synthego.com/#/) using the default parameters to determine potential gene editing events in each transgenic line.

2.4 Results and Discussion

2.4.1 Tetraspanins Define an Enriched Microdomain at the Sperm Cell Interface

In this chapter, we examined the expression patterns of *TET11* and *TET12* as well as other known sperm cell factors using confocal microscopy. The expression patterns previously identified using wide field fluorescent microscopy did not provide sufficient resolution for quantification of protein abundance or distribution of sperm cell factors at the plasma membrane.

Using Fiji, we selected tangential and median optical sections of a sperm cell pair to examine the distribution of each sperm cell factor (Fig. 2.3). Optical sections of sperm cells were acquired at intervals of 0.25µm using the corresponding wavelength on a spinning disk confocal

microscope. Z-stacks were then used to generate 2D maximum projections of all optical sections of a sperm cell pair (Fig. 2.3 and 2.4).

The analysis of optical sections indicates that the GFP signal for TET11 is not homogenously distributed throughout the plasma membrane. Rather these proteins seem to accumulate in a punctate form at the sperm cell surface as observed in a tangential plane of a sperm cell pair (Fig. 2.3B). These dots could potentially represent TET clusters (or nano-domains). On a median optical section, TET11 clearly delineates the SC plasma membrane accumulating at the SC-SC adhesion domain. The distribution at the SC-SC interface forms a linear and continuous membrane domain of about 2-3 µm, where no individual membranes can be distinguished (Fig. 2.3C). The protein distributes across the whole SC-SC contact area rather than forming an external ring (Fig. 2.3C). This pattern suggests a TET uniform accumulation at the SC-SC adhesion domain, which contrasts with the punctuated TET distribution at the cell surface (Fig. 2.3B). The apparent

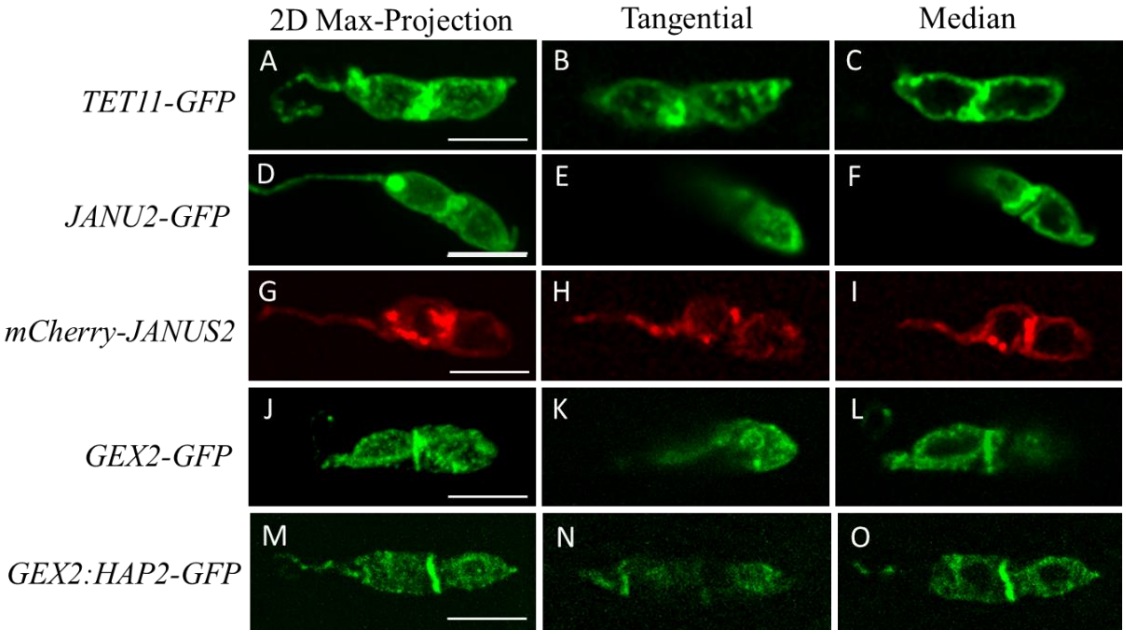

Figure 2.3 Distribution patterns of sperm cell factors. Representative 2D maximum projections of a z-stack (A, D, G, J, M) with corresponding tangential (B, E, H, K, N) and median (C, F, I, L, O) optical sections (0.25 µm) of a sperm cell pair in *Col qrt* background, except for GEX:HAP2-GFP which represents the pattern in *janus1/2* mutant. Scale bars: 5 µm.

uniformity of this domain might be due to overlap of multiple TET clusters which cannot be resolved by the resolution power of the spinning disk microscope. Of notice is that individual SC membranes cannot be distinguished at the SC-SC adhesion domain, suggesting that the two membranes are in very close proximity (<100 nm).

Interestingly the protein distribution of other sperm cell factors, including *JANUS2-GFP* (Fig. 2.3 D-F), *mCherry-JANUS2* (Fig. 2.3G-I), *GEX2-GFP* (Fig. 2.3J-L) follow a similar pattern. *JANUS1* and *JANUS2* were identified as sperm-specific TET interactors using Yeast Two-Hybrid (Y2H) and Bimolecular Fluorescent Complementation (BIFC) assays (unpublished results from Leonor Boavida).

Mutations in *JANUS1/2* disturb MGU organization by enhancing SC-SC adhesion which result in unbalanced fertilization events (see details in Chapter 3). Two translational fluorophore-fusions of *JANUS2* were analyzed in this experiment. A *mCherry-JANUS2* (*mCherry* fused to the N-terminus of *JANUS2*) and *JANUS2-GFP* (*GFP* fused to the C-terminus of *JANUS2*) both driven by *JANUS2* native promoter. Neither of the protein fusions complement the *janus1/2* double mutant phenotype indicating that both constructs generate non-functional proteins. The localization patterns for these two constructs are distinct, but neither cause visible defects when expressed in a wild type background (data not shown). *JANUS-GFP* is expressed evenly at the SC surface (Fig. 2.3D and E) but accumulates strongly at the plasma membrane (100x times more than any other SC factor with an equivalent mRNA transcript abundance). This accumulation suggests that the C-terminal fusion might be interfering with recycling of the protein from the SC membrane. The expression of *mCherry-JANUS2* is much weaker at the cell surface and accumulates in unknown intracellular vesicle-like bodies (Fig. 2.3G). These vesicle-like structures could represent retention of the protein in the ER or Golgi subcellular compartments, which would explain the

weaker expression at the plasma membrane (Gao et al., 2014). Median optical sections reveal that both protein fusions accumulate at the SC-SC adhesion interface and co-localize with TET11 in vesicles and at the plasma membrane (Fig. 2.4A and B). These results suggest that TET-JANUS complexes assemble in the ER before their export to the plasma membrane.

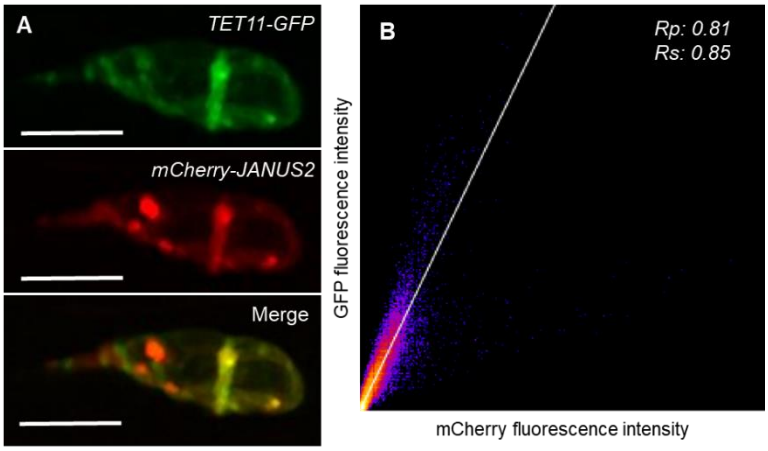

Figure 2.4 A. Colocalization of *TET11-GFP* and *mCherry-JANUS2* in sperm cells. From the top; *TET11-GFP*, *mCherry-JANUS2*, and the merged image. (B) 2D intensity histogram of *TET11-GFP vs. mCherry-JANUS2* as determined by Fiji co-localization plugin (Coloc2). Pearson's R value is shown (0.81), Spearman's rank correlation value is 0.8589, and the Costes *p-value* is 1.

Both *GEX2-GFP* and *HAP2-GFP* show a different expression pattern compared to other factors in this study (Fig. 2.3J-O). These two proteins localize in small organelles in the cytoplasm. This finding is surprising as GEX2, the sperm adhesion factor, was reported to be localized at the plasma membrane (Mori et al., 2014). The discrepancy between the results of Mori et. al. (2014) and this study likely result from the low image resolution in the former report. While GEX2 appears to accumulate adjacent to the membrane surface (Fig. 2.3K) in intracellular structures (Fig. 2.3L) the protein clearly polarizes to the membrane at the SC-SC interface. Sequestering GEX2 within the endomembrane system could be an efficient mechanism to protect the adhesion factor prior to fertilization. Upon reception of a signal from the egg cell, GEX2 may be transported to the plasma membrane during SC activation, similar to the mechanism described for HAP2 the sperm cell factor required for gamete fusion (Sprunck et al., 2012). Nevertheless, the localization of GEX2 and HAP2 at the SC-SC interface is clear and cannot be attributed to cytoplasmic localization, as individual sperm cells would be visible. These observations support direct or

indirect interactions and stabilization of GEX2 and HAP2 by unknown factors present at SC-SC adhesion domain, for instance, tetraspanins.

To determine if the distribution of TETs is polarized and accumulates at the SC-SC interface, we examined the fluorescent intensity across the SC-SC adhesion domain and on an adjacent membrane domain (Fig. 2.5A). A freehand line (width = 5 pixels) was drawn at the SC membrane (green line) (Fig. 2.5A) and at the membrane adhesion domain (red line) (Fig. 2.5A). The mean fluorescent intensity was recorded for each region in the same sperm cell pair. This data was used to calculate the protein enrichment at the SC-SC adhesion interface (Fig. 2.5G).

As predicted, TET11 seems to accumulate at the adhesion domain (Fig. 2.5B). The results, presented as fold enrichment, indicate that TET11 is enriched at the SC interface with a fold change (FC) of 2.5 with 75% of the SC pairs showing a value ≥ 2. As discussed previously, the SC-SC

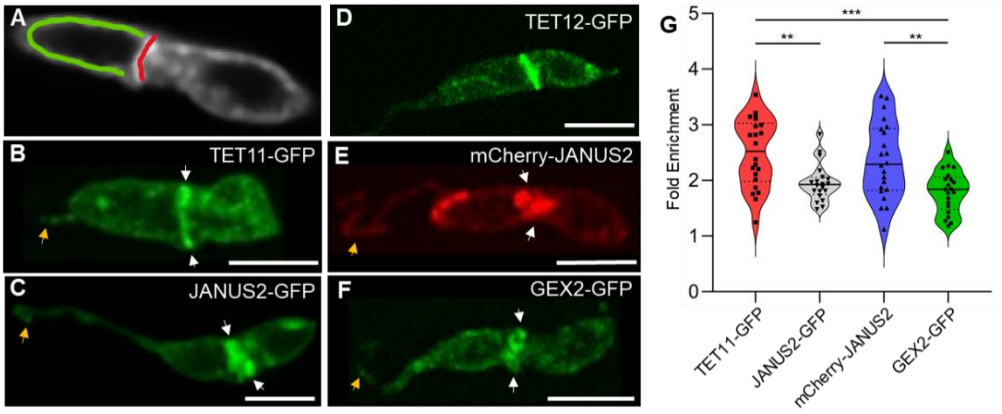

Figure 2.5 Expression analysis and quantification of protein distribution of sperm cell (SC) factors. (A) Representative image of fluorescence quantification. A freehand line in Fiji (width = 5 pixels) highlighting the SC membrane (green line) and the membrane adhesion domain (red line) was used to measure fluorescent intensity in each sperm cell pair. (B- F) Representative images of maximum projections of SC pairs for each marker line in the Columbia *quartet1* background (*Col qrt1*): *TET11-GFP* (B); *JANUS2-GFP* (C); *TET12-GFP* (D); *mCherry-JANUS2* (E) and *GEX2-GFP* (F). Yellow arrows indicate cytoplasmic extension connecting the SC to Vegetative Nucleus (VN), white arrows indicate SC-SC interface. Scale bars: 5 µm. (G) Violin plot depicting fold enrichment of sperm cell factors calculated as the ratio of mean fluorescent intensity between the adhesion domain and the adjacent plasma membrane. Solid black line represents mean, dotted black line represents the 25th to 75th percentiles. Individual measures are shown as dots. Statistical significance represented by * $p<0.05$, ** $p<0.01$, ***$p<0.001$ as calculated by one-way ANOVA followed by Dunnett's multiple comparison test.

adhesion domain is composed of two SC membranes facing each other with a small interstitial space (about 50-80 nm), while the SC surface is composed of two membranes, the vegetative external membrane and the internal SC membrane closely sticking to each other (see Fig. 2.2). Both TET11 and TET12 are sperm expressed membrane proteins, so we expect the distribution of the protein to be limited to individual sperm cell membranes (inner membrane). If a single membrane at the sperm cell surface is labeled, the FC expected would be close to 2, corresponding to 2 SC membranes adhering at the SC interface/1 SC plasma membrane at the cell surface. If both membranes (inner SC and outer vegetative membrane) are labeled, the FC would be close to 1. Our analysis reveals that TET11 is clearly enriched at the SC-SC interface (FC$\geq$ 2), while other factors show some variability. These observations suggest that the two plasma membranes may have unique lipid compositions to which certain proteins have higher affinity (Brown, 2013). Protein-protein interactions may be also involved in stabilizing the localization of proteins at the SC-SC interface. For instance, Lyn24 a mammalian factor known to associate with GPI- and cholesterol-enriched membrane domains (lipids rafts) (Li et al., 2013) and *AtGLR3.7* (Wudick et al., 2018) when expressed under a pollen-specific promoter (*LAT52*) (Twell et al., 1989) localize at the SC surface, suggesting the plasma membrane of SCs have unique compositional properties.

Our results show that TET11 accumulates at the plasma membrane and its distribution is asymmetric and polarized to the plasma membrane at the SC-SC adhesion interface. This enrichment cannot be solely explained by the juxtaposition of a double membrane. In the ultrastructural images of the SC interface (Fig. 2.2B), vesicular structures are visible at the interstitial space between the two SC membranes. It was reported that a polysaccharide-rich extracellular matrix fills the interstitial space between the two membranes (McCue et al., 2011). Since TETs are transmembrane proteins we do not expect them to be released into a polysaccharide

matrix. However, we cannot exclude the possibility that accumulation of TET11 at the SC-SC adhesion domain could be due to the presence of membranes or vesicles in this space.

Quantification of protein enrichment for two *JANUS2* translational fusions shows enrichment at the sperm cell interface. In the *mCherry-JANUS2* fusion, the accumulation of protein at the adhesion domain is highly variable with values ranging from non-enrichment to FC ≥ 2. The protein localization in vesicle-like structures in proximity to the SC-SC adhesion domain may have contributed to the variability of expression patterns (Fig. 2.3D-F, 2.4A, and 2.5E). In contrast, JANUS2-GFP protein fusion shows a clear localization at the plasma membrane (Fig. 2.3F), with a skewed FC=2, consistent with an even distribution of the protein at the SC surface (Fig. 2.5 G). Because these two translational fusions are not functional, JANUS2 enrichment at the SC-SC interface needs to be verified with a functional translational protein fusion. Nevertheless, JANUS involvement as a negative regulator of sperm cell-sperm cell adhesion and as direct TET interacting partners strongly support the hypothesis that TET/JANUS protein complexes form at the sperm-sperm cell adhesion domain.

Despite apparent retention in the endomembrane system (likely ER), GEX2 clearly localizes at the SC-SC interface with a fold enrichment around 2 (Fig. 2.5G). This distribution

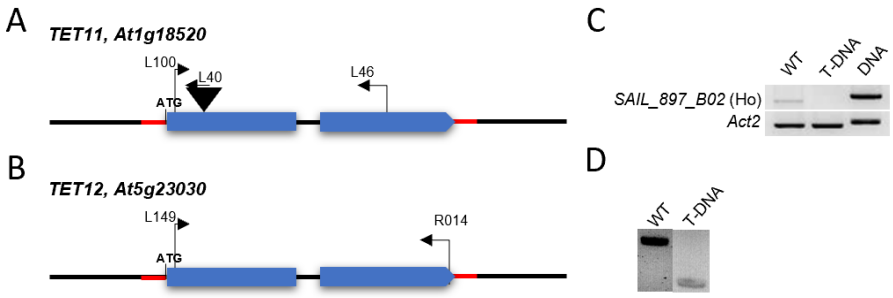

Figure 2.6 Overview of *TET11* and *TET12* gene structure and confirmation of *tet11* T-DNA insertion line. (A-B) Gene structure of *TET11* and *TET12*, showing location of primers used in this study. Black triangle represents T-DNA insertion. Red indicates 3' and 5' untranslated regions. Blue boxes show exons. (C) RT-PCR expression analysis of *TET11*. (D) Confirmation of *TET11* T-DNA insertion.

suggests that GEX2 might be direct or indirectly interacting or be stabilized by TETs or their partners at the SC-SC adhesion contact.

2.4.2 Generation of *TET12* CRISPR KO Lines Reveal Defects in Fertilization

The second goal of this study was to determine the function of TETs in SCs. Previous work recovered homozygous plants from a T-DNA insertion (SAIL_897_B02) in the *TET11* coding region (Boavida et al., 2013) (Fig. 2.6A). Homozygous plants did not produce any functional mRNA, confirming that the mutant is a knockout line (Fig. 2.6C and D). Examination of pollen morphology and seed set did not reveal any reproductive or other defects affecting plant development (data not shown). The absence of a phenotype in *tet11* suggested a possible functional redundancy with *TET12* in sperm cells. To address this hypothesis, we searched for *TET12* T-DNA insertions lines in all the mutant collections in the Arabidopsis seed stocks, with no success. For this reason, the examination on the function of *TET11* and *TET12* in SCs required generation of CRISPR/Cas9 transgenic lines specifically targeting the *TET12* coding region. The CRISPR/Cas9 editing system is composed of an endonuclease protein that targets specific DNA sequences lead by a short guide RNA (gRNA) (Adli, 2018). The components of the protein-RNA complex are cloned into a plasmid and transformed into the plant. The specificity of CRISPR/Cas9 is provided by the gRNA, which is bound to the Cas9 enzyme through interactions with the RNA phosphate backbone. Once bound, the complex searches for sites complementary to the gRNA with a conserved protospacer adjacent motif (PAM). PAM recognition is essential for CRISPR/Cas9 gene editing and is denoted as 5'-NGG-3' where N is any base pair. After identifying a complementary sequence with an appropriate PAM sequence, an RNA-DNA duplex is formed and Cas9 is activated for cleavage. Cas9 contains two nuclease domains that each cleave one strand of the target DNA sequence, producing a blunt-ended double strand break (Jiang and Doudna, 2017).

We used this technology to generate a CRISPR/Cas9 for *TET12* (Fig. 2.7A) and *JANUS1/2* (Fig. 2.7B). Our first approach used the 35S promoter to drive expression of the Cas9 protein. These constructs were unsuccessful in generating stable editing events (results not shown). In collaboration with Dr. Mily Ron (UC Davis), an expert in CRISPR/Cas9 technology and our collaborator, new constructs were generated aiming to induce gene editing more efficiently.

The new plasmid used the *RPS5* promoter to drive CAS9 expression and two gRNA sequences in the zygote (Fig. 2.7A) to improve the editing efficiency. The high rate of successful editing events is attributed to the promoter expression during early embryogenesis, reducing the proportion of chimeric plants and allows recovery of homozygous edited plants in the first generation (Ordon et al., 2020). The plasmid also contained an RFP or Citrine translational fusion under the control of the native OLE1 promoter. This promoter is expressed in the embryo during seed maturation (Baud et al., 2016), thus facilitating selection of positive transformants based on positive expression of a fluorescent protein in seeds (Fig. 2.7C). After identification of edited

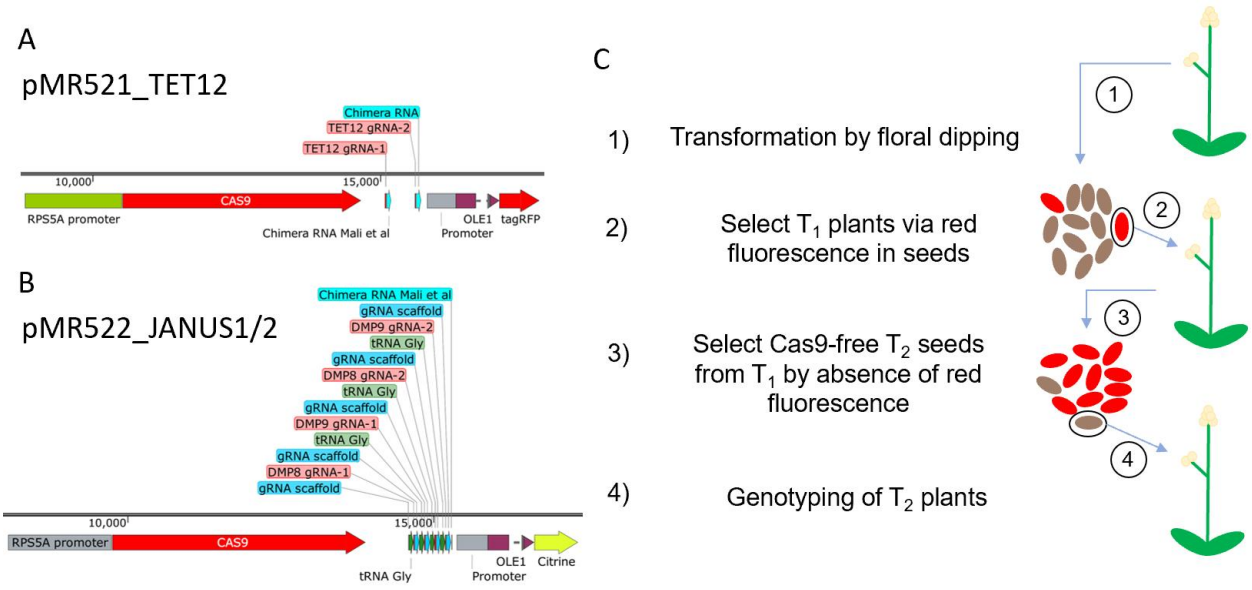

Figure 2.7 Overview of CRISPR/Cas9 plasmids used in this study and strategy for progeny selection. CRISPR/Cas9 plasmid maps used to induce genomic lesions in *TET12* (A) and *JANUS1/2* (B) coding sequences in the *tet11* mutant or *Col qrt* background. (C) Overview of selection of CRISPR edited progeny from T0 transformants.

plants, the CRISPR/Cas9 construct can be eliminated from the T1 progeny by screening for the absence of seed fluorescence (Fig. 2.7C).

The two CRISPR/Cas9 constructs targeting *TET12* or *JANUS1/2* coding regions were transformed into *tet11* Ho line and *Col qrt*. T1 seeds were germinated in the presence of the appropriate antibiotic to assure the selection of positive transformants and the plants grown to flowering (Fig. 2.7C). Here we present the preliminary results obtained for the individual transformations of the *TET12* CRISPR/Cas9 lines in the *Col qrt* and from the simultaneous transformation of both constructs, *TET12* CRISPR/Cas9 and *JANUS1/2* CRISPR/Cas9 in *Col qrt* and *tet11* Ho mutant.

Preliminary analysis of *TET12* CRISPR/Cas9 T1 transgenic plants identified several plants with consistent fertilization defects (Fig. 2.8A). These fertility defects lead either to the abortion of ovules that represent fertilized ovules that fail to develop endosperm or embryos or undeveloped ovules representing usually unfertilized embryo sacs (Fig. 2.8A). Interestingly *janus1/2* mutants show a somewhat similar phenotype. The proportion of seeds is consistent with the possibility of

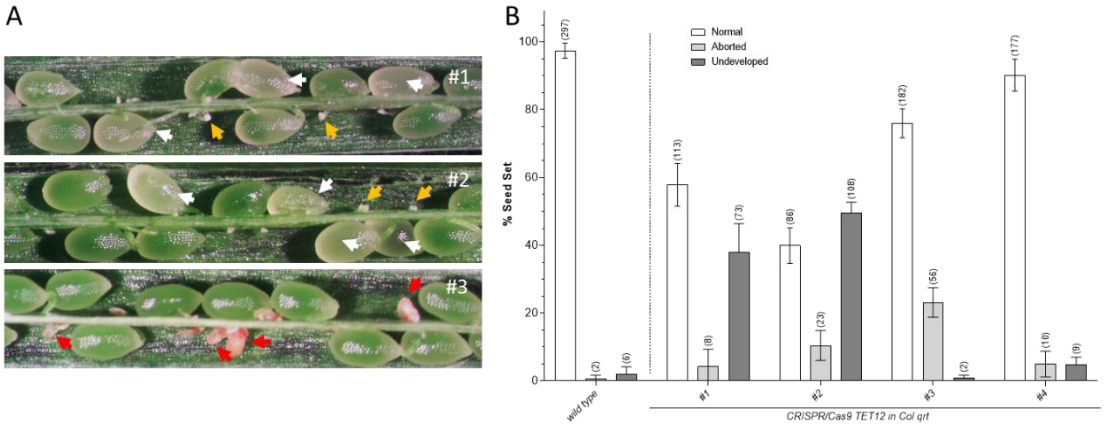

Figure 2.8 Phenotypical analysis of *TET12* CRISPR/Cas9 in Col qrt. (A) Representative images of siliques from three individual T1 plants showing fertilization defects. White arrows point to ovules with a developing endosperm but lack an embryo, yellow arrows indicate unfertilized ovules and red arrows ovules that were fertilized but aborted due to failure in developing endosperm. (B) Proportion of seed sets in 4 different T1 plants compared with Col qrt (wild type).

an incomplete penetrant phenotype and the presence of heterozygous and homozygous editing events. The different patterns of fertilization defects observed suggest that in addition to knockout (KO) plants, we may have phenotypes resulting from other types of editing events (frameshifts or SNPs) (Fig. 2.8B). The existence of a *TET12* CRISPR-associated phenotype in Col qrt does not exclude the hypothesis that *TET11/TET12* function redundantly in sperm cells. The analysis of *TET12* CRISPR editing events in the background of *tet11* will provide further insights into the function of these two genes in the male gametes and in double fertilization. Though these results are initial and require confirmation of *TET12* gene editing, we may finally have a tool to address the function of TETs in sperm cells. These lines and the *TET12* CRISPR/Cas9 in *tet11* homozygous background are currently under analysis.

We also decided to transform both *TET12* and *JANUS1/2* CRISPR/Cas9 constructs simultaneously into the *Col qrt* and *tet11* mutant background to generate possible triple and quadruple mutants. We recovered several T1 independent lines in both backgrounds. We amplified the genomic regions and analyzed the sequences to identify potential editing events.

Because the CRISPR/Cas9 constructs contain a double guide RNA for each gene (Fig. 2.7A and B), we expected that a substantial genomic region could be deleted between the two PAM regions. To verify if the construct was functioning as expected, genomic DNA from primary transformants was used to amplify the genomic region flanking the targeted region. Using gel electrophoresis, a large deletion could be detected by a shift of the band corresponding to the amplified fragment (Fig. 2.10C). As expected, the gel showed several band patterns consistent with homozygous edited plants (Fig. 2.10C). With confirmation that the construct was functional, we proceeded to examine the edited sequences.

The complete *TET12*, *JANUS1*, and *JANUS2* genes were amplified from selected transformants and sequenced. The Synthego ICE software (https://ice.synthego.com/#/) was used to examine the sequencing output and predict potential editing events (Fig. 2.9). The indel percentage represents editing efficiency, determined by comparing the edited sequence to the control sequence. The knockout score shows the proportion of cells that have a frameshift or 21 +

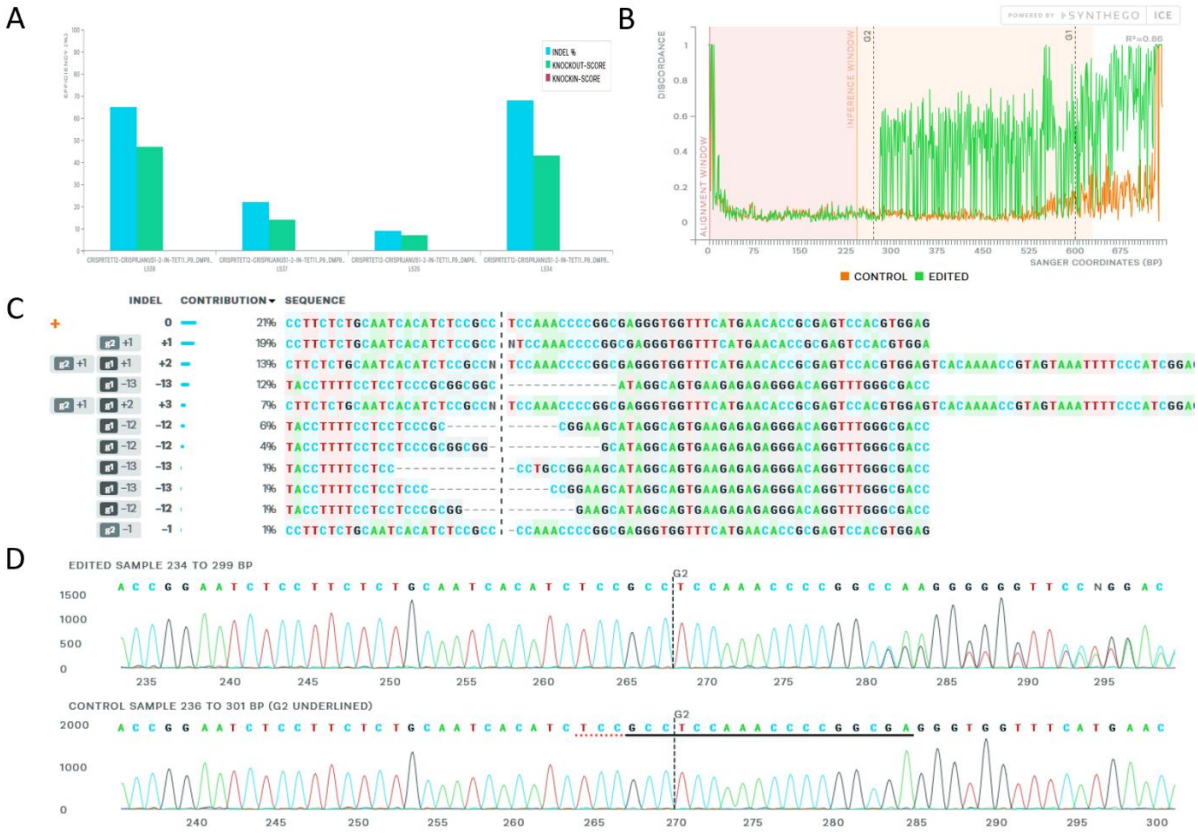

Figure 2.9 Representative output of *JANUS2* CRISPR/Cas9 edited sequence analysis using Synthego ICE software. (A) Graph showing % of editing efficiency based on 4 submitted sequences. Blue columns represent % of indels and Green the Knockout scores (%). (B) Discordance plot details the level of alignment per base between the wild type (control) and the edited sample (orange) in the inference window (the region around the cute site G1 and G2), i.e. it shows the average amount of signal that disagrees with the reference sequence derived from the control trace file. On the plot, the green line and orange line should be close together before the cut site, with a typical CRISPR edit resulting in a jump in the discordance near the cut site and continuing to remain far apart after the cut site (representing a high level of sequence discordance). (C) The contributions show the inferred sequences present in the edited sequences and their relative proportions. Cut sites are represented by black vertical dotted lines, and the wild-type sequence is marked by a "+" symbol on the far left. (D) Sanger sequence view showing edited and wild-type (control) sequences in the region around the guide sequence. This shows sequence base calls from both the control and the experimental sample .ab1 files, which will contain mixed base calls. The horizontal black underlined region represents the guide sequence. The horizontal red underline is the PAM site. The vertical black dotted line represents the actual cut site. Cutting and error-prone repair usually results in mixed sequencing bases after the cut.

bp indel (Fig. 2.9A). Both measurements were used to select potentially edited plants. The discordance plot (Fig. 2.9B) shows the level of alignment between the wild-type and edited samples. A typical CRISPR edited sequence shows high similarity prior to the cut site but a jump in the discordance following the PAM which is sustained throughout the rest of the gene. Indel contribution shows the sequences present in the edited population and their representation in the edited pool (Fig. 2.9C). Finally, the Sanger sequence view shows the edited, control, and non-edited traces near the gRNA binding sites (Fig. 2.9D).

Figure 2.10 is representative of the *TET12* output of Synthego ICE analysis (https://ice.synthego.com) of two *TET12/JANUS1/2* CRISPR edited plants (Fig. 2.10). Sequencing was performed with two primers (R014 and L149) whose annealing location was approximately 150 bp from the gRNA. The wild type (WT) sequence was used as a control. The predicted indels are consistent with the cleavage site of Cas9 downstream the PAM site. T1-1 had a small insertion on the region targeted by the gRNA-1 followed by a large deletion of (>400 bp). Similarly, T1-2

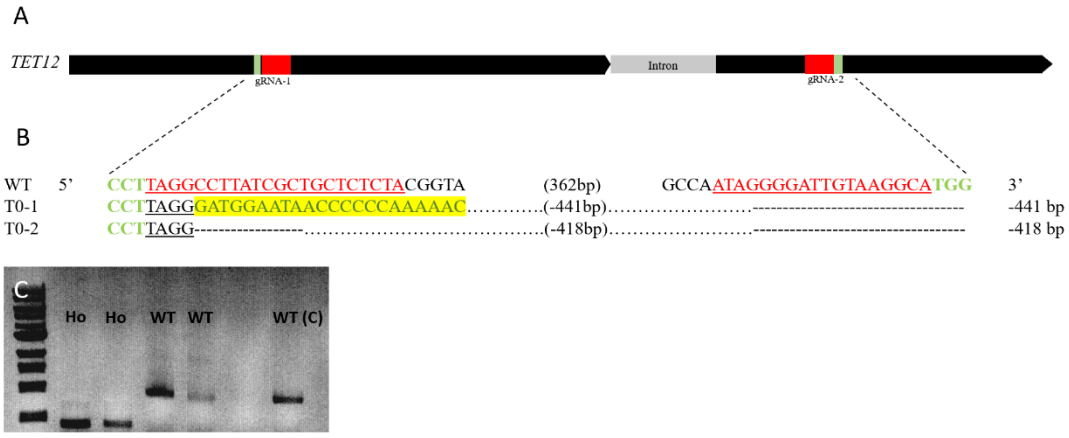

Figure 2.10 Analysis of CRISPR/Cas9 TET12 gene editing events in T1 lines. (A) Gene structure of *TET12* showing location of targeted sequences by the two guide RNAs (gRNA-1 and gRNA-2). Black blocks indicate exons, grey box indicates intron. Red box show sequences targeted by individual guide RNAs and the green box location of PAM motif. (B) Genomic sequences of wild type control and edited sequences from two independent T1 lines are shown. Underlined red sequence depicts the target sequence by the gRNAs with the protospacer-adjacent motif (PAM) shown in green. Highlighted yellow sequence indicate insertion, dashes show deletions within the gRNA target. Dots represent deletions between the two gRNA targets.

contains a large deletion of 418 bp starting 4 nucleotides downstream the gRNA-1 target sequence which extends beyond the location of the gRNA-2 target sequence (Fig. 2.10B).

Phenotypical analysis of the fertilization defects in *TET12/JANUS1/2* CRISPR edited plants revealed patterns consistent with editing events (Fig. 2.11). The seed set of CRISPR/Cas9 positive plants in the background of *tet11* showed severe fertility defects (Fig. 2.11C). A preliminary analysis determined that the transgenic lines contained consistent defects in pollen abortion (Fig. 2.11E and F) and female gametophyte arrest at the megaspore mother cell (MMC) stage (Fig. 2.11B). Because we transformed both constructs in the *Col qrt* and *tet11* homozygous background, the phenotypes can be due to multiple gene editing events. Since we have determined that *TET12* edited plants show fertilization defects, we expect that these early phenotypes in

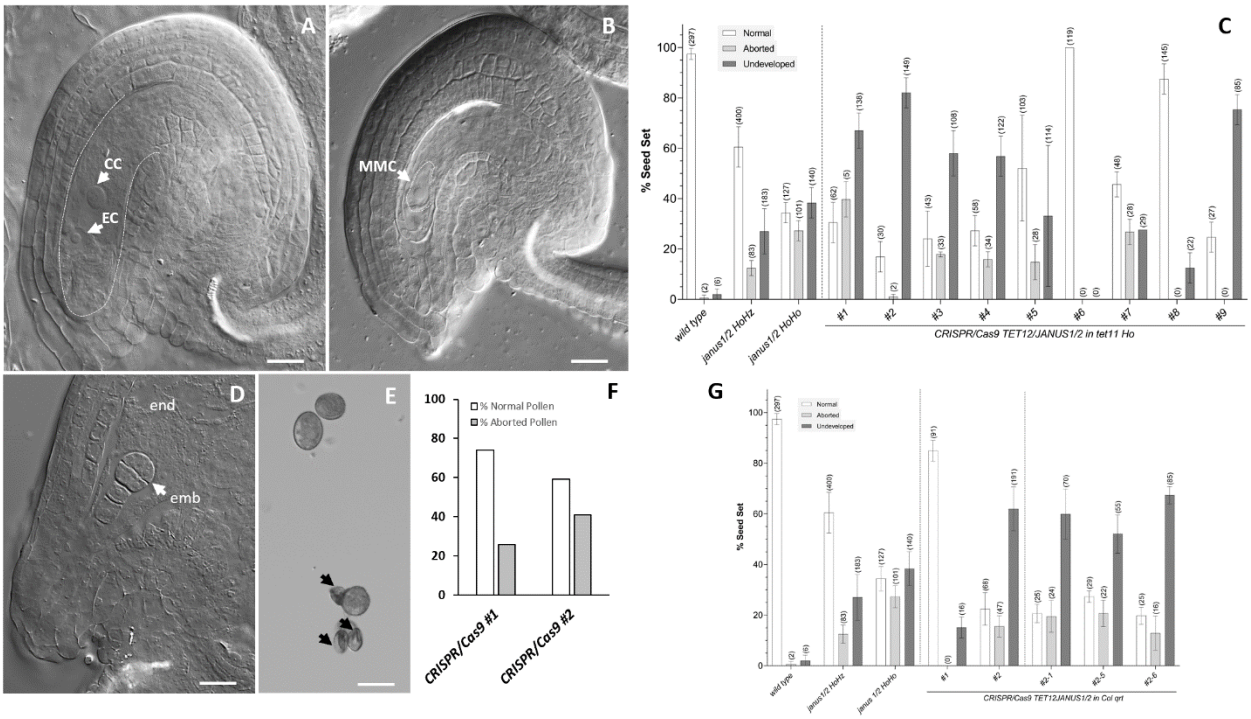

Figure 2.11 Phenotypical analysis of *TET12* and *JANUS1/2* CRISPR/Cas9 edited plants. (A) Wild type ovule containing an unfertilized embryo sac showing egg cell (EC) and central cell (CC). (B) Ovule arrested at the megaspore mother cell (MMC) stage in *TET12* edited plants. (D) Ovule containing a fertilized embryo sac with embryo (emb) and endosperm (end) in the same carpel as B. (C) Seed set analysis of CRISPR edited plants in the background of *tet11* with wild type, *janus1/2* HoHz, and *janus1/2* double mutant as controls. (E) Representative image of pollen abortion in *TET12* edited plants. (F) Quantification of pollen abortion. (G) Seed set analysis of CRISPR edited plants in the background of Col qrt , *janus1/2* HoHz, and *janus1/2* double mutant as controls.

gametophyte development may result from triple mutations likely affecting *TET12*, *JANUS1* and *JANUS2*. Further confirmation of all the phenotypes in the next generation and determination of the editing events will allow us to address the function of *TET11* and *TET12* in SCs and of potential lethal gametophytic defects in triple or quadruple mutants.

Since Tetraspanins are thought to function as central organizers of signaling proteins at the plasma membrane, we expect that *tet12* mutant will lead to disruption of SC-SC adhesion factors and other signaling molecules involved in the communication between SCs or affect double fertilization. A *tet12* mutant can be used to examine potential *TET* interactors and their involvement in the formation of SC adhesion domains.

The results in this section, suggest that *TET12* is necessary for double fertilization as we first anticipated. We currently do not have results to determine if *TET11* and *TET12* are functionally redundant. However, our CRISPR/Cas9 preliminary results are promising and further studies will verify *TET12* editing events, examine phenotypes, and associated alterations in gene expression. The possibility that CRISPR/Cas9 can create knockouts but also can cause Single Nucleotide Polymorphisms (SNP) or frameshifts that may lead to non-functional phenotypes or phenotypical variants is an exciting perspective. These tools can be critical to address structural and functional domains in plant tetraspanins and define their essential functions in plant development and reproduction.

2.5 References

Adli, M. 2018. "The CRISPR Tool Kit for Genome Editing and Beyond." *Nature communications* 9 (1). doi: 10.1038/s41467-018-04252-2.

Alexandersson, E, G Saalbach, C Larsson, and P Kjellbom. 2004. "Arabidopsis Plasma Membrane Proteomics Identifies Components of Transport, Signal Transduction and Membrane Trafficking." *Plant & cell physiology* 45 (11). doi: 10.1093/pcp/pch209.

Baud, S., Z. Kelemen, J. Thévenin, C. Boulard, S. Blanchet, A. To, M. Payre, N. Berger, D. Effroy-Cuzzi, J. M. Franco-Zorrilla, M. Godoy, R. Solano, E. Thevenon, F. Parcy, L. Lepiniec, and B. Dubreucq. 2016. "Deciphering the Molecular Mechanisms Underpinning the Transcriptional Control of Gene Expression by Master Transcriptional Regulators in Arabidopsis Seed1." In *Plant Physiol*, 1099-112.

Bent, A. 2006. "Arabidopsis thaliana floral dip transformation method." *Methods Mol Biol* 343:87-103. doi: 10.1385/1-59745-130-4:87.

Bentley, M, and G Banker. 2016. "The Cellular Mechanisms That Maintain Neuronal Polarity." *Nature reviews. Neuroscience* 17 (10). doi: 10.1038/nrn.2016.100.

Blazek, AD, BJ Paleo, and N Weisleder. 2015. "Plasma Membrane Repair: A Central Process for Maintaining Cellular Homeostasis." *Physiology (Bethesda, Md.)* 30 (6). doi: 10.1152/physiol.00019.2015.

Boavida, L. C., and S. McCormick. 2007. "Temperature as a determinant factor for increased and reproducible in vitro pollen germination in Arabidopsis thaliana." *Plant J* 52 (3):570-82. doi: 10.1111/j.1365-313X.2007.03248.x.

Boavida LC, Qin P, Broz M, Becker JD, McCormick S (2013) Arabidopsis tetraspanins are confined to discrete expression domains and cell types in reproductive tissues and form homo- and heterodimers when expressed in yeast. Plant Physiol 163: 696-712

Brown, D. A. 2013. "Lipid Rafts." In *Encyclopedia of Biological Chemistry (Second Edition)*, edited by William J. Lennarz and M. Daniel Lane, 741-744. Waltham: Academic Press.

Brown, DA, and E London. 1998. "Functions of Lipid Rafts in Biological Membranes." *Annual review of cell and developmental biology* 14. doi: 10.1146/annurev.cellbio.14.1.111.

Cacas, JL, F Furt, M Le Guédard, JM Schmitter, C Buré, P Gerbeau-Pissot, P Moreau, JJ Bessoule, F Simon-Plas, and S Mongrand. 2012. "Lipids of Plant Membrane Rafts." *Progress in lipid research* 51 (3). doi: 10.1016/j.plipres.2012.04.001.

Cenis, J. L. 1992. "Rapid extraction of fungal DNA for PCR amplification." *Nucleic Acids Res* 20 (9):2380.

Edwards, K., C. Johnstone, and C. Thompson. 1991. "A simple and rapid method for the preparation of plant genomic DNA for PCR analysis." *Nucleic Acids Res* 19 (6):1349.

Gao, C, Y Cai, Y Wang, BH Kang, F Aniento, DG Robinson, and L Jiang. 2014. "Retention Mechanisms for ER and Golgi Membrane Proteins." *Trends in plant science* 19 (8). doi: 10.1016/j.tplants.2014.04.004.

Hamamura, Y, C Saito, C Awai, D Kurihara, A Miyawaki, T Nakagawa, MM Kanaoka, N Sasaki, A Nakano, F Berger, and T Higashiyama. 2011. "Live-cell Imaging Reveals the Dynamics of Two Sperm Cells During Double Fertilization in Arabidopsis Thaliana." *Current biology : CB* 21 (6). doi: 10.1016/j.cub.2011.02.013.

Harder, T, P Scheiffele, P Verkade, and K Simons. 1998. "Lipid Domain Structure of the Plasma Membrane Revealed by Patching of Membrane Components." *The Journal of cell biology* 141 (4). doi: 10.1083/jcb.141.4.929.

Hemler, M. E. 2005. "Tetraspanin functions and associated microdomains." *Nat Rev Mol Cell Biol* 6 (10):801-11. doi: 10.1038/nrm1736.

Holowka, D, ED Sheets, and B Baird. 2000. "Interactions Between Fc(epsilon)RI and Lipid Raft Components Are Regulated by the Actin Cytoskeleton." *Journal of cell science* 113 (Pt 6).

Hooper, NM. 1999. "Detergent-insoluble Glycosphingolipid/Cholesterol-Rich Membrane Domains, Lipid Rafts and Caveolae (Review)." *Molecular membrane biology* 16 (2). doi: 10.1080/096876899294607.

Jiang, F, and JA Doudna. 2017. "CRISPR-Cas9 Structures and Mechanisms." *Annual review of biophysics* 46. doi: 10.1146/annurev-biophys-062215-010822.

Johnson-Brousseau, S. A., and S. McCormick. 2004. "A compendium of methods useful for characterizing Arabidopsis pollen mutants and gametophytically-expressed genes." *Plant J* 39 (5):761-75. doi: 10.1111/j.1365-313X.2004.02147.x.

Krügel, U, LM Veenhoff, J Langbein, E Wiederhold, J Liesche, T Friedrich, B Grimm, E Martinoia, B Poolman, and C Kühn. 2008. "Transport and Sorting of the Solanum Tuberosum Sucrose Transporter SUT1 Is Affected by Posttranslational Modification." *The Plant cell* 20 (9). doi: 10.1105/tpc.108.058271.

Li, S, LZ Zhou, QN Feng, S McCormick, and Y Zhang. 2013. "The C-terminal Hypervariable Domain Targets Arabidopsis ROP9 to the Invaginated Pollen Tube Plasma Membrane." *Molecular plant* 6 (4). doi: 10.1093/mp/sst098.

Li, X., X. Wang, Y. Yang, R. Li, Q. He, X. Fang, D. T. Luu, C. Maurel, and J. Lin. 2011. "Single-molecule analysis of PIP2;1 dynamics and partitioning reveals multiple modes of Arabidopsis plasma membrane aquaporin regulation." *Plant Cell* 23 (10):3780-97. doi: 10.1105/tpc.111.091454.

Marhava, Petra, Ana Cecilia Aliaga Fandino, Samuel W. H. Koh, Adriana Jelínková, Martina Kolb, Dorina P. Janacek, Alice S. Breda, Pietro Cattaneo, Ulrich Z. Hammes, Jan Petrášek, and Christian S. Hardtke. 2020. "Plasma Membrane Domain Patterning and Self-Reinforcing Polarity in Arabidopsis." *Developmental Cell* 52 (2):223-235.e5. doi: https://doi.org/10.1016/j.devcel.2019.11.015.

McCue, AD, M Cresti, JA Feijó, and RK Slotkin. 2011. "Cytoplasmic Connection of Sperm Cells to the Pollen Vegetative Cell Nucleus: Potential Roles of the Male Germ Unit Revisited." *Journal of experimental botany* 62 (5). doi: 10.1093/jxb/err032.

Mori, T., T. Igawa, G. Tamiya, S. Y. Miyagishima, and F. Berger. 2014. "Gamete attachment requires GEX2 for successful fertilization in Arabidopsis." *Curr Biol* 24 (2):170-5. doi: 10.1016/j.cub.2013.11.030.

Ordon, J, M Bressan, C Kretschmer, L Dall'Osto, S Marillonnet, R Bassi, and J Stuttmann. 2020. "Optimized Cas9 Expression Systems for Highly Efficient Arabidopsis Genome Editing Facilitate Isolation of Complex Alleles in a Single Generation." *Functional & integrative genomics* 20 (1). doi: 10.1007/s10142-019-00665-4.

Preuss, D., S. Y. Rhee, and R. W. Davis. 1994. "Tetrad analysis possible in Arabidopsis with mutation of the QUARTET (QRT) genes." *Science* 264 (5164):1458-60. doi: 10.1126/science.8197459.

Qiu, QS, BJ Barkla, R Vera-Estrella, JK Zhu, and KS Schumaker. 2003. "Na+/H+ Exchange Activity in the Plasma Membrane of Arabidopsis." *Plant physiology* 132 (2). doi: 10.1104/pp.102.010421.

Raggi, S, E Demes, S Liu, S Verger, and S Robert. 2020. "Polar Expedition: Mechanisms for Protein Polar Localization." *Current opinion in plant biology* 53. doi: 10.1016/j.pbi.2019.12.001.

Reimann, R., B. Kost, and J. Dettmer. 2017. "TETRASPANINs in Plants." *Front Plant Sci* 8. doi: 10.3389/fpls.2017.00545.

Robinson, SJ, LH Tang, BA Mooney, SJ McKay, WE Clarke, MG Links, S Karcz, S Regan, YY Wu, MY Gruber, D Cui, M Yu, and IA Parkin. 2009. "An Archived Activation Tagged Population of Arabidopsis Thaliana to Facilitate Forward Genetics Approaches." *BMC plant biology* 9. doi: 10.1186/1471-2229-9-101.

Schindelin, J., I. Arganda-Carreras, E. Frise, V. Kaynig, M. Longair, T. Pietzsch, S. Preibisch, C. Rueden, S. Saalfeld, B. Schmid, J. Y. Tinevez, D. J. White, V. Hartenstein, K. Eliceiri, P. Tomancak, and A. Cardona. 2012. "Fiji: an open-source platform for biological-image analysis." *Nat Methods* 9 (7):676-82. doi: 10.1038/nmeth.2019.

Simons, K, and D Toomre. 2000. "Lipid Rafts and Signal Transduction." *Nature reviews. Molecular cell biology* 1 (1). doi: 10.1038/35036052.

Sprunck, S., S. Rademacher, F. Vogler, J. Gheyselinck, U. Grossniklaus, and T. Dresselhaus. 2012. "Egg cell-secreted EC1 triggers sperm cell activation during double fertilization." *Science* 338 (6110):1093-7. doi: 10.1126/science.1223944.

Wang, F., A. Muto, J. Van de Velde, P. Neyt, K. Himanen, K. Vandepoele, and M. Van Lijsebettens. 2015. "Functional Analysis of the Arabidopsis TETRASPANIN Gene Family in Plant Growth and Development1[OPEN]." In *Plant Physiol*, 2200-14.

Wisniewska, J, J Xu, D Seifertová, PB Brewer, K Ruzicka, I Blilou, D Rouquié, E Benková, B Scheres, and J Friml. 2006. "Polar PIN Localization Directs Auxin Flow in Plants." *Science (New York, N.Y.)* 312 (5775). doi: 10.1126/science.1121356.

Wudick, MM, MT Portes, E Michard, P Rosas-Santiago, MA Lizzio, CO Nunes, C Campos, D Santa Cruz Damineli, JC Carvalho, PT Lima, O Pantoja, and JA Feijó. 2018. "CORNICHON Sorting and Regulation of GLR Channels Underlie Pollen Tube Ca 2+ Homeostasis." *Science (New York, N.Y.)* 360 (6388). doi: 10.1126/science.aar6464.

Yuan, J, Y Ju, DS Jones, W Zhang, N Lucca, CJ Staiger, and SA Kessler. 2020. "Pollen tube-triggered accumulation of NORTIA at the filiform apparatus facilitates fertilization in Arabidopsis thaliana." doi: 10.1101/621599.

Yáñez-Mó, M, O Barreiro, M Gordon-Alonso, M Sala-Valdés, and F Sánchez-Madrid. 2009. "Tetraspanin-enriched Microdomains: A Functional Unit in Cell Plasma Membranes." *Trends in cell biology* 19 (9). doi: 10.1016/j.tcb.2009.06.004.

CHAPTER 3. TET/JANUS SIGNALLING COMPLEXES PLAY A ROLE IN DOUBLE FERTILIZATION

3.1 Abstract

Cell-to-cell adhesion is an essential cellular process in all multicellular organisms. Animal cells can adhere to one another directly across the membrane while most plant cells contain a cell wall that prevents direct contact between two adjacent plasma membranes. The male gametes of plants do not contain cell walls, and therefore cell-cell interactions occur directly across the plasma membranes. Two recently identified Tetraspanin interactors in plant sperm cells (SCs), *JANUS1* (*DMP8)* and *JANUS2* (*DMP9),* act as negative regulators of SC-SC adhesion. *JANUS1/2* share structural similarities to known matrix metalloproteases (MMPs). In animals, MMPs typically digest proteins in the extracellular matrix (ECM) but are also known to activate signaling and adhesion factors through proteolytic shedding of their prodomain. In *janus1/2* mutants, the twin SCs exhibit an extended adhesion interface consistent with alterations in the membrane composition. In this chapter we examined the structural homology of JANUS1/2 to MMPs and tested whether these proteins have unique functions within their family. We also tested the hypothesis that GEX2 is the adhesion factor regulating homotypic interactions between the twin SCs. Our results show that JANUS1/2 may perform unique functions as membrane proteases in SCs and that GEX2 could be part of a TET-JANUS protein complex regulating SC-SC adhesion.

3.2 Introduction

3.2.1 Cell-Cell Adhesion

Cell-to-cell adhesion is essential in all multicellular organisms. In animals, intercellular adhesion is a highly dynamic process, essential for development and cell migration (Halbleib and

Nelson, 2006). In animal cells, cell-cell interactions can occur via the plasma membrane (cell–cell adhesion) or between the plasma membrane and the extracellular matrix (cell-ECM). Some of the molecules which facilitate adhesion events in animals include immunoglobulin-like adhesion molecules (CAMs), cadherins, selectins, integrins, occludins, claudins, and tricellulins (Mariano et al., 2011; Bendas and Borsig, 2012; Campbell et al., 2017). Tetraspanins (TETs) are also actively involved in regulating cell-to-cell adhesion events via their interactions with integrins and proteolytic remodelers of the ECM, for instance, ADAM proteins (Yanez-Mo et al., 2011).

Most plant cells are surrounded by a cell wall which prevents the direct adhesion between the plasma membrane of adjacent cells. During cytokinesis, a cell plate is formed where new cell wall materials are deposited between each daughter cell. A pectin-rich middle lamella resembling a gel forms between adjacent cells walls and contributes to cell-cell adhesion. Plant cell walls are rigid and therefore cells have a fixed position in the tissue. This positional information is important for cell differentiation (De Smet and Beeckman, 2011). Cell growth and morphogenesis involves remodeling of the cell walls to make them less stiff and allow for cell expansion. The middle lamella is mainly composed of pectin a highly methyl-esterified polysaccharide. Pectin can be modified by removing the methyl groups, resulting in de-esterified pectin. This form of pectin can be promptly crosslinked via calcium, producing a stiff, gel-like material that promotes adhesion of two adjacent cells (Daher and Braybrook, 2015). For instance, mutants in the *TUMOROUS SHOOT DEVELOPMENT2* (*TSD2*) gene encoding a pectin methyltransferase expressed primarily in meristems and young tissues show defects in cell-cell adhesion that lead to cellular over-proliferation of tumor-like structures (Krupková et al., 2007).

In plants, cell-cell adhesion is necessary for plant development and growth and is critical for sexual reproduction. In flowering plants, many reproductive processes including adhesion of

pollen grains to stigma papilla and pollen tube growth and guidance along the female tissue involves adhesion molecules. In lily, the Stigma/stylar Cysteine-rich Adhesin (SCA) was shown to promote adhesion of the pollen tube to the female transmitting tract (Lord, 2000; Sang-Youl and Elizabeth M., 2003). Plant gametes are unique, in that they are the only plant cells that lack entirely organized cell walls. Cell-cell interactions and adhesion between gametes are thought to occur directly across the plasma membrane of gametes. For instance, adhesion between the two twin sperm cells (SCs) and the Vegetative Nucleus (VN) is thought to be essential for the simultaneous delivery of sperm cells into the embryo sac (McCue et al., 2011) SC-SC adhesion might be mediated by TET-JANUS complexes (see Chapter 2). However, the adhesion factors involved in this process are not currently known.

Male-to-female gamete adhesion prior to gamete fusion in double fertilization depends on a SC-specific factor *GEX2* (*Generative Cell Expressed 2*) (Mori et al., 2014). GEX2 is a large (~120 kDa) single-pass transmembrane protein containing two extracellular Immunoglobulin-like (Ig-like) domains (Mori et al., 2014). In animals, Ig-like proteins mediate cell-cell adhesion and signal transduction processes (Horstkorte and Fuss, 2012).

Cellular adhesion is essential for both plant and animal development. Although recent advances have increased our understanding of cell-cell adhesion in plants, the identity and function of adhesion factors remain elusive. This is especially true with respect to factors that affect gamete adhesion during double fertilization in which the only adhesion factor currently known is GEX2.

3.2.2 Function of TET/JANUS Complexes in Plant Gamete Adhesion

Chapter 2 demonstrated that several SC signaling proteins (*JANUS2*, *GEX2*, *HAP2*) with roles in double fertilization, co-localize with *TET11/TET12* within the Tetraspanin-enriched microdomain (TEM) at the SC-SC adhesion interface. I also have shown that GEX2 and HAP2,

despite their subcellular localization in the endomembrane system, localize in the plasma membrane at the SC-SC adhesion domain.

JANUS1/2, known as *DMP8/9* (*DUF679 domain membrane protein)* belong to a plant-specific gene family of 10 members with no known recognizable functional motifs (Kasaras and Kunze, 2010) (Fig. 3.1A). The genes are small (< 1Kb) and contain no introns (Fig. 3.1B and C). A double homozygous mutant isolated from T-DNA insertions located in the coding region of *JANUS1* and *JANUS2* was recovered *(*SK30238 and SK29952, respectively) (Fig. 3.1D and E). The mutants do not produce any functional mRNA (Fig. 3.1F and G) and are true knockout lines (Fig. 3.1B and C, F, and G).

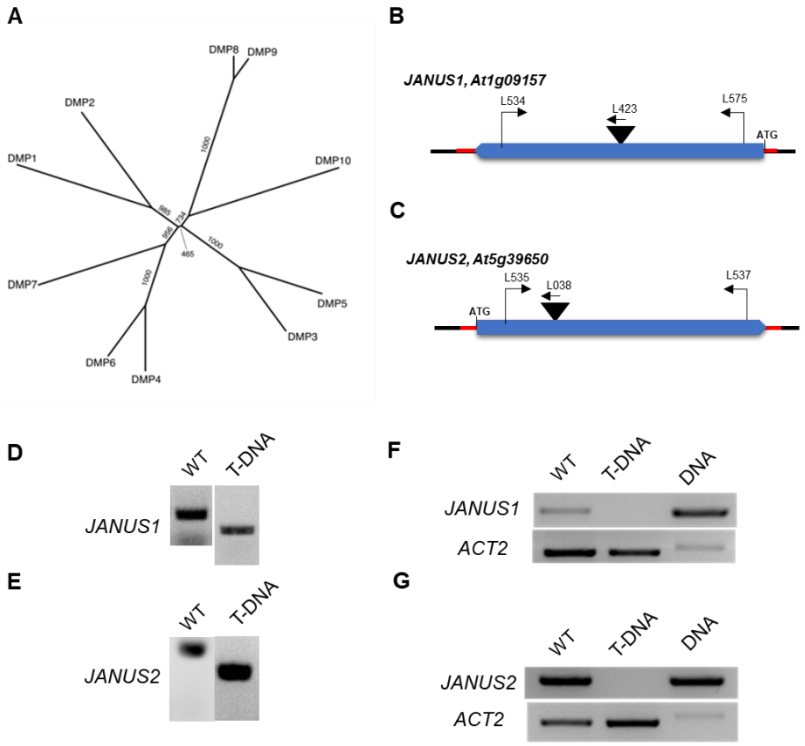

Figure 3.1 Phylogeny of JANUS protein family and JANUS1 and JANUS 2 gene structure and mutant analysis. (A) Unrooted phylogenetic tree built from aligned DMP (JANUS) protein sequences (*adapted from Kasaras, et. al. 2013*). Gene structure of *JANUS1 (B)* and *JANUS2 (C)*, showing location of primers used in this study. Black triangle represents T-DNA insertion. Red bar indicates 3' and 5' untranslated regions. Blue boxes show exons. Confirmation of *janus1* (D) and *janus2* (E) heterozygous T-DNA insertion lines. RT-PCR expression analysis of *janus1 (F)* and *janus2* (G) homozygous T-DNA insertion lines.

JANUS1/2 are specifically expressed in Arabidopsis male gametes and are verified interactors of the SC-expressed *TET11* and *TET12* (unpublished results from Leonor Boavida). The fertility defects observed in *janus1/2* double mutant (Fig. 3.2A) were recently reported to be due to the inability of SCs to fuse with the egg cell (EC) (Cyprys et al., 2019). A second publication reported that *janus1/2* produces approx. 2% of haploid progeny (Yu et al., 2020). However, the mechanisms and the causes of these two independent phenotypes are not understood.

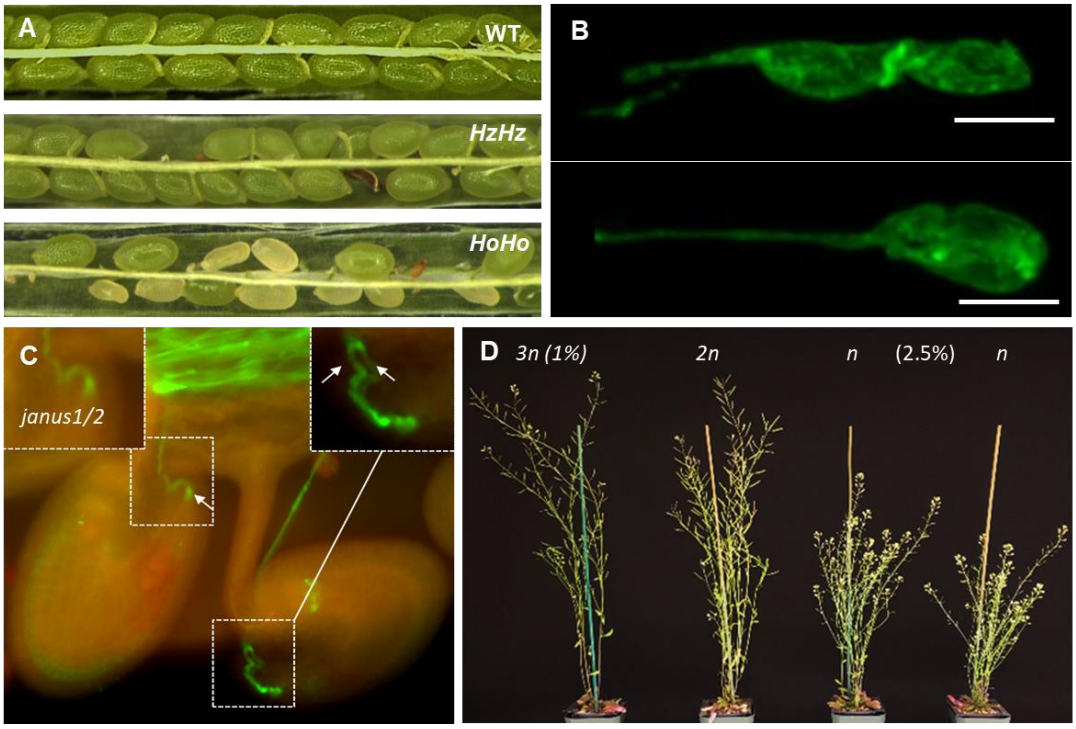

Figure 3.2 Phenotypes associated to *janus1/2* mutants. **(A)** Representative images of siliques from the wild type (Col), *janus1/2* heterozygous mutant, and *janus1/2* homozygous mutant. **(B)** Representative images of SCs pair morphology in *janus1/2* mutants. 32% of the SCs show a spindle morphology (top), 68% show the extended adhesion domain (bottom). Scale bars = 5 µm. **(C)** Representative image showing multiple pollen tubes targeting the same ovule (polytubey) in a *janus1/2* mutant. **(D)** Self-cross of *janus1/2* results in triploid (3n), diploid (2n), and haploid progeny (n).

In parallel with the work of these two groups, Leonor Boavida found that *janus1/2* mutants have alterations on the MGU assembly (Fig. 3.2B). In the double mutant, the two SCs adhere to

each other through an extended plasma membrane domain, that contrasts with the typical SC-SC adhesion that assembles the MGU in a spindle-like form (Fig. 3.2B). In *janus1/2* double mutant the two SCs fail to separate upon their delivery into the embryo sac leading to delayed or impaired SC fusion with female gametes. This defect triggers attraction of multiple pollen tubes towards a single ovule (polytubey effect) (Fig. 3.1C). Eventually, some of the delivered SC pairs (> 1 SC pair) will fuse with the egg and central cell. Exposure of female gametes to an excess of sperm cells lead to multiple sperm cell fusions (polyspermy) producing polyploid progeny (Fig. 3.2D). Usually polyspermy in the central cell leads to abnormal endosperm development and eventual abortion due to excess paternal genome (2m:>1p) (Dilkes et al., 2008). A polyspermy block in the egg cell usually prevent multiple sperm cell fusions. However stimulation or release of sperm membrane signaling factors could be sufficient to induce egg activation (Kelliher et al., 2017) without paternal contribution (haploid induction) if a balanced maternal : paternal (2m:1p) ratio is achieved in the endosperm (Fig. 3.2D) (Barroso et al., 2009; Kelliher et al., 2017). JANUS proteins are therefore essential for multiple aspects of cell-cell interactions during double fertilization. We believe the phenotypes associated occur due to impaired or defective cell-cell signaling across the plasma membranes.

Structural homology modelling showed JANUS proteins have high similarity to matrix metalloproteases (MMPs) (Kwok Ki Ho, unpublished). MMPs belong to a family of proteases which require zinc and/or calcium for catalytic activity. They have been well studied in mammals but are also found in plants (Marino and Funk, 2012). Studies in animal systems show that MMPs are important for remodeling of the extracellular matrix (ECM) and are involved in cellular processes like cell migration, adhesion, and signaling (Marino et al., 2014). In animals, the ECM is complex, forming a network of polysaccharides and proteins. MMPs are secreted into the ECM

space and degrade or cleave proteins, leading to their recognized function as ECM remodelers (Marino and Funk, 2012). Five genes encoding MMP-like proteins were identified in *A. thaliana* (Maidment et al., 1999). The five *AtMMPs* (denoted as *MMP1 to MMP5*) are expressed throughout the plant and have been detected in the root, stem, leaf, and flowers of *A. thaliana* (Flinn, 2020). Currently, little is known about the mechanism underlying MMP function in plants but homologues in soybean and cucumber were found to have roles in leaf expansion/development and senescence (Delorme et al., 2000).

Although extensive research has been performed to identify factors that regulate male-female gamete interactions, the knowledge of signaling pathways and factors required for SC-SC or SC-egg cell interactions are still lacking. We have identified a potential signaling pathway in double fertilization that may function through the regulation of Tetraspanin-JANUS complexes. Since JANUS1/2 functions as a negative regulator of sperm cell-sperm cell adhesion, a major goal of this study was to understand how this process is mediated.

In this Chapter, we examined JANUS1/2 protein structure to identify potential functional domains. We also examined the hypothesis that GEX2, a SC adhesion factor required for male-female gamete adhesion, could also function as a homotypic (SC-SC) cell adhesion factor in *Arabidopsis* sperm cells.

3.3 Materials and Methods

3.3.1 Plant Material and Growth Conditions

Mutant lines and ecotypes if not otherwise indicated were obtained from ABRC stock center (https://abrc.osu.edu/). *Arabidopsis* seeds were surface sterilized using the vapor phase methodology with chlorine gas. Briefly, seeds were aliquoted into 1.5mL eppendorf tubes at ~

30µL volume. The eppendorf tubes containing the seeds were placed open in a desiccator located in a fume hood. Three ml of concentrated HCl was quickly added to a beaker containing 50 mL of bleach (5-10% NaOCl) and the desiccator was immediately sealed. Primary transformants were sterilized for 4-6 hours and F2 seeds or greater were sterilized for 2 hours. After sterilization, seeds were removed from the desiccator and covered with aluminum foil to avoid contamination. The seeds were transferred to a flow hood and the tubes were left open for 30 minutes to allow diffusion of chlorine gas before plating. Sterilized seeds were plated on 1x basal Murashige and Skoog (MS) (Sigma) medium supplemented with Gamborg vitamins (Sigma), 0.5 g L^{-1} MES (Sigma), 1% (w/v) sucrose (Fisher Scientific), and 0.8% (w/v) plant agar (Fisher Scientific) and the pH adjusted to 5.7. Seeds were stratified for 48 h at 4°C in the dark before transfer to a growth chamber with long-day conditions (16 h light/8h dark at 21°C) Transgenic plants and mutant lines were selected in MS medium containing the appropriate selection agent. After 14 days seedlings were transferred to soil and grown in short-day conditions (8h light/16 h dark at 22°C) for 2 weeks to promote vegetative growth. Flowering was induced by transferring the plants to long day conditions (16h light/8h dark) with day/night temperatures of 22°C/18°C.

All transgenic markers lines used in this study were previously generated (Boavida et al., 2013 and unpublished results from Leonor Boavida). The *quartet 1-2* (*qrt1-2*) mutant (Preuss et al., 1994) in the Columbia ecotype was used for stable transformations. Ten to twenty resistant plants resulting from each transformation were analyzed for expression pattern and single insertions. One or two lines with stable GFP expression were chosen for propagation, used to recover homozygous lines and for further analysis. Lines with possible phenotypes in plant development and seed set were discarded if not related with protein expression levels. All the analysis of this study was performed using homozygous stable lines.

3.3.2 DNA Extractions

DNA extractions were performed according to (Edwards et al., 1991; Cenis, 1992) with small adaptations. DNA extraction buffer was prepared with 1M Tris HCl (pH: 8), 5M NaCl, 0.5M EDTA, and 20% SDS. Young, fresh rosette leaves were collected and grinded in a 1.5 ml eppendorf tube with 300 ul of DNA extraction buffer using a plastic pellet or a grinding machine. 150 ul of 3M sodium acetate (pH = 5.2) was added to the tube. The samples were vortexed and incubated at -20^{o}C for 10 minutes. After incubation, samples were spun at 14,800 rpm for 3 minutes. The supernatant was transferred to a clean 1.5 mL eppendorf tube. Isopropanol was added at a 1:1 ratio (450ul). Samples were incubated at room temperature (RT) for 15 min before centrifugation at 14,800 rpm for 5 min. The supernatant was removed, and the DNA pellet washed by adding 450ul of ice-cold 70% ethanol. The samples were spun for 1 minute at 14,800 rpm. The ethanol was removed, and samples were air-dried for 1 hour before elution with 30 ul of 1x TE buffer. Extracted genomic DNA was stored at -20^{o}C.

3.3.3 Characterization of Insertion and Marker Lines

Genotyping of *janus1/2* (SK30238/ SK29952), *tet11* (SAIL_897_B02), and *gex2* (FLAG_441D08) homozygous mutant lines was performed by PCR using genomic DNA extracted from individual plants. All PCR amplifications used DreamTaq polymerase (ThermoFisher) according with the manufacturer's instructions. Two primer pairs were used to determine the plant genotype. For TET11 SAIL line the primer pairs were L151 and L152 for the genomic region flanking the T-DNA insertion and the second primer pair L151 and L040 were used as a gene specific primer and as T-DNA left border specific, respectively. For *GEX2* FLAG line the primer pairs were L458 and L498 for the genomic region flanking the T-DNA insertion and the second primer pair L039 and L498 were used a primer specific to the T-DNA left border and a gene

specific primer, respectively. For *JANUS1/2* SK lines the primer pairs used were L534, L575 and L537, L535 respectively for the genomic region flanking the T-DNA insertion. The second primer pair for *janus1 and2* T-DNA insertion used L575/L423 and L535/L038 as gene specific and T-DNA specific primers pairs. Sequences of the primers used in this study can be found in Appendix A.

3.3.4 Seed Set Analysis

Pistils with 7-10 Days After Pollination (DAP) were collected from self-pollinated plants and dissected under a stereoscope to expose ovules. The number of developing seeds, aborted seeds, and undeveloped ovules were counted for each silique. A minimum of 5 siliques were used for the quantification of seed set.

3.3.5 Pollen Germination Assays

Arabidopsis pollen was collected from fresh day open flowers and germinated *in vitro* as previously described (Boavida and McCormick, 2007). Briefly, ~ 40 open flowers were incubated in 1 mL of freshly prepared pollen germination medium (5mM $CaCl_2$, 0.01% H_3BO_3, 5mM KCl, 10% sucrose, 1mM $MgSO_4$, pH adjusted to 7.5-7.8) and vortexed for 3 minutes to release the pollen from anthers. After removing flower parts and debris with a tweezer, the solution was centrifuged at 8,000 rpm for 3 min and the supernatant removed. The pollen pellet was then resuspended in 100-200 µL of fresh pollen germination medium, depending on the size of the pellet. The pollen solution was transferred to a 25mm glass bottom petri dish coated with 0.01% poly-L lysine (Sigma). The dish was placed in a humidity chamber as described in (Johnson-Brousseau and McCormick, 2004) and incubated at 22^{o}C for 4 hours.

3.3.6 Microscopy Imaging and Data Processing

For quantification of protein enrichment in sperm cells, germinated pollen tubes were imaged using a spinning disk CSU-10 confocal head (Yokogawa Electric) mounted on a Zeiss Observer.Z1 inverted microscope equipped with a Prime 95B camera (Teledyne Photometrics) and controlled by Slidebook software (Intelligent Imaging Innovations). Optical sections of 0.25 µm were collected from sperm cell pairs expressing single or double fluorophores were acquired using a 100x Plan-APO oil-immersion objective (1.46 NA) with the following settings: GFP and mCherry excited by 488 nm and 561 nm laser lines, respectively. Samples were exposed for 500 *ms* using 30% laser power using the respective band-pass filters (482/35 and 617/73; Semrock). A minimum of 20 sperm cell pairs were analyzed for quantification.

Image analysis and 2D projections were performed using ImageJ/Fiji (Schindelin et al., 2012). All images were processed using the following functions available in Fiji prior to analysis: smooth, sharpen, de-speckle, and background subtraction with a rolling-ball radius of 30 pixels. To quantify fluorescent intensity, median optical sections from sperm cell pairs were selected and a freehand line (width = 5 pixels) was drawn on the SC-SC adhesion domain and outer sperm membrane and the mean intensity value recorded. Relative intensity was determined as the ratio between the mean fluorescence intensity at the adhesion domain and the outer sperm membrane. Co-localization analysis was carried out using the Fiji plugin Coloc2 (Schindelin et al., 2012).

3.3.7 Statistical Analysis

Statistical analysis and graphs were generated using R (R Development Core Team, 2010) and GraphPad (Prism version 8.4.2; GraphPad Software). One- or two-way *ANOVA* was used to analyze significant differences between multiple groups. Unpaired *Student's t-test* was used to determine statistical significance between two groups.

3.3.8 Plasmid Construction and Plant transformation

All PCR amplifications were performed from genomic DNA using Phusion Taq polymerase (Fisher), according to the manufacturer's instructions. All clones were constructed using Gateway technology (Invitrogen). For complementation analyses, PCR fragments corresponding to *JANUS2* promoter (R021 and R022), *JANUS2* N-terminal truncation (R003 and R004), *JANUS2* C-terminal truncation (R005 and R006), site directed mutagenesis replacing two aspartic acid (D) residues with Alanine (A) in the *JANUS2* coding sequence (D156A and D176A) corresponding to the putative catalytic domain (R004 and R005), *DMP1* coding sequence (R001 and R002), or *DMP10* coding sequence (R007 and R008) (Fig. 3.4) were amplified using the noted primer pairs and following the conditions previously described. Full primer sequences can be found in Appendix A. The PCR products were purified with the QIAquick PCR Purification Kit (Qiagen) and cloned via a BP reaction into pDONR-221 (Invitrogen) and verified by sequencing. The pK2GW7 was digested with the restriction enzymes SacI-HF and SpeI-HF (New England Biolabs) to remove the 35S promoter. The PCR product of the *JANUS2* promoter was amplified, equally digested, and ligated into pK2GW7. The pK2GW7 with the *JANUS2* promoter, now referenced as *JANUS2prom*-pK2GW7, was used as the destination vector in all LR reactions performed with the described BP clones to generate the final expression constructs. These constructs were transformed into *A. thaliana* using the Agrobacterium flower dip method (Zhang et al., 2006) to generate stable transgenic lines. Positive transgenics were selected in plates containing the appropriate antibiotic as previously described.

3.3.9 Sequencing Reactions

All sequencing reactions were performed using the Sanger method. Prior to December 2019, sequencing reactions were performed using Purdue's Genomic Core Facility. Reactions that occurred following January 2020 were performed by Genewiz.

Purdue Genomics Core Facility: 10 µl reactions were used for Sanger sequencing. 5 µl of PCR product template diluted with water was provided at a concentration dependent on product size (100-200 bp: 3 ng/ µl; 200-500 bp: 10 ng/µl; 500-1000 bp: 20 ng/µl; 1000-2000 bp: 40 ng/µl; plasmid DNA: 10 ng/µl). 10 µM of the respective primer was added with 2 µl of Terminator Ready Reaction mix and Big Dye Sequencing Buffer (Fisher). Sequencing reactions were performed in a thermal cycler with the following conditions: *1)* 96 ^{o}C for 1 min; *2)* 96 ^{o}C for 10 sec; *3)* appropriate primer annealing temperature for 5 sec; *4)* 60 ^{o}C for 4 min. After the reaction, the sequencing products were precipitated by adding an equivalent volume of water, 2 µl of 3M NaAc (pH: 4.6), 2 µl of 0.125M EDTA, and 50 µl of 100% ethanol. The solution was transferred to a 1.5 mL eppendorf tube, vortexed, and stored at -20 ^{o}C for 10 min upon which the mix was centrifuged at 14,800 rpm for 15 min at RT. The supernatant was carefully removed, and the pellet washed twice with ice-cold 70% ethanol. The pellet was left to dry in the dark for 1 hour, before elution in 15 ul of MiliQ water. The sequencing products were then delivered to Purdue's Genomic Core Facility.

Genewiz: The purified PCR product, was mixed with the appropriate primer according to the Genewiz guidelines for Sanger sequencing and shipped for the sequencing reaction.

All sequences were analyzed with SnapGene software (GSL Biotech LLC).

3.4 Results and Discussion

3.4.1 JANUS1/2 Structural and Functional Analysis

The Arabidopsis *DMP8/9* (*JANUS1/2*) share 90% of amino acid similarity but have significant differences from other members of the family, forming a clade of their own (Fig. 3.1A). These differences suggest that the two proteins may have functions that are unique to sperm cells. JANUS1 and JANUS2 are predicted to have four transmembrane domains with a long N-terminal sequence and a C-short terminal domain. The proteins lack a recognizable signal peptide or any other annotated functional domain.

Simulations using structural homology modelling (in collaboration with Dr. Kwok Ki Ho, a research specialist in the lab) identified structural similarities of JANUS1 protein with a class of metalloproteases in humans, the collagenase 3 protein also known as matrix metalloprotease 13 (MMP-13) (Fig. 3.3A) (Stura et al., 2013). In animals, there are numerous examples of TET-MMP interactions where Tetraspanins function in cell adhesion through the regulation of matrix metalloprotease (MMP) expression at the cell surface (Bourboulia and Stetler-Stevenson, 2010). For instance, silencing of Tetraspanin CD9 suppresses expression of MMP ADAM17 in human endothelial cells (Gutiérrez-López et al., 2011). CD9 also mediates the interaction between ADAM2, an MMP, and the integrin $\alpha 6\beta 1$ to promote adhesion and fusion between rodent egg and sperm (Chen et al., 1999). Interestingly, Testase 1 (ADAM24) a sperm surface metalloprotease prevents polyspermy at the level of the oocyte plasma membrane in mice (Zhu et al., 2009).

JANUS1/2 contain some basic features of metalloproteases while it lacks others. Metalloproteases are translated as inactive proteins, requiring the removal of a prodomain to become functional (Hadler-Olsen et al., 2011). Two primary mechanisms are known to induce activation in MMPs. The first is cleavage and removal of the prodomain either by another protease

or by autolytic cleavage. The second mechanism is allosteric activation of the MMP, wherein an interacting partner induces the displacement of the prodomain from the catalytic region allowing for activation (Hadler-Olsen et al., 2011). The long N-terminus domain of JANUS is particularly rich in Prolines, motifs usually involved in protein-protein interactions (Ball et al., 2005). The N terminus ends with a conserved furin cleavage motif (Schaller and Ryan, 1994) (Fig 3B). Furin-like proteins have been identified in plants (Schaller and Ryan, 1994) and show homology to subtilisin-like serine proteases (Hirokazu et al., 2001).

Metalloproteases share a conserved structural topology that comprise a catalytic domain containing three histidine residues that constitutes a zinc-binding domain and a "methionine turn"

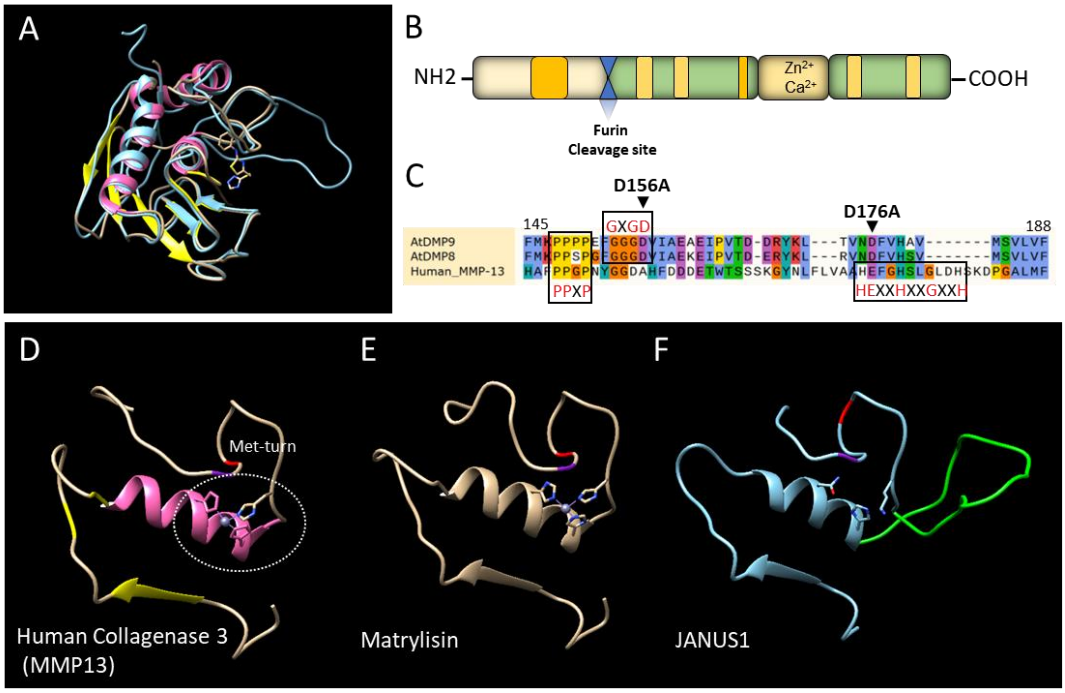

Figure 3.3. Structure homology modeling of JANUS1 with the human collagenase 3 (MMP13) and Matrylisin. (A) Overlap of structural model of MMP13 and JANUS1 as predicted by Chimera (Petterson, EF. et. al., 2004); (B) Predicted protein model for JANUS1/2 (DMP8/9) showing pro-domain, predicted furin–cleavage site (Blue), location transmembrane domains (yellow), pro-rich domains (orange) and predicted Zn^{2+}/Ca^{2+} catalytic/binding site; (C) Amino acid sequence alignment of JANUS1/2 and MM13 catalytic domain showing predicted SH3-binding motif (PPXP) adjacent to aspartyl-protease motif (GXGD), followed by the Zn^{2+} and Ca^{2+}-binding metalloprotease catalytic site (HEXXHXXGXXH) missing 2 critical histidine residues in JANUS1/2 (DMP8/9). D156A and D176A indicate location of targeted mutated residues; (D-F) Minimal structure required for metalloprotease catalytic activity of human collagenase 3 (D), Matrylisin (E) and corresponding region in JANUS1 (F).

that lies close to the catalytic domain and is required for its activity (Fig. 3.3D). Matrylisin represents the minimal structural organization required for MMP activity (Uría and López-Otín, 2000) (Fig. 3.3E). The typical metalloprotease catalytic site (HEXXHXXGXXH) contains three histidines (Fig. 3.3C). JANUS1 shares the same topology (Fig. 3E-F), containing the Met-turn needed for catalytic activity with an alpha helix and the spatial placement of amino acid residues hypothesized to be necessary for catalytic function, but lacks two of the histidine residues and has an extra-long loop close to the catalytic domain (Fig. 3.3C-F). JANUS structural organization is well conserved (Fig. 3.3D and F). We identified a second motif, the GXGD motif (Fig. 3.3C), upstream the predicted metalloprotease catalytic site which functions as a catalytic site in intramembrane peptidases (I-CLIPS) (Ha, 2009). Adjacent to the GXGD motif we found a Src Homology-3 (SH3) domain (Fig. 3.3C), a proline-rich motif which could function as a intracellular substrate binding site (Landgraf et al., 2004).

The similarity between metalloproteases and JANUS proteins led to the hypothesis that JANUS1/2 may function as a metalloprotease or intramembrane protease. Accordingly, these two proteins share stark differences from other DMP members (Fig. 3.2A and Fig 3.4A) which miss most of the identified motifs and topology. These observations lead us to hypothesize that JANUS1/2 may perform unique functions within their protein family.

To test this hypothesis, we examined whether other DMP family members (*DMP1* and *DMP10*) (Fig. 3.1A and 3.4A) complement the *janus1/2* phenotype in sperm cells. *DMP1* is a membrane protein that was implicated in membrane fission during ER and tonoplast breakdown during leaf senescence and is required for membrane fusion during vacuole biogenesis in roots (Kasaras et al., 2012). *DMP1* is one of the two family members with lower similarity to *JANUS1/2*.

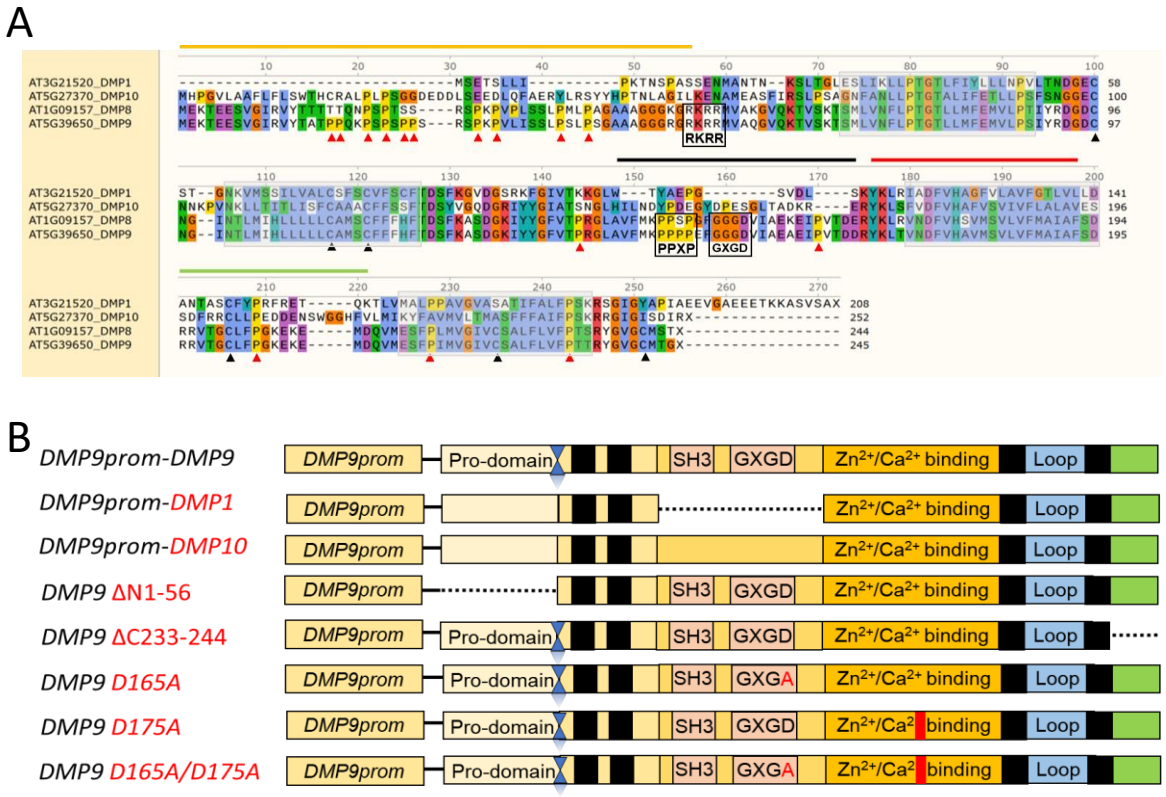

Figure 3.4. (A-B) Amino acid sequence alignment of DMP1, DMP10, DMP8 and DMP9 and schematic of constructs used to address JANUS2 (DMP9) functional motifs. Transmembrane domains are boxed shaded in grey. Yellow bar indicates JANUS1/2 pro-domain with predicted RKRR furin-cleavage site. Black bar highlights predicted SH3-motif (PPXP) and aspartyl-protease catalytic motif (GXGD) unique to JANUS1/2. Red bar indicates predicted zinc-binding motif missing the two Histidines from the canonical metalloprotease (HEXXHXXGXXH) catalytic motif. The green bar indicates intracellular loop only present in JANUS1/2. Red arrows highlight conserved prolines and black arrows conserved cysteines. (B) Complementation constructs (*JANUS2prom:DMP1* and *JANUS2prom:DMP10*), *JANUS2* N-terminus (*JANUS2ΔN1-53*) and C-terminus (*JANUS2ΔN233-244*) truncation and constructs containing mutations that replace the aspartic acid (D) by Alanine (A) on the predicted GXGD motif (D165A) or on the predicted metalloprotease catalytic domain (D176A). Blue hourglass indicates prodomain cleavage site only present in JANUS2.

Comparison of amino acid sequences revealed that *DMP1* lacks the hypothesized pro-domain found in *JANUS1/2* (Fig. 3.4A) and all the region containing the predicted SH3-like binding site and aspartyl-protease (GXGD) motifs. *DMP10* is the closest related member to *JANUS1/2* (Fig. 3.1A). Transcripts of *DMP10* were also detected in *A. thaliana* flowers (Kasaras and Kunze, 2010), but are absent from pollen and SCs. Both DMP1 and DMP10 do not contain the predicted furin-cleavage site (RKRR) and several of the conserved cysteine and proline residues found in

JANUS1/2 protein sequence. In addition, the SH3-like binding and aspartyl-protease catalytic motif seem to be unique to JANUS1/2 proteins (Fig. 3.4A and B).

We generated constructs expressing *DMP1* and *DMP10* driven by the *DMP9* promoter and transformed these constructs into the wild type (*Col qrt*) and *janus1/2* double mutant. We examined 45 primary transformants in *Col qrt* and in *janus1/2* background. The results presented here are representative of a preliminary analysis of primary transformants (T1 generation). Further confirmation and characterization of the phenotypes in stable lines (T2 and following generations) need to be performed.

Our analysis indicates that both *DMP1* and *DMP10*, when ectopically expressed in wild type cause fertility defects (Fig. 3.5A and B). Consistently *DMP1* and *DMP10* expression in sperm cells of *janus1/2* double mutant (Fig. 3.5) did not rescue the seed set phenotype and increased the proportion of abnormal seeds (Fig. 3.5A and B). Most plants show varying degrees of pollen abortion suggesting that the ectopic expression of these two proteins has negative consequences in pollen development.

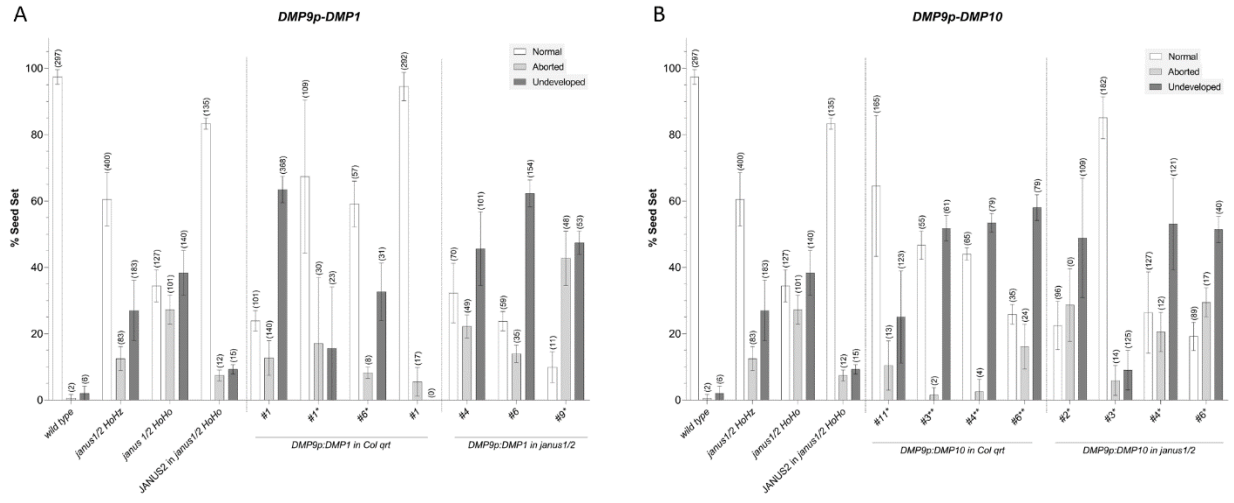

Figure 3.5. *DMP1* and *DMP10* ectopic expression in sperm cells causes deleterious effects in double fertilization. Representative transgenic T1 lines are shown for each background, *Col qrt* (wild type) and *janus1/2*. (A) Quantification of seed sets in T1 *DMP9prom::DMP1* transgenic lines (B) Quantification of seed sets in T1 *DMP9prom::DMP10* transgenic lines.

No function has been assigned to *DMP10*, but *DMP1* was implicated in membrane remodeling affecting both the ER and the vacuole (Kasaras et al., 2012). Our findings also support a function of JANUS1/2 as membrane remodelers. This experiment demonstrates, however, that JANUS1/2 are indeed unique within the DMP protein family performing essential functions in SCs, possibly by targeting specific substrates in sperm cells. While only two of the fellow members were tested in this experiment, it is likely that these results remain consistent when compared to all the DMP protein members.

In Chapter 2 we have shown that both *mCherry-JANUS2* and *JANUS2-GFP* fusions are non-functional proteins, however the untagged JANUS2 coding sequence, under control of the native promoter, is sufficient to complement the *janus1/2* phenotype (Fig. 3.5, Leonor Boavida *unpublished results*). Moreover, the expression levels and the subcellular localization of these two proteins fusions are drastically different. These observations suggested that both JANUS2 N-terminus and C-terminus have essential functions.

We thus generated N-terminus (*DMP9prom*::*DMP9* ΔN1-56) or C-terminus (DMP9prom::*DMP9* ΔC233-244) *JANUS2* truncated constructs and expressed them in wild type and *janus1/2* mutant background. We analyzed 66 primary transformants for seed set phenotypes (Fig. 3.6). The analysis of transformants from the T1 generation seems to confirm our hypothesis. JANUS2 N-truncated construct, when expressed in Col *qrt*, resulted in a significant increase of aborted and undeveloped ovules (Fig. 3.6A). This truncated protein was also unable to complement the *janus1/2* phenotype and led to an increased number of undeveloped ovules which likely result from failed gamete fusions. The expression of *JANUS2* C-terminus truncation constructs also resulted in an increased seed abortion in the Col *qrt* background, but with predominance of aborted

ovules that usually result from unbalanced fertilization events (Fig. 3.6B). Consistently the construct did not rescue the *janus1/2* mutant phenotype.

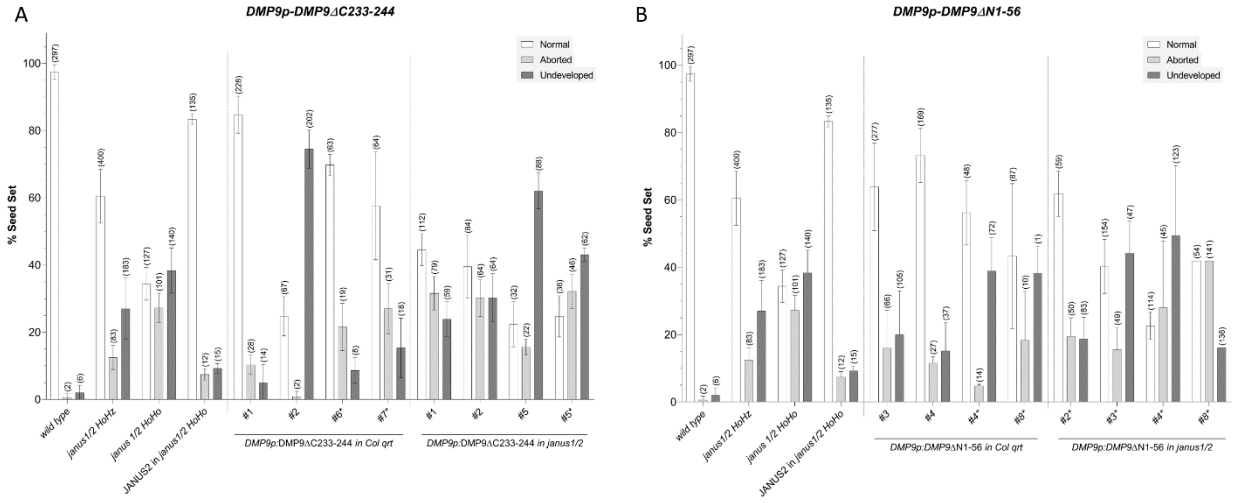

Figure 3.6. Analysis of *JANUS2* (*DMP9*) N- and C-terminus truncation constructs. Representative transgenic T1 lines are shown for each background, Col qrt (wild type) and *janus1/2*. (A) Quantification of seed sets of *DMP9prom*::*DMP9* ΔN1-56 and (B) *DMP9prom*::*DMP9* ΔC233-244 transgenic lines.

While the results presented here are still preliminary and we cannot conclusively assign a specific function to the domains tested, we can predict some characteristics based on the structural analysis and observations from the fluorophore-protein constructs. Both the GFP and mCherry fusion were successfully targeted to the plasma membrane (see Chapter 2 for more information) but show different levels of expression and localization patterns. The *JANUS2* N-terminus is extremely rich in prolines, providing sites for potential protein-protein interactions. The N terminus also contains the predicted cleavage motif of the *JANUS* pro-domain. In animals, the pro-domain of metalloproteases seems is cleaved in the ER (Kang et al., 2002) after which the protein is secreted as catalytically active (Seals and Courtneidge, 2003). Tetraspanins have been shown to promote metalloprotease maturation and trafficking to and from the cell surface (Saint-Pol et al., 2017). We know by BIFC analysis *in planta*, that TETs and JANUS interact in the ER and at the plasma membrane, suggesting that TET-JANUS complexes form in the ER before trafficking to

the plasma membrane. The *mCherry-JANUS2* construct is weakly detected in the SC membrane, *albeit* some enrichment at the SC-SC interface, co-localizing with *TET11-GFP* (Chapter 2). However, the protein seems to accumulate in bright, vesicle-like, cytoplasmic endomembrane structures, suggesting that the N-terminus fluorophore fusion might be interfering with cleavage of the pro-domain and exit from the ER to the plasma membrane, which would explain the reduced expression at the cell surface. If the N-terminus is required for ER exit, through interactions with the Tetraspanins, or if TETs are required for JANUS maturation needs to be address with further experiments.

In contrast, *JANUS2-GFP* shows clear localization and an even distribution at the SC plasma membrane with a skewed enrichment at the SC-SC interface. The levels of protein expression are however, 100-fold above those typically detected for *TET12* in SCs, despite their mRNA levels being similar (data not shown). This may indicate that *JANUS2-GFP* is trafficked to the plasma membrane and somehow stabilized. Though the SC-SC interface domain is visible, the enrichment is not as pronounced as for *TET11*, suggesting that *JANUS* enrichment at the SC-SC interface may depend on TET interactions. There are several possible explanations for the observed accumulation and even localization of *JANUS2* at the SC surface: The C-terminus domain is involved in JANUS-TET interactions, which in turn modulate its expression at the membrane maybe through regulation of *JANUS* autocatalytic activity. A second possible explanation is that the C-terminus contains an endocytic signal which might be blocked on JANUS2-GFP. While all these hypotheses need to be further explored, the phenotypes indicate that both the N- and C-terminus play essential functions in the localization and activity of the protein. Co-localization, expression studies (e.g. BIFC), and assays *in planta* using truncated forms

of the protein and imaging of subcellular localization/interactions with TETs should provide clarification on the function of specific domains.

Finally, we generated three different constructs to address the function of predicted catalytic domains in JANUS proteins. As previously mentioned, JANUS has a conserved topology and several conserved amino acid residues with similarities to the MMP catalytic domain (HEXXHXXGXXH) but lack two of the three critical histidine residues (the first and the 3rd histidine). The histidine (H), the glutamic acid (E) and the glycine (G) are conserved, invariable residues in the catalytic site of all metalloproteases. It has been shown that mutations of the glutamic acid (E) of MMP catalytic site is sufficient to abolish the catalytic activity of MMPs (Arza et al., 2001).

We thus reasoned that a mutation in the aspartic acid (D176A) of JANUS, corresponding to the glutamic acid (E) in the MMP catalytic site, could provide information about possible activity of this predicted domain. We also identified homology with a second motif (GXGD), located upstream the predicted MMP catalytic domain, which is present in aspartyl-peptidases (Fig. 3.4A). We generated a construct with a similar mutation in the aspartic acid (D165A) of this motif as well as a third construct where the two mutations were present simultaneously (D165A/D176A) (Fig. 3.4B). We hypothesized that, if D165 and D176 are essential for catalytic function, these constructs would be unable to complement the *janus1/2* fertilization defects. We obtained 14 primary transformants containing mutations in both catalytic sites. In the background of Col *qrt*, the expression of *DMP9prom::DMP9 D165A/D175A* lead to significant fertilization defects with the presence of numerous aborted and unfertilized ovules (Fig. 3.7). Consistently, *janus1/2* phenotype was not rescued by this construct (Fig. 3.7), suggesting that either one or both residues are responsible for JANUS2 function. Transgenic lines containing individual mutations can

provide further insights into the specificity of the domain which might be involved in JANUS1/2 function in *Arabidopsis* SCs. As mentioned previously, this graph shows preliminary data from primary transformants. Stable lines must be isolated before identifying a consistent phenotype and determining statistical significances on the observed values. Further biochemical studies will confirm the association of one or both residues with potential catalytic activity of JANUS2 as an intramembrane protease or as a zinc/calcium-dependent metalloprotease.

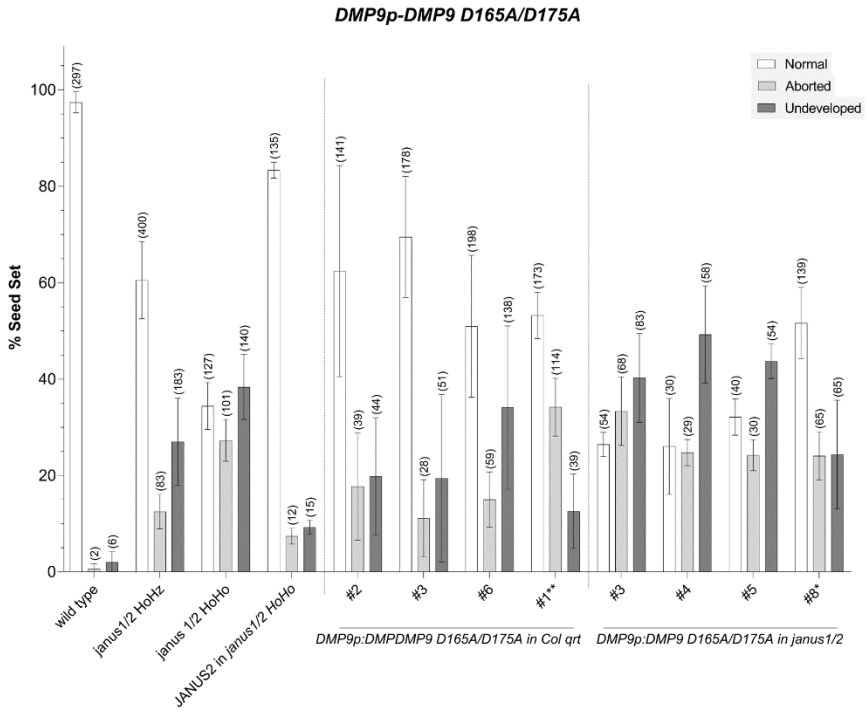

Figure 3.7 Seed set analysis of transgenic lines transformed with a construct containing a double mutation in two of the predicted catalytic residues of JANUS2 (*DMP9prom:DMP9 D165A/D175A*). Representative transgenic T1 lines are shown for each background, *Col qrt* (wild type) and *janus1/2*.

Since all these constructs cause defects in fertility when introduced into the wild type background, we should assume that the modified, exogenous protein interferes with the native protein function likely acting in a dominant negative interaction.

3.4.2 GEX2 Contributes to Increased Sperm Cell-Sperm Cell Adhesion in *janus1/2*

JANUS1/2 functions as a negative regulator of SC-SC adhesion, meaning that the proteins are not directly implicated as a physical adhesion molecule, but regulate expression or localization of a potential adhesion molecule. The predicted function of JANUS1/2 as a membrane remodeler seemingly fits with our hypothetical model: JANUS2 interacts directly with an adhesion molecule, which is recruited to the SC-SC Tetraspanin-enriched microdomain through JANUS-TET interactions. At the SC-SC adhesion domain the adhesion molecule is protected from unspecific interactions occurring at the SC plasma membrane. In the absence of JANUS1/2, the adhesion factor is not recruited to the SC-SC interface, spreading through the SC surface which leads to increased SC-SC adhesion. It is also possible that JANUS1/2 are activated by interactions with TETs, acting as a membrane sheddase or protease exposing or degrading the adhesion molecule in SCs. GEX2 functions as an adhesion factor between male and female gametes in double fertilization (Mori et al., 2014). We hypothesized that GEX2 could also function as an adhesion factor between the twin SCs. To test this hypothesis, we developed a triple *gex2/janus1/2* mutant. We expected that, if GEX2 is the adhesion factor promoting the extended adhesion between *janus1/2* sperm cells, introducing *gex2* mutant into the *janus1/2* background would decrease the proportion of SC-SC pairs with extended adhesion phenotype, that would be able to successfully separate but would have delayed SC-egg adhesion resembling the gex2 mutant phenotype. In contrast, increased expression of *GEX2* (*GEX2-GFP*) in the *janus1/2* background would lead to a higher proportion of SC-SC pairs showing the extended adhesion phenotype likely resulting in an increased seed abortion.

To test this hypothesis, we generated a triple *gex2/janus1/2* mutant and examined the seed set in the triple mutant (Fig. 3.8). The seed set was highly variable, reflecting an intermediate

phenotype between *janus1/2* and *gex2* mutants. The number of undeveloped ovules was not affected when compared to *janus1/2* (Fig. 3.8).

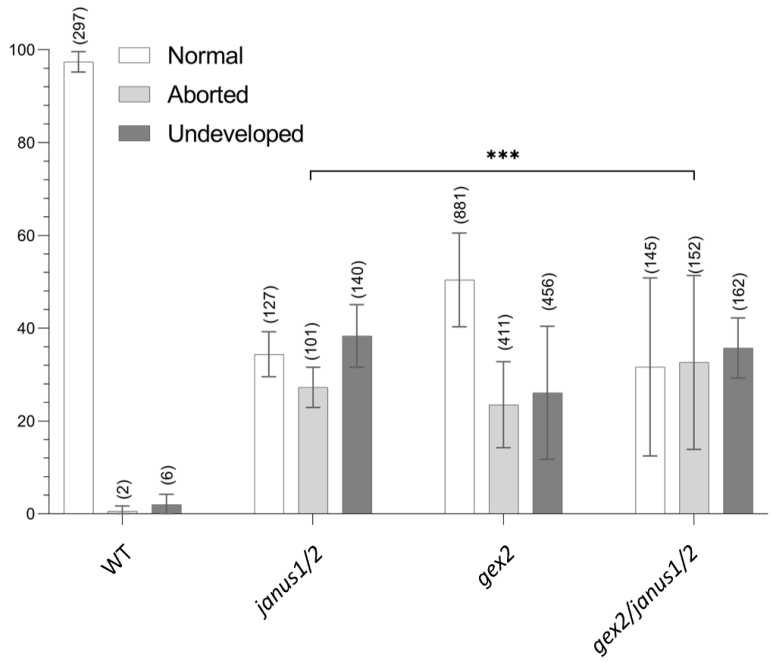

Figure 3.8. Seed set analysis of the triple *gex2/janus1/2 mutant*. Seed set quantification is shown for wild type (*Col qrt*), *janus1/2* homozygous, *gex2* homozygous, and *gex2/janus1/2* triple mutant. Number of ovules analyzed is shown between bracts. A 2-way ANOVA followed by Tukey's multiple comparison was used to determine statistical significance. *** $p < 0.01$

While these results are not conclusive, the absence of *gex2* seems to increase the probability of fertilized ovules, which might be due to a lower proportion of sperm cells presenting an extended adhesion. Moreover, this data provides evidence that GEX2 may contribute the extended adhesion phenotype observed in *janus1/2* SCs.

When we introduced GEX2-GFP into the *janus1/2* background we observed a significant reduction in the proportion of undeveloped ovules and an equivalent increase of aborted ovules (Fig. 3.9), which agrees with the hypothesis that an increase of GEX2 expression leads to more SC pairs with increased SC-SC adhesion that fail to separate during double fertilization. In this case more polyspermic fusions are expected, explaining the increase on the number of aborted ovules.

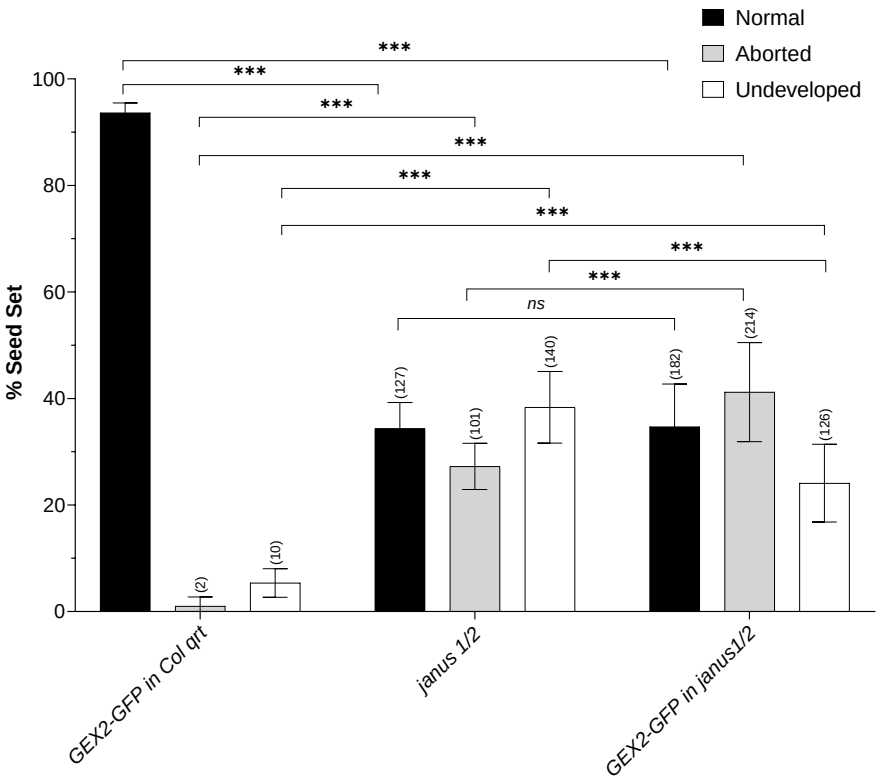

Figure 3.9. Seed set analysis of *GEX2-GFP* in *janus1/2*. Seed set quantification is shown for *janus1/2* homozygous mutant and GEX2-GFP in *Col qrt* and *janus1/2*. Sample size of ovules is indicated above the respective bar. A 2-way ANOVA followed by Tukey´s multiple comparison analysis was used to determine statistical significance. *n.s. non-significant* ***p<0.0001.

We then examined the morphology of the MGU *janus1/2* and the triple *gex2/janus1/2* mutant using *JANUS2-GFP* marker line and *janus1/2* in the background of *GEX2-GFP* (Fig. 3.10A). In the *JANUS2-GFP* background the proportion of SC pairs displaying the adhesion morphology is decreased in triple *gex2/janus1/2* mutant when compared to *janus1/2* (Fig. 3.10A), supporting the hypothesis that *GEX2* contributes as a SC-SC adhesion factor. However in the background of *GEX2-GFP* the number of *janus1/2* sperm cell pairs with the extended adhesion phenotype is higher than in the wild type as expected for the *janus1/2* mutation. The adhesion phenotype is not increased when compared to the proportion (40-50%) typically observed in the *janus1/2* background (JANUS2-GFP this study and TET12-GFP, not shown) (Fig. 3.10 A and B)..

These results are not conclusive to whether GEX2 contributes as a homotypic cell-cell adhesion factor in *Arabidopsis* SCs. The number of SCs sampled for GEX2-GFP in the wild type and

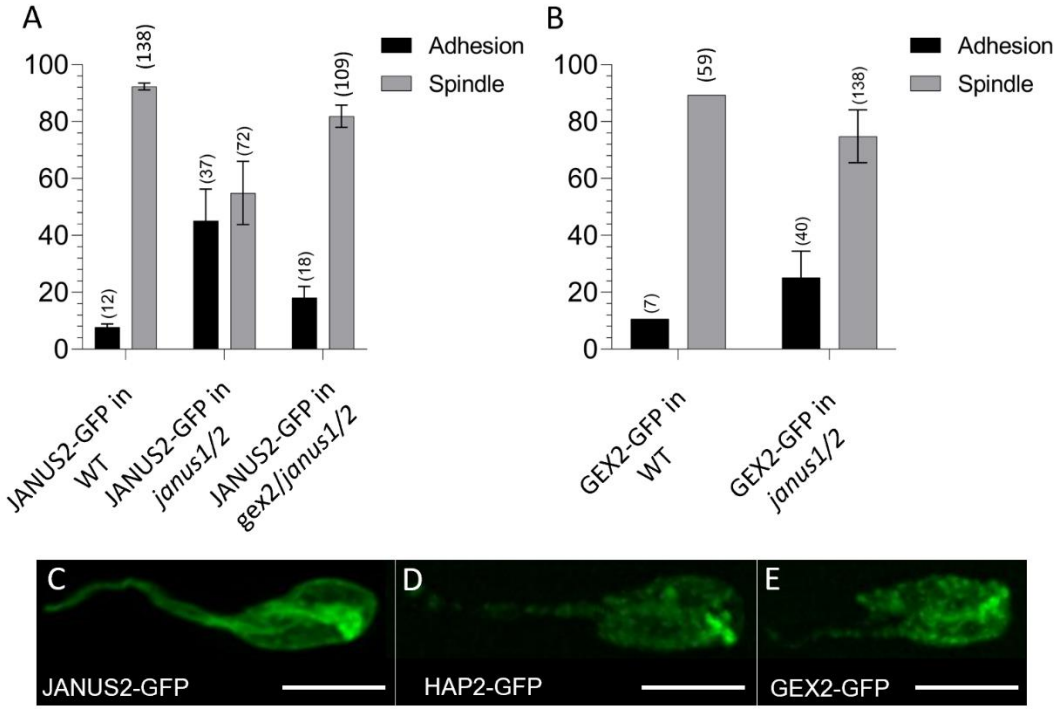

Figure 3.10. Examining GEX2 as a homotypic SC-SC adhesion factor. (A) Quantification of Male Germ Unit morphology in JANUS2-GFP expressed in the background of *wild type* (WT), *janus1/2*, and *gex2/janus1/2*. (B) Quantification of Male Germ Unit morphology in GEX2-GFP expressed in the background *of wild type* (WT) and *janus1/2*. (C-D) Representative images of SC pairs showing the extended adhesion phenotype in *janus1/2* in the background of different marker lines.

janus1/2 background need to be increased and the *GEX2-GFP* construct verified to be functional. Moreover, *GEX2* expression under the native promoter may not be sufficient to cause a significant and clear effect in SC-SC adhesion, other SC promoters with stronger expression need to be tested.

Finally, we examined if the distribution and localization of sperm cell factors was altered in the background of *janus1/2*. When we compare *GEX2-GFP* expression in *Col qrt* (wild type) and in the *janus1/2* background, GEX2 localization and its enrichment at the SC-SC adhesion domain is only slightly increased in *janus1/2*, suggesting that JANUS1/2 do not influence GEX2 localization. However, for this quantification we only used sperm cell pairs that had a typical spindle morphology. Quantification and subcellular localization of GEX2 in sperm cells pairs with the extended adhesion morphology should provide conclusive information of possible mobilization of GEX2 to the extended SC-SC adhesion domain (Fig. 3.10D, Fig. 3.11B and E).

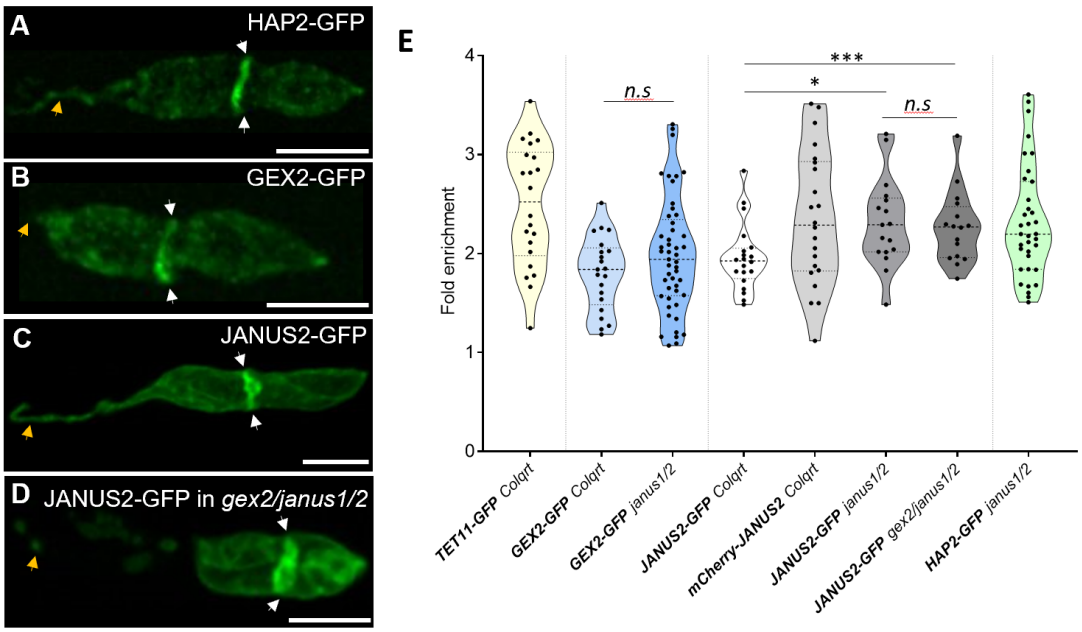

Figure 3.11. Expression analysis and quantification of enrichment of sperm cell (SC) factors at the SC-SC interface. (A-D) Representative 2D maximum projections of Z-stacks for each marker line in *janus1/2* background: *HAP2-GFP* (A); *GEX2-GFP* (B); *JANUS2-GFP* (C); *JANUS2-GFP* in *gex2/janus1/2* (D). Yellow arrows indicate cytoplasmic SC extension connecting to Vegetative Nucleus (VN), white arrows indicate SC-SC interface. Scale bars: 5 µm. (E) Violin plot depicting fold protein enrichment calculated as ratio of mean fluorescent intensity between SC-SC adhesion domain and plasma membrane. Values from all analyzed marker lines in Col qrt and in *janus1/2* mutant are shown. Dashed line represents mean, dotted line represents the 25th to 75th percentiles. Statistical significance represented by *p<0.05, **p<0.01, ***p<0.001 as calculated by unpaired t-test with Welch's correction

In addition, we examined the distribution of other SC factors (Fig. 3.11A-E) in the background of *janus1/2*. The expression of *JANUS2-GFP* in the *janus1/2* double and *gex2/janus1/2* triple mutant lines is similar but shows significant enrichment at the SC-SC adhesion domain when compared to wild type (Fig. 3.11E). These results are interesting, as we previously hypothesized that the C-terminus of *JANUS2*-GFP could be blocking *JANUS-TET* interactions and its recruitment to the SC-SC interface. The observation that in *janus1/2* background, *JANUS2-GFP* accumulates at the adhesion domain, may suggest that *JANUS2* could have another interacting partner that recruits it to the adhesion domain. It is also possible that in the absence of the endogenous JANUS, TET recruits more JANUS-GFP (a non-functional protein) to the SC-SC interface to compensate for its absence. For this reason, these observations should be taken carefully.

The expression of *HAP2* shows that despite its localization in the endomembrane system, both *HAP2* and *GEX2* accumulate at the SC-SC adhesion domain (Fig.3.11A). Quantification of *HAP2-GFP* in *Col qrt* will allow us to determine if HAP2 enrichment at the SC-SC interface is increased in *janus1/2* background.

In this chapter, we provide evidence that JANUS1/2 may function as a plasma membrane remodeler in *Arabidopsis* sperm cells. Although the results are preliminary, these proteins seem to contain conserved residues and motifs which are consistent with their unique functions within their protein family and in SCs. In addition, our results suggest that GEX2 could act as a homotypic cell adhesion factor between the twin sperm cells, although further experiments are needed to confirm the results here presented. This chapter has emphasized a possible function of JANUS1/2 proteins in double fertilization shedding light into new levels of regulation and functions of sperm cell factors in plant reproduction.

3.5 References

Arza, B, M De Maeyer, J Félez, D Collen, and HR Lijnen. 2001. "Critical Role of Glutamic Acid 202 in the Enzymatic Activity of stromelysin-1 (MMP-3)." *European journal of biochemistry* no. 268 (3). doi: 10.1046/j.1432-1327.2001.01943.x.

Ball L, Kühne R, Schneider-Mergener J, Oschkinat H (2005) Recognition of Proline-Rich Motifs by Protein-Protein-Interaction Domains. Angewandte Chemie (International ed. in English) 44Barroso G, Valdespin C, Vega E, Kershenovich R, Avila R, Avendaño C, Oehninger S (2009) Developmental Sperm Contributions: Fertilization and Beyond. Fertility and sterility 92

Bendas, Gerd, and Lubor Borsig. 2012. "Cancer Cell Adhesion and Metastasis: Selectins, Integrins, and the Inhibitory Potential of Heparins." *International Journal of Cell Biology* no. 2012. doi: https://doi.org/10.1155/2012/676731.

Boavida, L. C., and S. McCormick. 2007. "Temperature as a determinant factor for increased and reproducible in vitro pollen germination in Arabidopsis thaliana." *Plant J* no. 52 (3):570-82. doi: 10.1111/j.1365-313X.2007.03248.x.

Boavida LC, Qin P, Broz M, Becker JD, McCormick S (2013) Arabidopsis tetraspanins are confined to discrete expression domains and cell types in reproductive tissues and form homo- and heterodimers when expressed in yeast. Plant Physiol 163: 696-712

Bourboulia, D, and WG Stetler-Stevenson. 2010. "Matrix Metalloproteinases (MMPs) and Tissue Inhibitors of Metalloproteinases (TIMPs): Positive and Negative Regulators in Tumor Cell Adhesion." *Seminars in cancer biology* no. 20 (3). doi: 10.1016/j.semcancer.2010.05.002.

Campbell, HK, JL Maiers, and KA DeMali. 2017. "Interplay Between Tight Junctions & Adherens Junctions." *Experimental cell research* no. 358 (1). doi: 10.1016/j.yexcr.2017.03.061.

Cenis, J. L. 1992. "Rapid extraction of fungal DNA for PCR amplification." *Nucleic Acids Res* no. 20 (9):2380.

Chen, MS, KS Tung, SA Coonrod, Y Takahashi, D Bigler, A Chang, Y Yamashita, PW Kincade, JC Herr, and JM White. 1999. "Role of the Integrin-Associated Protein CD9 in Binding Between Sperm ADAM 2 and the Egg Integrin alpha6beta1: Implications for Murine Fertilization." *Proceedings of the National Academy of Sciences of the United States of America* no. 96 (21). doi: 10.1073/pnas.96.21.11830.

Cyprys, P., M. Lindemeier, and S. Sprunck. 2019. "Gamete fusion is facilitated by two sperm cell-expressed DUF679 membrane proteins." *Nat Plants* no. 5 (3):253-257. doi: 10.1038/s41477-019-0382-3.

Daher, F. B., and S. A. Braybrook. 2015. "How to let go: pectin and plant cell adhesion." *Front Plant Sci* no. 6:523. doi: 10.3389/fpls.2015.00523.

De Smet, I, and T Beeckman. 2011. "Asymmetric Cell Division in Land Plants and Algae: The Driving Force for Differentiation." *Nature reviews. Molecular cell biology* no. 12 (3). doi: 10.1038/nrm3064.

Delorme, V. G., P. F. McCabe, D. J. Kim, and C. J. Leaver. 2000. "A Matrix Metalloproteinase Gene Is Expressed at the Boundary of Senescence and Programmed Cell Death in Cucumber1." *Plant Physiol* no. 123 (3):917-28.

Edwards, K., C. Johnstone, and C. Thompson. 1991. "A simple and rapid method for the preparation of plant genomic DNA for PCR analysis." *Nucleic Acids Res* no. 19 (6):1349.

Flinn, Barry S. 2020. "Plant extracellular matrix metalloproteinases." *Functional Plant Biology* no. 35 (12):1183-1193. doi: 10.1071/FP08182.

Gutiérrez-López, MD, A Gilsanz, M Yáñez-Mó, S Ovalle, EM Lafuente, C Domínguez, PN Monk, I González-Alvaro, F Sánchez-Madrid, and C Cabañas. 2011. "The Sheddase Activity of ADAM17/TACE Is Regulated by the Tetraspanin CD9." *Cellular and molecular life sciences : CMLS* no. 68 (19). doi: 10.1007/s00018-011-0639-0.

Ha, Y. 2009. "Structure and mechanism of intramembrane protease." *Semin Cell Dev Biol* no. 20 (2):240-50. doi: 10.1016/j.semcdb.2008.11.006.

Hadler-Olsen, E, B Fadnes, I Sylte, L Uhlin-Hansen, and JO Winberg. 2011. "Regulation of Matrix Metalloproteinase Activity in Health and Disease." *The FEBS journal* no. 278 (1). doi: 10.1111/j.1742-4658.2010.07920.x.

Hirokazu, Tanaka, Onouchi Hitoshi, Kondo Maki, Hara-Nishimura Ikuko, Nishimura Mikio, Machida Chiyoko, and Machida Yasunori. 2001. "A subtilisin-like serine protease is required for epidermal surface formation in Arabidopsis embryos and juvenile plants." *Development*.

Horstkorte, Rüdiger, and Babette Fuss. 2012. "Chapter 9 - Cell Adhesion Molecules." In *Basic Neurochemistry (Eighth Edition)*, edited by Scott T. Brady, George J. Siegel, R. Wayne Albers and Donald L. Price, 165-179. New York: Academic Press.

Johnson-Brousseau, S. A., and S. McCormick. 2004. "A compendium of methods useful for characterizing Arabidopsis pollen mutants and gametophytically-expressed genes." *Plant J* no. 39 (5):761-75. doi: 10.1111/j.1365-313X.2004.02147.x.

Kang, T, YG Zhao, D Pei, JF Sucic, and QX Sang. 2002. "Intracellular Activation of Human Adamalysin 19/disintegrin and Metalloproteinase 19 by Furin Occurs via One of the Two Consecutive Recognition Sites." *The Journal of biological chemistry* no. 277 (28). doi: 10.1074/jbc.M203532200.

Kasaras, A, and R Kunze. 2010. "Expression, Localisation and Phylogeny of a Novel Family of Plant-Specific Membrane Proteins." *Plant biology* no. 12 Suppl 1. doi: 10.1111/j.1438-8677.2010.00381.x.

Kasaras, A., M. Melzer, and R. Kunze. 2012. "Arabidopsis senescence-associated protein DMP1 is involved in membrane remodeling of the ER and tonoplast." *BMC Plant Biol* no. 12:54. doi: 10.1186/1471-2229-12-54.

Krupková, E, P Immerzeel, M Pauly, and T Schmülling. 2007. "The TUMOROUS SHOOT DEVELOPMENT2 Gene of Arabidopsis Encoding a Putative Methyltransferase Is Required for Cell Adhesion and Co-Ordinated Plant Development." *The Plant journal : for cell and molecular biology* no. 50 (4). doi: 10.1111/j.1365-313X.2007.03123.x.

Landgraf, C, S Panni, L Montecchi-Palazzi, L Castagnoli, J Schneider-Mergener, R Volkmer-Engert, and G Cesareni. 2004. "Protein Interaction Networks by Proteome Peptide Scanning." *PLoS biology* no. 2 (1). doi: 10.1371/journal.pbio.0020014.

Lord, E. 2000. "Adhesion and Cell Movement During Pollination: Cherchez La Femme." *Trends in plant science* no. 5 (9). doi: 10.1016/s1360-1385(00)01744-1.

Maidment, JM, D Moore, GP Murphy, G Murphy, and IM Clark. 1999. "Matrix Metalloproteinase Homologues From Arabidopsis Thaliana. Expression and Activity." *The Journal of biological chemistry* no. 274 (49). doi: 10.1074/jbc.274.49.34706.

Mariano, C, H Sasaki, D Brites, and MA Brito. 2011. "A Look at Tricellulin and Its Role in Tight Junction Formation and Maintenance." *European journal of cell biology* no. 90 (10). doi: 10.1016/j.ejcb.2011.06.005.

Marino, G, and C Funk. 2012. "Matrix Metalloproteinases in Plants: A Brief Overview." *Physiologia plantarum* no. 145 (1). doi: 10.1111/j.1399-3054.2011.01544.x.

Marino, G, PF Huesgen, U Eckhard, CM Overall, WP Schröder, and C Funk. 2014. "Family-wide Characterization of Matrix Metalloproteinases From Arabidopsis Thaliana Reveals Their Distinct Proteolytic Activity and Cleavage Site Specificity." *The Biochemical journal* no. 457 (2). doi: 10.1042/BJ20130196.

Mori, T., T. Igawa, G. Tamiya, S. Y. Miyagishima, and F. Berger. 2014. "Gamete attachment requires GEX2 for successful fertilization in Arabidopsis." *Curr Biol* no. 24 (2):170-5. doi: 10.1016/j.cub.2013.11.030.

Preuss, D., S. Y. Rhee, and R. W. Davis. 1994. "Tetrad analysis possible in Arabidopsis with mutation of the QUARTET (QRT) genes." *Science* no. 264 (5164):1458-60. doi: 10.1126/science.8197459.

Saint-Pol, J, E Eschenbrenner, E Dornier, C Boucheix, S Charrin, and E Rubinstein. 2017. "Regulation of the Trafficking and the Function of the Metalloprotease ADAM10 by Tetraspanins." *Biochemical Society transactions* no. 45 (4). doi: 10.1042/BST20160296.

Sang-Youl, Park, and Lord Elizabeth M. 2003. "Expression studies of SCA in lily and confirmation of its role in pollen tube adhesion." *Plant Molecular Biology* no. 51 (2):183-189. doi: doi:10.1023/A:1021139502947.

Schaller, A. 2004. "A Cut Above the Rest: The Regulatory Function of Plant Proteases." *Planta* no. 220 (2). doi: 10.1007/s00425-004-1407-2.

Schaller, A., and C. A. Ryan. 1994. "Identification of a 50-kDa systemin-binding protein in tomato plasma membranes having Kex2p-like properties." *Proc Natl Acad Sci U S A* no. 91 (25):11802-6.

Schindelin, J., I. Arganda-Carreras, E. Frise, V. Kaynig, M. Longair, T. Pietzsch, S. Preibisch, C. Rueden, S. Saalfeld, B. Schmid, J. Y. Tinevez, D. J. White, V. Hartenstein, K. Eliceiri, P. Tomancak, and A. Cardona. 2012. "Fiji: an open-source platform for biological-image analysis." *Nat Methods* no. 9 (7):676-82. doi: 10.1038/nmeth.2019.

Seals, DF, and SA Courtneidge. 2003. "The ADAMs Family of Metalloproteases: Multidomain Proteins With Multiple Functions." *Genes & development* no. 17 (1). doi: 10.1101/gad.1039703.

Uría, JA, and C López-Otín. 2000. "Matrilysin-2, a New Matrix Metalloproteinase Expressed in Human Tumors and Showing the Minimal Domain Organization Required for Secretion, Latency, and Activity." *Cancer research* no. 60 (17).

Yanez-Mo, M., F. Sanchez-Madrid, and C. Cabanas. 2011. "Membrane proteases and tetraspanins." *Biochem Soc Trans* no. 39 (2):541-6. doi: 10.1042/bst0390541.

Yu, Zhong, Chen Baojian, Li Mengran, Wang Dong, Jiao Yanyan, Qi Xiaolong, Wang Min, Liu Zongkai, Chen Chen, Wang Yuwen, Chen Ming, Li Jinlong, Xiao Zijian, Cheng Dehe, Liu Wenxin, Boutilier Kim, Liu Chenxu, and Chen Shaojiang. 2020. "A DMP -triggered in vivo maternal haploid induction system in the dicotyledonous Arabidopsis." *Nature Plants* no. 6 (5):466-472. doi: doi:10.1038/s41477-020-0658-7.

Zhang, Xiuren, Rossana Henriques, Shih-Shun Lin, Qi-Wen Niu, and Nam-Hai Chua. 2006. "Agrobacterium -mediated transformation of Arabidopsis thaliana using the floral dip method." *Nature Protocols* no. 1 (2):641-646. doi: doi:10.1038/nprot.2006.97.

Zhu, G. Z., S. Gupta, D. G. Myles, and P. Primakoff. 2009. "Testase 1 (ADAM 24) a sperm surface metalloprotease is required for normal fertility in mice." *Mol Reprod Dev* no. 76 (11):1106-14. doi: 10.1002/mrd.21076.

CHAPTER 4. CONCLUSIONS AND FUTURE PERSPECTIVES

4.1 Introduction

Humans have been modifying and breeding crops for millennia, however, only recently advances in our understanding of the basic principles of plant reproduction, at both the genetic and cellular level, has enabled more applied approaches. Understanding the signaling pathways and the molecular components involved in regulating cell-cell communication during plant reproduction is essential to improve breeding strategies and overall crop production.

This thesis focused on the characterization of *Tetraspanins* (*TET*s) and their signaling partners, *JANUS1/2* in *Arabidopsis* sperm cells (SCs). Although tetraspanins have been previously implicated in development and immunity in animal systems (García-Frigola et al., 2001; Levy and Shoham, 2005), the knowledge of their functions and signaling interactors in plants is very scarce. Published results on the function of *AtTETs* supports the hypothesis that they are evolutionarily conserved and perform similar functions across all multicellular organisms (Cnops et al., 2006; Wang et al., 2015; Cai et al., 2018; Cai et al., 2019). This study is the first to provide a quantitative analysis of *TETs* distribution and localization in the plasma membrane of SCs. We have shown that these patterns are consistent with the existence of a Tetraspanin-Enriched Microdomain (TEMs) at the SC-SC interface. Future studies should examine how TEMs are regulated and control the expression and function of potential interacting partners in double fertilization.

4.2 The SC-SC Adhesion Interface Defines a Tetraspanin-Enriched Microdomain

This thesis provides quantitative evidence for the existence of a Tetraspanin-Enriched Microdomain (TEM) that forms at the SC-SC adhesion interface. The Male Germ Unit (MGU) is a structural assembly that organizes the twin sperm cells and the Vegetative Nucleus (VN) in a

functional unit (McCormick, 2004). The MGU has long been suggested to be essential to ensure the simultaneous delivery of the sperm cells to the ovule (McCue et al., 2011). Recent findings suggest that this functional assembly may also assure the intercellular communication (small RNAs and mRNAs) between the VN and both sperm cells (Slotkin et al., 2009; Jiang et al., 2015). The cytoplasmic extension from one SC to the VN allows directional transport of information from the VN membrane to SCs, while the TEM structure may function as a platform for secretion or transport of factors across the plasma membrane of sperm cells.

In this study we examined if plant tetraspanins accumulate at the adhesion interface of SCs, thus defining a TET-enriched microdomain, as reported for their functions in animal systems (Latysheva et al., 2006; Mazurov et al., 2006). Our results suggest that TETs do not only accumulate at the SC-SC adhesion domain, but this accumulation cannot be solely explained by the existence of a double membrane at the SC-SC interface. The close proximity of both SC membranes, on the range of 50-80 nm at the adhesion site, potentially allow direct protein-protein interactions between adjacent cells (Wu et al., 2015). Although *cis* interactions have been reported in TEMs, consistent with their ability to form homo- and heterodimers in plants (Boavida et al., 2013), TET interactions in *trans,* across cells have not yet been reported. A possible explanation for enrichment of TETs at the SC-SC interface could be a local membrane enrichment, similar to the embryo sac filiform apparatus. However, transmission electron microscopy of the SC-SC interface does not reveal any apparent membrane enrichment or folding (Fig. 2.2, unpublished results from Leonor Boavida). We observe that both membranes are separated by an interstitial space, which is likely filled with a polysaccharide-enriched extracellular matrix (McCue et al., 2011) where occasional membrane structures, similar to vesicles can be observed.

This study also provides evidence for localization at the SC-SC adhesion domain of several sperm cells factors with known functions in double fertilization. GEX2 and HAP2 are both transmembrane proteins essential for adhesion and fusion of male-female gametes (von Besser et al., 2006; Mori et al., 2014). HAP2 is localized at the endomembrane system and is only mobilized to the plasma membrane upon sperm cell delivery. This mobilization is dependent of sperm cell activation by the egg cell cysteine-rich peptide, EC1 (Sprunck et al., 2012). GEX2, the factor regulating male-female gamete adhesion, was previously described to be plasma membrane localized (Mori et al., 2014). Our analyses indicate that GEX2, similar to HAP2, is sequestered in the endomembrane system. It remains to be determined how GEX2 is mobilized to the plasma membrane, and if this mobilization is also EC1-dependent.

Both HAP2 and GEX2, independent of their intracellular localization, are polarized at the plasma membrane to the SC-SC adhesion interface. These two factors should only be active during sperm-female gamete interactions and be inactive (or non-functional) in SCs during pollen tube growth. Our findings thus support the hypothesis that the SC-SC interface may function as a protective domain for sperm-expressed fertilization factors. Future studies should focus on determining if this localization is TET-dependent. Potential molecular interactions of HAP2 and GEX2 with Tetraspanins could easily be verified using yeast two-hybrid interactions, pull-down assays, or BIFC. Single-molecule high-resolution microscopy (Sergé, 2016) is a powerful tool to obtain spatial and temporal resolution of molecular interactions, co-localization, and protein-specific dynamics within TEM clusters at the SC-SC adhesion domain.

Because all sperm cell factors analyzed in this study localize and, in different degrees, are enriched at the SC-SC interface, information in the distribution of plasma membrane components unrelated with double fertilization (e.g. GPI anchored, lipid-raft associated and other

transmembrane proteins) must be examined to determine the specificity of TET-enriched microdomains and potential molecular interactions. A second aspect relates with the cellular origin of these markers. As previously discussed, SCs are enclosed by a plasma membrane of vegetative origin. A few reports described localization of pollen-derived membrane associated proteins to the sperm cell surface. For instance, Lyn24 know as a GPI-anchored protein in animal cells when expressed in the vegetative pollen cell is targeted to the SC surface (Li et al., 2013). These observations suggest that SC membranes may have special protein or lipid compositions. While a *bonafide* marker for the outer vegetative SC membrane has not been reported, co-localization of known sperm cell markers with Lyn24 driven by a pollen-specific and a sperm-specific promoter may provide some clues about the composition of these two membranes.

At the cellular level it will be interesting to identify components that stabilize the TET microdomain. In animal systems, TETs are stabilized by palmitoylation and associations with cytoskeleton components (Sala-Valdés et al., 2006; Espenel et al., 2008). The role of the cytoskeleton, namely of actin filaments and microtubules in MGU integrity is poorly understood. The participation of the cytoskeleton in the stabilization of the MGU and of SC-SC TET microdomains is an interesting aspect to explore.

In the second part of Chapter 2, we generated CRISPR/Cas9 transgenic plants to examine the function of *TET11/TET12* in SCs and of functional interactions between JANUS and TETs. The analysis of a knockout *tet11* mutant did not reveal any apparent phenotype, suggesting that *TET11/TET12* could function redundantly in the SCs. Preliminary analysis identified fertility-associated phenotypes on several transgenic *TET12* CRISPR/Cas9 T1 plants. The fertility phenotypes affect fertilization and range from 25-50% suggesting that we may have identified *tet12* heterozygous and homozygous mutants with partial penetrance. While these results would

be consistent with a possible functional redundancy of *TET11* and *TET12* in SCs, only the analysis of *TET12* CRISPR edited plants in the background of *tet11* can reveal how the function of these two genes is related.

In transgenic CRISPR/Cas9 plants targeting both *TET12* and *JANUS1/2*, we observed fertilization defects associated with pollen abortion, late aborted ovules, and arrest in embryo sac development. The phenotype is similar, independent of the background, *tet11* or *wild type*, suggesting that *TET12* and *JANUS1/2* may play unknown and essential roles in early male and female gametophyte development.

Tetraspanins are expressed throughout the plant in a cell-type specific manner (Boavida et al., 2013). *TET8* and *TET9* are highly expressed in female gametes. Future studies could identify functional roles in double fertilization for these proteins, and if some type of Tetraspanin-enriched microdomains is present or form in female gametes. In mice, the egg cell-expressed Tetraspanin CD9, is required for sperm-egg cell fusion and is mobilized to the gamete contact site through interactions with its partner JUNO during fertilization. Interestingly, CD9 was hypothesized to be involved in developing the polyspermic barrier following fertilization (Jankovičová et al., 2020), since the CD9/JUNO are rapidly shed from the egg membrane after sperm-egg fusion (Chalbi et al., 2014). Perhaps tetraspanins expressed in *Arabidopsis* female gametes are also involved in facilitating gamete adhesion and fusion or regulating polyspermy block in the egg cell. *TET8* and *TET9* were reported to be induced upon plant-pathogen invasion, leading to a defense mechanism by which plants secrete TET8/TET9-coated exosomes which carry small RNAs able to silence virulent genes in fungi (Cai et al., 2018). EC1, a cysteine-rich peptide responsible for sperm cell activation in Arabidopsis, is secreted by the egg cell binding to an unknown receptor on the sperm plasma membrane (Sprunck et al., 2012). Similar to cell-cell signaling during the plant immune

response, we can envision that TET8/9 could also be involved in facilitating signaling between the egg cell and SCs.

4.3 JANUS1/2 potential function as Matrix Metalloproteases in *Arabidopsis* Sperm Cells

Matrix Metalloproteases (MMPs) were associated to degradation and shedding of extracellular matrix components, contributing to several important biological processes, such as signaling, cell growth, and cell migration (Itoh, 2015). Five homologues of matrix metalloproteases (MMPs) were identified in *A. thaliana* (Maidment et al., 1999), although none of them are expressed in SCs. The Arabidopsis JANUS1/2 proteins display striking structural similarities and share some known functional motifs with matrix metalloproteases. JANUS1/2 are distinct within their small protein family, forming a unique clade (Chapter 3). We have shown that *janus1/2* phenotype cannot be rescued by ectopic expression of any other member of the DMP protein family, suggesting that JANUS1/2 functions in SC are unique or have some type of substrate specificity. These proteins are annotated with unknown functions (Kasaras and Kunze, 2010), and a single study suggested that DMP proteins could function as membrane remodelers in the tonoplast and ER (Kasaras et al., 2012).

Preliminary results obtained from transgenic plants containing mutations on two of the predicted catalytic sites cause fertilization defects when expressed in a wild type background. These results strongly support our structural analysis and the potential proteolytic function of JANUS1/2. In addition, it seems clear that JANUS1/2 have some sort of membrane remodeling function, since the phenotype observed in *janus1/2* SCs is consistent with alterations in the composition of the SC membranes. However, biochemical studies are necessary to confirm JANUS1/2 function as a protease. This research direction is currently being followed in the lab.

Other possible studies include the identification of JANUS substrates, inhibitors and activators in sperm cells and female gametes.

It is also not known if JANUS1/2 are acting only in sperm cells or their functions as membrane remodelers extend to the surface of female gametes after male-female gamete contact. In animals, matrix metalloproteases are necessary for sperm-egg fusion. In mice, the sperm-expressed matrix metalloprotease, ADAM24, is required for the sperm to penetrate the zona pellucida of the egg and is also involved in establishing an egg polyspermy block (Zhu et al., 2009). A single report for a gamete-expressed metalloprotease in plants, comes from *Chlamydomonas reinhardtii*, where the Gamete Lytic Enzyme, GLE is responsible for removing the cell walls of gametes prior to fusion (Kinoshita et al., 1992).

4.4 GEX2 may promote Homotypic Cell-Cell Adhesion in *A. thaliana* Sperm Cells

GEX2 is a sperm-specific single-pass transmembrane protein previously described as a male-female gamete adhesion factor (Mori et al., 2014). As a primary candidate for an adhesion factor, we hypothesized that *GEX2* could also function as an adhesion factor between the two sperm cells.

We have shown that when we remove GEX2 from the background of *janus1/2* proportion of SCs showing the typical MGU spindle morphology increases. Similarly, the increased expression of GEX2 significantly enhanced the fertilization defects (aborted ovules) expected to result from a higher proportion of SC pairs with extended adhesion that fail to separate causing polyspermic fusions. However, we were not able to correlate these results with an extended adhesion morphology when we introduced GEX2-GFP into *janus1/2* SC. This last result was unexpected but could be easily explained by the low sample size in this particular experiment.

Finally, we examined the distribution and accumulation of GEX2 in *janus1/2* SCs. We found that GEX2 was enriched at the SC-SC interface of *janus1/2* and in the triple *gex2/janus1/2* mutant when compared to wild type, but the fold enrichment was similar between *janus1/2* and the triple *gex2/janus1/janus2* mutant (Chapter 3, Fig. 3.11). Together, these results suggest that GEX2 may be involved in reinforcing SC-SC adhesion, however additional experiments are required to conclusively determine the contribution of GEX2 to *janus1/2* phenotype. These include the quantification of a higher or similar number of SC pairs in *janus1/2* expressing GEX2-GFP. The *gex2* phenotype is relatively mild and homozygous mutants are relatively easy to recover, suggesting that GEX2 is not the only adhesion factor involved in gamete interactions.

4.5 References

Boavida LC, Qin P, Broz M, Becker JD, McCormick S (2013) Arabidopsis tetraspanins are confined to discrete expression domains and cell types in reproductive tissues and form homo- and heterodimers when expressed in yeast. Plant Physiol 163: 696-712

Cai Q, He B, Weiberg A, Buck AH, Jin H (2018) Small RNAs and extracellular vesicles: New mechanisms of cross-species communication and innovative tools for disease control. *In* PLoS Pathog, Vol 15

Chalbi M, Barraud-Lange V, Ravaux B, Howan K, Rodriguez N, Soule P, Ndzoudi A, Boucheix C, Rubinstein E, Wolf J, Ziyyat A, Perez E, Pincet F, Gourier C (2014) Binding of Sperm Protein Izumo1 and Its Egg Receptor Juno Drives Cd9 Accumulation in the Intercellular Contact Area Prior to Fusion During Mammalian Fertilization. Development (Cambridge, England) 141

Cnops G, Neyt P, Raes J, Petrarulo M, Nelissen H, Malenica N, Luschnig C, Tietz O, Ditengou F, Palme K, Azmi A, Prinsen E, Van Lijsebettens M (2006) The TORNADO1 and TORNADO2 genes function in several patterning processes during early leaf development in Arabidopsis thaliana. Plant Cell 18: 852-866

Espenel C, Margeat E, Dosset P, Arduise C, Le Grimellec C, Royer CA, Boucheix C, Rubinstein E, Milhiet PE (2008) Single-molecule analysis of CD9 dynamics and partitioning reveals multiple modes of interaction in the tetraspanin web. J Cell Biol 182: 765-776

García-Frigola C, Burgaya F, de Lecea L, Soriano E (2001) Pattern of Expression of the Tetraspanin Tspan-5 During Brain Development in the Mouse. Mechanisms of development 106

Itoh Y (2015) Membrane-type matrix metalloproteinases: Their functions and regulations. Matrix Biol 44-46: 207-223

Jankovičová J, Neuerová Z, Sečová P, Bartóková M, Bubeníčková F, Komrsková K, Postlerová P, Antalíková J (2020) Tetraspanins in Mammalian Reproduction: Spermatozoa, Oocytes and Embryos. Medical microbiology and immunology

Jiang H, J Y, Boavida L, Chen Y, Becker J, Köhler C, McCormick S (2015) Intercellular Communication in Arabidopsis Thaliana Pollen Discovered via AHG3 Transcript Movement From the Vegetative Cell to Sperm. Proceedings of the National Academy of Sciences of the United States of America 112

Kasaras A, Kunze R (2010) Expression, Localisation and Phylogeny of a Novel Family of Plant-Specific Membrane Proteins. Plant biology 12 Suppl 1

Kasaras A, Melzer M, Kunze R (2012) Arabidopsis senescence-associated protein DMP1 is involved in membrane remodeling of the ER and tonoplast. BMC Plant Biol 12: 54

Kinoshita T, Fukuzawa H, Shimada T, Saito T, Matsuda Y (1992) Primary Structure and Expression of a Gamete Lytic Enzyme in Chlamydomonas Reinhardtii: Similarity of Functional Domains to Matrix Metalloproteases. Proceedings of the National Academy of Sciences of the United States of America 89

Latysheva N, Muratov G, Rajesh S, Padgett M, Hotchin N, Overduin M, Berditchevski F (2006) Syntenin-1 Is a New Component of Tetraspanin-Enriched Microdomains: Mechanisms and Consequences of the Interaction of syntenin-1 With CD63. Molecular and cellular biology 26

Levy S, Shoham T (2005) The Tetraspanin Web Modulates Immune-Signalling Complexes. Nature reviews. Immunology 5

Li S, Zhou L, Feng Q, McCormick S, Zhang Y (2013) The C-terminal Hypervariable Domain Targets Arabidopsis ROP9 to the Invaginated Pollen Tube Plasma Membrane. Molecular plant 6

Maidment J, Moore D, Murphy G, Murphy G, Clark I (1999) Matrix Metalloproteinase Homologues From Arabidopsis Thaliana. Expression and Activity. The Journal of biological chemistry 274

Mazurov D, Heidecker G, Derse D (2006) HTLV-1 Gag Protein Associates With CD82 Tetraspanin Microdomains at the Plasma Membrane. Virology 346

McCormick S (2004) Control of male gametophyte development. Plant Cell 16 Suppl: S142-153

McCue A, Cresti M, Feijó J, Slotkin R (2011) Cytoplasmic Connection of Sperm Cells to the Pollen Vegetative Cell Nucleus: Potential Roles of the Male Germ Unit Revisited. Journal of experimental botany 62

Mori T, Igawa T, Tamiya G, Miyagishima SY, Berger F (2014) Gamete attachment requires GEX2 for successful fertilization in Arabidopsis. Curr Biol 24: 170-175

Sala-Valdés M, Ursa A, Charrin S, Rubinstein E, Hemler M, Sánchez-Madrid F, Yáñez-Mó M (2006) EWI-2 and EWI-F Link the Tetraspanin Web to the Actin Cytoskeleton Through Their Direct Association With Ezrin-Radixin-Moesin Proteins. The Journal of biological chemistry 281

Sergé A (2016) The Molecular Architecture of Cell Adhesion: Dynamic Remodeling Revealed by Videonanoscopy. Front Cell Dev Biol 4

Slotkin R, Vaughn M, Borges F, Tanurdzić M, Becker J, Feijó J, Martienssen R (2009) Epigenetic Reprogramming and Small RNA Silencing of Transposable Elements in Pollen. Cell 136

Sprunck S, Rademacher S, Vogler F, Gheyselinck J, Grossniklaus U, Dresselhaus T (2012) Egg cell-secreted EC1 triggers sperm cell activation during double fertilization. Science 338: 1093-1097

von Besser K, Frank AC, Johnson MA, Preuss D (2006) Arabidopsis HAP2 (GCS1) is a sperm-specific gene required for pollen tube guidance and fertilization. Development 133: 4761-4769

Wang F, Muto A, Van de Velde J, Neyt P, Himanen K, Vandepoele K, Van Lijsebettens M (2015) Functional Analysis of the Arabidopsis TETRASPANIN Gene Family in Plant Growth and Development1[OPEN]. *In* Plant Physiol, Vol 169, pp 2200-2214

Wu Y, Kanchanawong P, Zaidel-Bar R (2015) Actin-delimited Adhesion-Independent Clustering of E-cadherin Forms the Nanoscale Building Blocks of Adherens Junctions. Developmental cell 32

Zhu GZ, Gupta S, Myles DG, Primakoff P (2009) Testase 1 (ADAM 24) a sperm surface metalloprotease is required for normal fertility in mice. Mol Reprod Dev 76: 1106-1114

APPENDIX A. LIST OF PRIMERS

Primer Number	Primer Name	Gene	Primer Sequence
L038	LBb1XL	SALK T-DNA Insertion	ACCAGCGTGGACCGCTTGCTGCAACTCTCTCAGGG
L039	FLAG_lb	FLAG T-DNA Insertion	CGTGTGCCAGGTGCCCACGGAATAGT
L040	SAIL_LB1	SAIL T-DNA Insertion	GCCTTTTCAGAAATGGATAAATAGCCTT
L151	OX_TET11CDS_F	TET11	GGGGACAAGTTTGTACAAAAAAGCAGGCTATGTTTCGAGTTAGCAATTTC
L152	OX_TET11CDS_R	TET11	GGGGACCACTTTGTACAAGAAAGCTGGGTCGACAGAATCACTTTTCCTAG
L423	pSKTAIL-L2	SAIL T-DNA Insertion	TGGACGTGAATGTAGACACGTCG
L458	GEX2_GW_F	GEX2	GGGGACAAGTTTGTACAAAAAAGCAGGCTATGGTTGGTATCTTCAATAT
L498	GEX2_R2	GEX2	CCTGCATATACTTCCTTGATGAAAGG
L534	DMP8_F	DMP8	AACTATTGAGTCACAAAACACAGAGA
L535	DMP9_F	DMP9	GAAAAAAACAGAGAGAAACACACGAA
L537	DMP9_R	DMP9	CCAAAAAACAGAAAAGTGAAAATAAATTAACC
L575	DMP8_R3	DMP8	GCAAGAGTTTATTTTAGGCACGTG
R001	DMP1_CDS_GWR1-2_F	DMP1	GGGGACAAGTTTGTACAAAAAAGCAGGCTATGTCCGAAACTTCTTTGCTC
R002	DMP1_CDS_GWR1-2_R	DMP1	GGGGACCACTTTGTACAAGAAAGCTGGGTTTAGGCAGAGACCGAGG
R003	DMP9N-trunc_CDS_GWR1-2_F	DMP9	GGGGACAAGTTTGTACAAAAAAGCAGGCTATGGTGGCGCAAGGAGTTC
R004	DMP9_CDS_GWR1-2_R	DMP9	GGGGACCACTTTGTACAAGAAAGCTGGGTTTAACCAGTCATGCAACCAAC
R005	DMP9C-trunc_CDS_GWR1-2_F	DMP9	GGGGACAAGTTTGTACAAAAAAGCAGGCTATGGAGAAAACAGAGGAAAGC
R006	DMP9C-trunc_CDS_GWR1-2_R	DMP9	GGGGACCACTTTGTACAAGAAAGCTGGGTTTACGGAAAAACAAGAAACAAAGC
R007	DMP10_CDS_GWR1-2_F	DMP10	GGGGACAAGTTTGTACAAAAAAGCAGGCTATGGAGGCGTCGTTCATTAG
R008	DMP10_CDS_GWR1-2_R	DMP10	GGGGACCACTTTGTACAAGAAAGCTGGGTTCAACGAATGTCTGAAATTCCG
R021	DMP9p_SacI_F	DMP9	ATGCGAGCTCACTGATATGGGATTCTAATAGAAAAAAAAGAAAAATATACATTCTATT
R022	DMP9p_SpeI_R	DMP9	ACTAGTGGTTTCGTGTGTTTCTCTCTGTTTTTTTCTTTT